GSBS Dissertations and Theses   Graduate School of Biomedical Sciences

2000-08-07

Allosteric Regulation of Recombination Enzymes *E. coli* RecA and Human Rad51: A Dissertation

Julie Kelley De Zutter
University of Massachusetts Medical School

Let us know how access to this document benefits you.

Repository Citation

Allosteric Regulation of Recombination Enzymes:

E. coli RecA and Human Rad51

A Dissertation Presented

By

Julie Kelley De Zutter

Submitted to the Faculty of the

University of Massachusetts

Graduate School of Biomedical Sciences

in partial fulfillment of the requirements for the degree of

Doctor of Philosophy

August 7, 2000

Biochemistry and Molecular Biology

Parts of this dissertation have appeared in:

Kelley, J. A. & Knight, K. L. (1997). Allosteric regulation of RecA protein function is mediated by Gln194. *J Biol Chem* 272(41), 25778-82.

De Zutter, J. K. & Knight, K. L. (1999). The hRad51 and RecA proteins show significant differences in cooperative binding to single-stranded DNA. *J Mol Biol* **293**(4), 769-80.

De Zutter, J. K., Forget, A. L., Logan, K. M. and Knight, K. L. (2000). Phe217 regulates the transfer of allosteric information across the subunit interface of the RecA filament. *Structure, in press.*
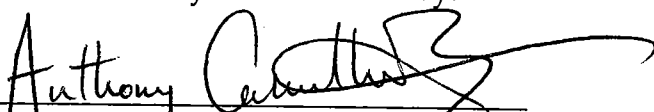
Allosteric Regulation of Recombination Enzymes:
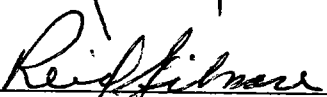
E. coli RecA and Human Rad51
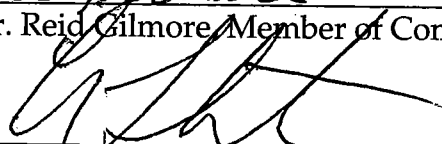
A Dissertation Presented
By

Julie Kelley De Zutter

Approved as to style and content by:

_____
Dr. Anthony Carruthers, Chair of Committee

_____
Dr. Reid Gilmore, Member of Committee

_____
Dr. Craig Peterson, Member of Committee

_____
Dr. Celia Schiffer, Member of Committee

_____
Dr. Sue Lovett, Member of Committee

_____
Dr. Kendall Knight, Thesis Advisor

_____
Dr. Thomas B. Miller, Jr.
Dean, Graduate School of Biomedical Sciences

Department of Biochemistry and Molecular Biology
August 7, 2000

Acknowledgements

First and foremost, I would like to thank my husband, Philip, for his unconditional love and support throughout my entire graduate career. I truly feel as if we have accomplished this together! He has always been a constant source of motivation, providing me with a unique perspective through both the highs and lows of graduate school. He has always reminded me of what is most important in life.

Secondly, I would like to thank my parents, Patsy and Frank Kelley. Although I have had many teachers in my life, they have always been the most instrumental. They taught me the importance of an education and to always strive to be the best person poss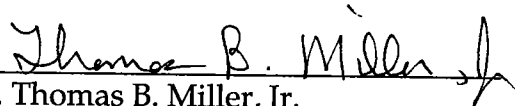ible. Furthermore, they have shown me through their actions, that no goal is ever too large, or out of reach with a little hard work and a lot of perseverance. Their love, guidance and ability to help me keep my feet planted firmly on the ground will continue to help me grow, both personally and professionally throughout my entire life.

Also, I would not be where I am today without the rest of my family; Peggy, Frankie, Marianne, Patrick, Tricia, Megan, Buddy, MaryKate, Sean, Stevie, Lori, Catie, Lizzie, Ellen, Michael, Brigid, Kathleen, Michael, Lynda, Carl, James, Ryan, Matthew, Kristine, Abigail and Matthew. They have supported me in every endeavor throughout my life and are a constant reminder of how lucky I am to

have such a great family. Most importantly, they have taught me the importance of laughter, especially at myself, which has been an invaluable tool in graduate student life!

Next, I want to extend my gratitude to the members of the Knight lab- both past and present, including Janice Lloyd, Karen Logan, Tony Forget and Erin Wallace. Each of them has contributed in their own unique way to the great experience that I have had while in graduate school. I always knew I could rely on them for advice, to listen and to help, and of course, for a good laugh! We have shared so much as labmates and friends, and I wish them each success in their own personal endeavors. I will always value each of them as true friend. Additionally, I would like to acknowledge the other people in the Department of Biochemistry and Molecular Biology who made my life at UMass so much more enjoyable on a daily basis. The members of the Carruthers Lab- Kara Levine, Erin Cloherty and Stephanie Hamill, as well as the Departmental Secretaries- Annette Stratton and Karen Welch. I will truly miss interacting with them all, and although further apart, I know we will remain friends.

Finally, I would like to thank Ken Knight for providing me with this opportunity to grow as both a person and a scientist. In the course of the time that I have spent in his lab, he has patiently helped me to develop confidence in my own scientific abilities. He has a unique ability to answer the most basic or difficult question, without making you feel stupid and can motivate you to tackle the most complex of all problems while making you think that it was your own

vi

idea. His door is always open to talk, not only about science, but any topic that concerns you. His love and enthusiasm for science and are truly both inspirational and contagious, and I hope that, one day, I can be the type of mentor he has been for me.

Abstract

ATP plays a critical role in the regulation of many enzyme processes. In this work, I have focused on the ATP mediated regulation of the recombination processes catalyzed by the *E. coli* RecA and the human Rad51 proteins. The RecA protein is a multifunctional enzyme, which plays a central role in the processes of recombinational DNA repair, homologous genetic recombination and in the activation of the cellular SOS response to DNA damage. Each of these functions requires a common activating step, which is the formation of a RecA-ATP-ssDNA nucleoprotein filament. The binding of ATP results in the induction of a cooperative, high affinity ssDNA binding state within RecA (Menetski & Kowalczykowski, 1985b; Silver & Fersht, 1982). Data presented here identifies Gln194 as the NTP binding site "γ- phosphate sensor", in that mutations introduced at this residue disrupt all ATP induced RecA activities, while basal enzyme function is maintained. Additionally, we have dissected the parameters contributing to cooperative nucleoprotein filament assembly in the presence of cofactor. We show that the dramatic increase in the affinity of RecA for ssDNA in the presence of ATP is a result of a significant increase in the cooperative nature of filament assembly and not an increase in the intrinsic affinity of a RecA monomer for ssDNA.

Previous work using both mutagenesis and engineered disulfides to study the subunit interface of the RecA protein has demonstrated the importance of Phe217

for the maintenance of both the structural and functional properties of the protein (Skiba & Knight, 1994; Logan *et al.*, 1997; Skiba *et al.*, 1999) . A Phe217Tyr mutation results in a striking increase in cooperative filament assembly. In this work, we identify Phe217 as a key residue within the subunit interface and clearly show that Phe217 is required for the transmission of ATP mediated allosteric information throughout the RecA nucleoprotein filament.

The human Rad51 (hRad51) protein, like its bacterial homolog RecA, catalyzes genetic recombination between homologous single and double stranded DNA substrates. This suggests that the overall process of homologous recombination may be conserved from bacteria to humans. Using IAsys biosensor technology, we examined the effect of ATP on the binding of hRad51 to ssDNA. Unlike RecA, we show that hRad51 binds cooperatively and with high affinity to ssDNA both in the presence and absence of nucleotide cofactor. These results show that ATP plays a fundamentally different role in hRad51 *vs.* RecA mediated processes.

In summary, through the work presented in this dissertation, we have defined the critical molecular determinants for ATP mediated allosteric regulation within RecA. Furthermore, we have shown that ATP is not utilized by Rad51 in the same manner as shown for RecA, clearly defining a profound mechanistic difference between the two proteins. Future studies will define the requirement for ATP in hRad51 mediated processes.

Table of Contents

List of Tables

List of Figures

List of Abbreviations

ADP-AlF$_4^-$	adenosine diphosphate aluminum fluoride
ATPγS	adenosine 5´-O-(3-thiophosphate)
β-ME	β-mercaptoethanol
CHT	ceramic hydroxyapatite
ds	double stranded
DTT	dithiothreitol
DSB	double stranded break
EDTA	ethylenediaminetetraacetic acid
hRad51	human Rad51
IPTG	isopropyl-β-D-thiogalactopyranoside
jm	joint molecule
ScRad51	S. cerevisiae Rad51
SDS	sodium dodecyl sulfate
ss	single stranded
SSB	single stranded binding protein
MMS	Methyl methanesulfonate
nc	nicked circular
nt	nucleotide
NTPs	nucleoside triphosphates

PEI   polyethylenimine

RPA   replication protein A

Chapter I

Introduction and Literature Review

Homologous genetic recombination is a highly complex and absolutely critical process, fundamental to the existence of all living organisms. Some recombinational events result in the generation of genetic diversity within an organism, while others function to repair DNA damage encountered by the cell. Recombinational repair mechanisms are a major pathway by which cells repair DNA, and in this way, the processes of recombination and DNA repair are very closely related.

Over 30 years of scientific investigation, utilizing both genetic and biochemical approaches, has provided insight into the processes of recombination and recombinational DNA repair. As a result, a large number of genes and gene products have been shown to be essential to these processes. In *E. coli*, the *recA* gene was initially identified as a result of a mutation that led to a 50,000 fold reduction in conjugal recombination (Clark & Margulies, 1965). Subsequently, the RecA protein was shown to be essential for the repair of UV damage in DNA and in nearly every other aspect of recombination, providing the first link between recombination and DNA repair. Furthermore, RecA is highly conserved among prokaryotes. Homology among 64 bacterial RecA proteins ranges from 54% to 100%, with 105 amino acids reported as "invariant" (Roca & Cox, 1997). Extensive biochemical studies have defined RecA as a multifunctional enzyme,

which acts as the central component in both the regulation and catalysis of recombinational DNA repair (Bianco *et al.*, 1998; Cox, 1999; Kowalczykowski *et al.*, 1994; Roca & Cox, 1990; West, 1992). RecA is a 352 amino acid protein (M_r=37,842 Da) which has been shown to both bind and hydrolyze ATP as well as other nucleoside triphosphates (NTPs). It has also been shown to bind to both single-stranded (ss) and double-stranded (ds) DNA and can promote the ATP dependent annealing of complementary single-stranded-DNA molecules. It forms regular helical filaments both in the presence and absence of DNA. Importantly, RecA has been shown to catalyze the processes of homologous pairing, strand exchange and branch migration; the critical central reactions of recombination. RecA also plays a pivotal role in the induction of the SOS response, by catalyzing the cleavage of the LexA repressor in response to DNA damage. This event results in the activation of more than 20 genes, including *recA*, which are involved in DNA repair.

One of the first models for homologous recombination was proposed by Holliday in 1964 (Holliday, 1964) (Figure 1A). Holliday proposed that recombination and the exchange of DNA strands took place between two dsDNA substrates, both of which had a break or nick in one of the strands. A symmetric invasion and exchange of DNA strands was shown to produce a symmetric region of heteroduplex DNA, as well as a "crossover structure", termed a Holliday junction. Cleavage of the Holliday junction in a specific orientation results in the formation of recombinant products. Additional models of recombination which differ in the designation of the initial DNA substrates

Figure 1.

A   B   C

OR

OR

OR
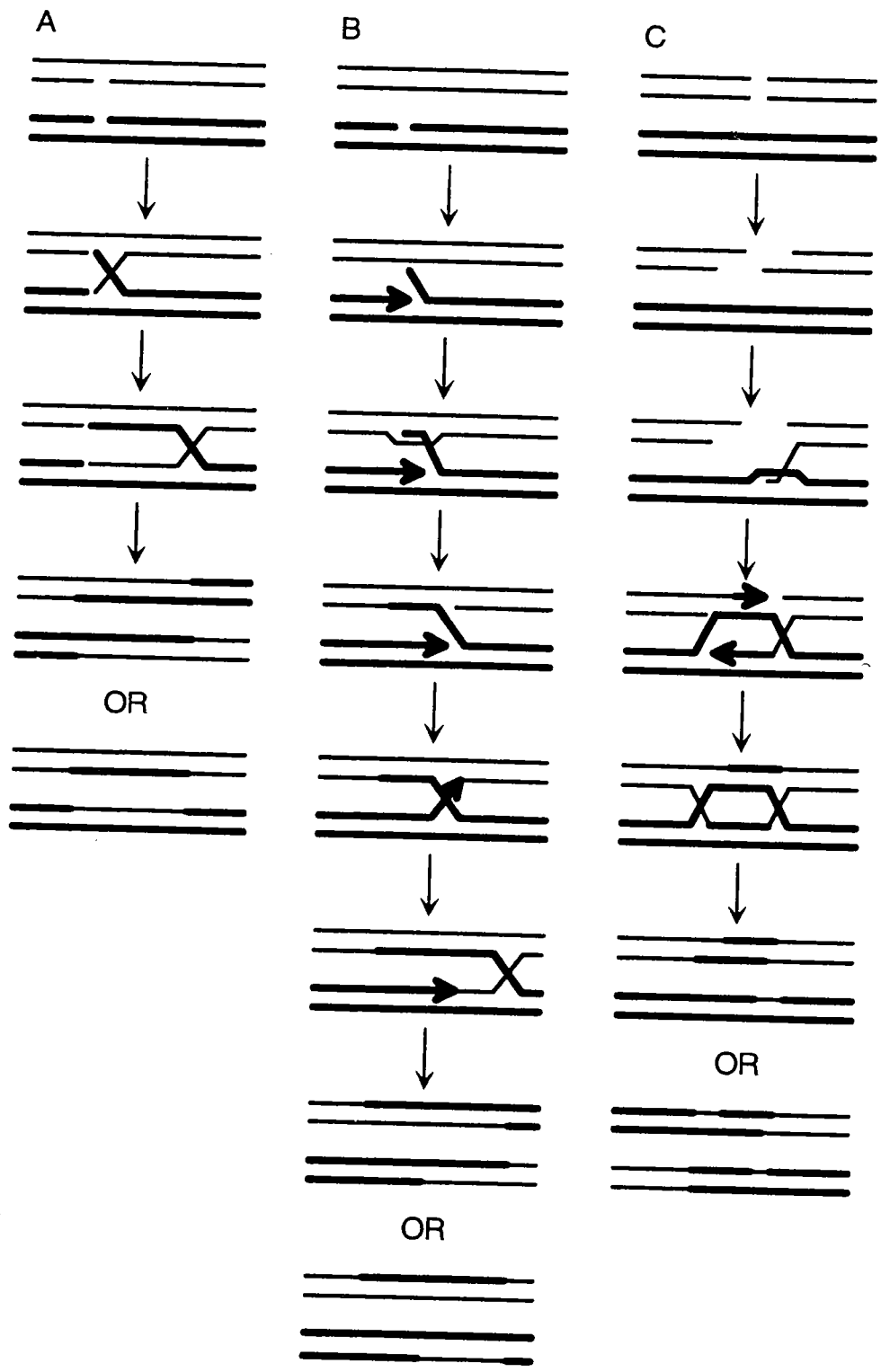
Figure 1. **Models of Genetic Recombination.** **(A)** Holliday Model **(B)** Messelson-Radding Model **(C)** Double-Strand Break Repair Model. Arrows in the panels indicate DNA synthesis. From Kowalczykowski, S., *et al.* (1994). *Microbiol Rev* **58**(3), 401-465.

have been proposed, however, the central steps of the Holliday model remain unchanged. Meselson and Radding proposed a model in which recombination is initiated at a ssDNA break (Figure 1B) (Meselson & Radding, 1975). Strand invasion and exchange results in asymmetric regions of heteroduplex DNA, followed by DNA replication to repair the break. The double strand break repair model proposes that recombination is initiated at dsDNA breaks (Figure 1C) (Resnick, 1976; Szostak *et al.*, 1983). In this model one of the DNA strands invades the homologous region in the complement, creating a D-loop. The region of heteroduplex DNA is extended by DNA synthesis, which is primed by the 3' end of the break, using the intact homolog as a template to repair the DNA.

In retrospect, recombination has been shown to occur between each of the substrates proposed above, under different conditions; at ssDNA nicks, at ssDNA gaps and at dsDNA breaks. Although the chromosome of *E. coli* is circular, each of these substrates can be encountered by the cell through a variety of events. A ssDNA nick can arise from enzymatic cleavage of the DNA, or from the action of free radicals generated during metabolism. A ssDNA gap can arise as a direct result of the DNA repair process. For example, if a primary lesion, such as a pyrimidine dimer, is not excised by RecA-independent processes (such as nucleotide excision repair) and the chromosome replicates, the replication machinery encounters the DNA damage and collapses. Replication is restarted beyond the lesion, leaving a ssDNA gap. Repair of the gap occurs through homologous pairing of the damaged strand with its complementary strand on the opposite side of the replication fork.

Double-stranded DNA breaks (DSBs) are encountered by the cell under a variety of circumstances. They can occur following the introduction of linear dsDNA during conjugation or transduction, resulting in recombination events between the linear double-stranded "donor" and the supercoiled "recipient" chromosome. Double strand breaks can also result from chemical or physical insults to the DNA, such as exposure to ionizing radiation. More commonly, a dsDNA break can occur as a consequence of normal cellular processes. For example, if the replication fork encounters a ssDNA nick in either the leading or lagging strand, a DSB is generated. If left unrepaired, DSBs are lethal to the cell, and it is at these sites that the recombination machinery is activated to repair the breaks. The repair of single-stranded gaps and double-stranded breaks constitutes the process of post-replicative or "recombinational" DNA repair. In *E. coli*, genetic studies have demonstrated a role for many proteins in the repair of DSBs including RecA, RecBCD, single-stranded binding protein (SSB), DNA polymerase I, DNA gyrase, DNA ligase, RuvA, B and C as well as many others. Figure 2 illustrates the double strand break repair model.

The recombination reaction in the repair of double strand breaks can be separated into 4 definable biochemical steps: 1) initiation 2) homologous pairing and strand exchange 3) DNA heteroduplex extension and 4) resolution (Kowalczykowski, 1991; Kowalczykowski & Eggleston, 1994). Initiation of recombination at a DSB requires the resection of the dsDNA substrate to produce a ssDNA tail. In *E. coli*, the RecBCD enzyme, which possesses both helicase and nuclease activity is responsible for this function. Other helicases and/or

Figure 2.
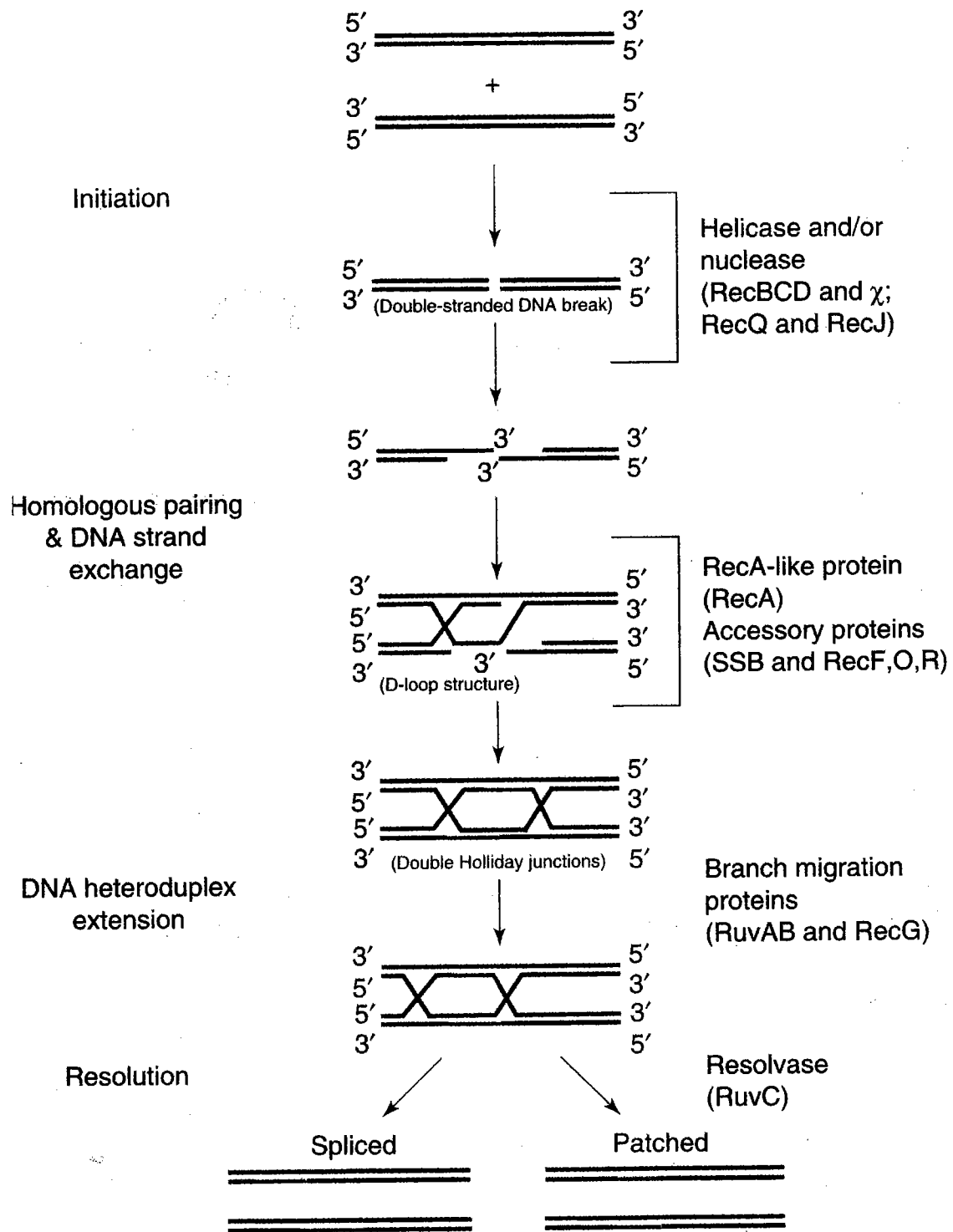
Figure 2. **General model for double-strand break repair (DSBR).** Proteins involved at each step are indicated in parenthesis. Light blue lines indicate regions of newly synthesized DNA. From Kowalczykowski, S. (2000). *TIBS* **25**, 156-165.

nucleases, such as RecE (Joseph & Kolodner, 1983), RecQ (Umezu *et al.*, 1990) and RecJ, (Lovett & Kolodner, 1989) may also function at this step. Following the generation of a 3' tail, RecA assembles cooperatively, in a 5'→3' direction onto the ssDNA forming a RecA-ATP-ssDNA nucleoprotein filament. This nucleoprotein filament, also termed the presynaptic complex, is the active species in recombination. Single-stranded binding protein (SSB) facilitates nucleoprotein filament formation by removing secondary structure within the ssDNA. Other factors such as the RecBCD and the RecF, RecO and RecR proteins also function at this step by helping to load RecA onto the ssDNA (Shan *et al.*, 1997). The presynaptic complex then invades the recipient dsDNA molecule. Initial, non-homologous contacts are made, followed by an efficient and directional search for homology, catalyzed by the RecA filament. Once the two DNA molecules are homologously aligned, DNA strand exchange occurs. Initially paranemic joint molecules, which require the protein for stability, are formed. If there is a homologous DNA end, the heteroduplex DNA becomes inherently stabilized by base pairing, forming a plectonemic joint molecule. Following joint molecule formation, pairing of the remaining donor and recipient strands produces a crossover structure known as a Holliday junction. Branch migration of this crossover intermediate, or DNA heteroduplex extension, is catalyzed by the RuvAB heterodimer, and extends the region of transferred, heteroduplex DNA. The final step in the process is resolution, which involves the nucleolytic cleavage of the Holliday junction by the RuvC protein, resulting in recombinant DNA products.

Strand exchange has been reconstituted *in vitro* utilizing a variety of DNA substrates (Figure 3). The use of supercoiled DNA and linear ssDNA as substrates results in the formation of joint molecules containing a D-loop (Figure 3A). If linear dsDNA and gapped circular dsDNA are utilized in the reaction, nicked circular and linear dsDNA with a ssDNA overhang are generated (Figure 3C). The most common DNA substrates used in the *in vitro* strand exchange reaction are linear dsDNA and single-stranded circular DNA, which generate gapped circular dsDNA and linear ssDNA products (Figure 3B). In all of these reactions, substrates, intermediates and products can be resolved by gel electrophoresis. This *in vitro* reaction requires that one of the substrates is linear, and therefore possesses a DNA end. Secondly, one substrate must have a region of ssDNA and finally, the two substrates must share homology. RecA has been shown to efficiently catalyze the *in vitro* strand exchange reaction, which is central to the process of recombination.

The strand exchange reaction does not require an input of energy, as the reaction is isoenergetic; i.e. for each base pair broken during the search for homology, another is formed (Cox, 1994; Roca & Cox, 1997). Despite the fact that a significant amount of ATP is hydrolyzed during the strand exchange reaction, hydrolysis of a nucleotide cofactor is not required for DNA strand exchange to occur. Using ATPγS, a non-hydrolyzable analog of ATP (Menetski *et al.*, 1990), as well as ADP-AlF$_4^-$ (Kowalczykowski & Krupp, 1995), it was shown that both homologous pairing and strand exchange occur. Additionally, a RecA mutant, Lys72Arg, which possesses a mutation of the catalytic lysine within the Walker

Figure 3.

A
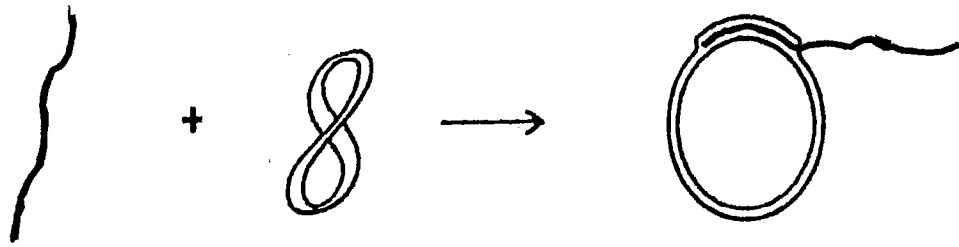
B
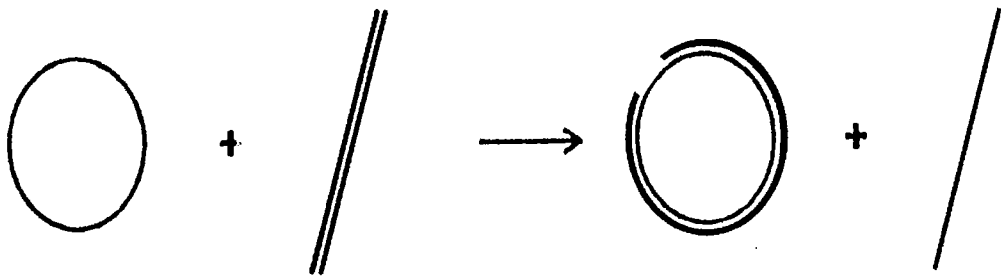
C
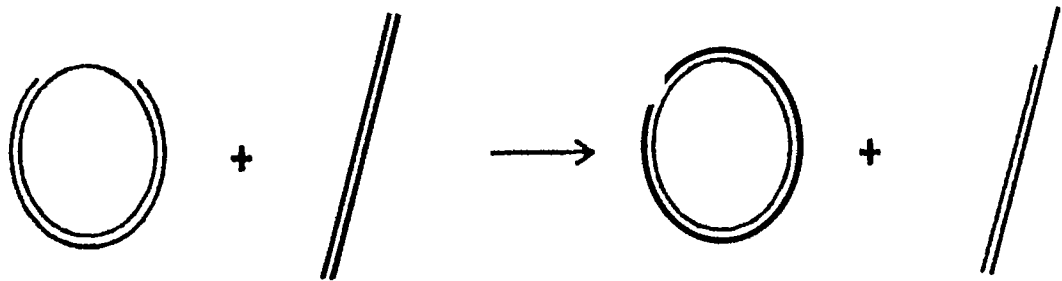
Figure 3. DNA substrates used in the homologous *in vitro* strand exchange reaction promoted by the RecA protein. (A) Linear single-stranded (ss) DNA and supercoiled double-stranded (ds) DNA substrates and D-loop structure product. (B) Circular ssDNA and linear ds DNA substrates. Products are nicked circular dsDNA and linear ssDNA. (C) Gapped duplex DNA and linear dsDNA substrates. Products are nicked circular dsDNA and linear dsDNA with a ssDNA tail. From Kowalczykowski, S. (1991). *Annu Rev Biophys Biophys Chem* **20**, 539-575.

A-box (GXXXXGKT) has been shown to bind but not hydrolyze ATP, and promotes the efficient formation of joint molecules (Rehrauer & Kowalczykowski, 1993). Although RecA catalyzes the formation of joint molecules and the reaction undergoes branch migration in the presence of ATPγS, products are not formed in the absence of ATP hydrolysis (Kowalczykowski & Krupp, 1995; Rehrauer & Kowalczykowski, 1993). Although ATP does not appear to play a role as an energy source to drive the search for homology, it plays a critical role in regulation of the process. ATP acts as a critical allosteric effector of RecA. In the absence of any nucleotide cofactor, RecA exhibits a low affinity for ssDNA (Menetski & Kowalczykowski, 1985b; Silver & Fersht, 1982). Upon binding ATP, a high affinity ssDNA binding state is induced, resulting in the activation of the protein for all of its functions (Menetski & Kowalczykowski, 1985b; Silver & Fersht, 1982). Upon hydrolysis of ATP, ADP supports the return back to the inactive, low affinity ssDNA binding state of RecA. By regulating the formation as well as the disassembly of the presynaptic complex, ATP regulates the initiation of the process of strand exchange. It has also been shown that RecA assembles and dissassembles from opposite ends of the nucleoprotein filament. As a result, filament formation is a highly dynamic process. However, the rates of ATP hydrolysis are constant at each end of the nucleoprotein filament. Lindsley and Cox (1990) concluded that this treadmilling-like process of assembly and dissasembly does not necessarily drive the strand exchange reaction and hypothesizes that its function may be to recycle RecA within the cell.

Further evidence suggests that RecA can exist in 2 distinct conformations. Nucleoprotein filaments formed in the absence of nucleotide cofactor can be visualized by electron microscopy and exhibit a pitch of 64Å with an axial rise per nucleotide of 2.1Å. There appear to be 30 nucleotides per turn of the helix in this "collapsed" filament. In contrast, filaments formed in the presence of ATP or ATPγS are extended, with a 95Å pitch, 6 monomers/turn and a rise per base pair of 5.1Å (Egelman & Stasiak, 1986; Stasiak & Egelman, 1994). Furthermore, limited proteolytic digestion of the RecA protein indicates that large conformational changes take place in the presence of a nucleotide cofactor (Kobayashi *et al.*, 1987). Finally, Stole and Bryant (1994) have constructed a mutant RecA protein (His163Trp) and have used this mutant to follow structural changes induced in the presence of ATP (Stole & Bryant, 1994). Taken together, these data provides strong evidence for the hypothesis that RecA can exist in one of two conformational states: an inactive state, induced by the absence of cofactor or in the presence of ADP and an activated state, induced in the presence of ATP.

An additional role for ATP hydrolysis may be to allow strand exchange to bypass regions of heterology within the DNA. In the presence of ATP, RecA can promote strand exchange across fairly large regions of heterology. In the presence of ATPγS, however, even small regions of heterology disrupt the ability of RecA to promote strand exchange. Although ATP hydrolysis is not required for efficient joint molecule formation by RecA, it is required for extensive DNA heteroduplex extension and resolution of intermediate joint molecules to nicked circular and single-stranded linear DNA products hydrolysis (Kowalczykowski

& Krupp, 1995; Rehrauer & Kowalczykowski, 1993).

In the absence of DNA, RecA exists as a heterogeneous population of oligomeric species including monomers, hexamers, protein filaments of varying lengths, as well as bundles of filaments. This has been shown both by electron microscopy and light scattering techniques (Brenner *et al.*, 1988; Ruigrok & DiCapua, 1991; Wilson & Benight, 1990) as well as by gel filtration chromatography (Logan & Knight, 1997). The presence of magnesium supports self-association into filaments, while the presence of ATP disrupts bundles and decreases the length of filaments (Brenner *et al.*, 1988; Logan & Knight, 1997). Self-association into long filaments as well as bundles is concentration dependent (Brenner *et al.*, 1988; Logan *et al.*, 1997; Ruigrok & DiCapua, 1991; Wilson & Benight, 1990).

The crystal structure of the RecA monomer and polymer was solved to 2.3Å resolution in the absence of a nucleotide cofactor (Story *et al.*, 1992). Additionally, the RecA-ADP structure was also solved by diffusing ADP into preformed crystals of RecA (Story & Steitz, 1992) (Figure 4). The RecA monomer structure consists of 3 domains: a small amino terminal domain, a large central domain and a smaller carboxy-terminal domain. In the structure, there are 2 disordered regions, corresponding to amino acids 156-164 (Loop L1) and amino acids 195-209 (Loop L2). Although the primary (ssDNA) and secondary (dsDNA) binding domains of RecA have not been definitively identified to date, several lines of evidence implicate these disordered regions in DNA binding.

Both Loops L1 and L2 are positioned along the filament axis where DNA is proposed to bind within the helical filament (Figure 5). Crosslinking studies have identified determinants within both L1 and L2 which crosslink to both single and double-stranded DNA (Malkov & Camerini-Otero, 1995; Morimatsu & Horii, 1995; Morimatsu et al., 1995). It has also been shown that His163, which lies within L1 is protected from chemical modification in the presence of dsDNA (Stole & Bryant, 1994). Proteolytic digestion of RecA in the presence of ssDNA protects a fragment of RecA which encompasses Loop 2 (Gardner et al., 1995). Moreover, using fluorescence quenching, Phe203, the central aromatic residue of L2, has been shown to interact directly with DNA (Maraboeuf et al., 1995). Further, a 20 amino acid peptide which includes the entire sequence of L2 has been shown to adopt a β-sheet conformation in the presence of a nucleotide cofactor. This peptide was also shown to bind both single and double-stranded DNA and promote the formation of joint molecules (Voloshin, 1996). Taken together, these data strongly implicates L2 as the primary single-stranded DNA binding site within RecA, with L1 possible serving as the secondary or double-stranded DNA binding site.

The crystal structure has also provided insights into the determinants of nucleotide binding and hydrolysis (Story et al., 1993). Asp100, Tyr103 and Gly265 all make contacts with the adenine base. The α and β-phosphates are bound by the Walker A nucleotide binding motif, found in many nucleotide binding proteins, which is positioned from residues 66-73 within RecA. Asp144 and Glu96 play critical roles in catalysis. Asp144, within the Walker B nucleotide

Figure 4.
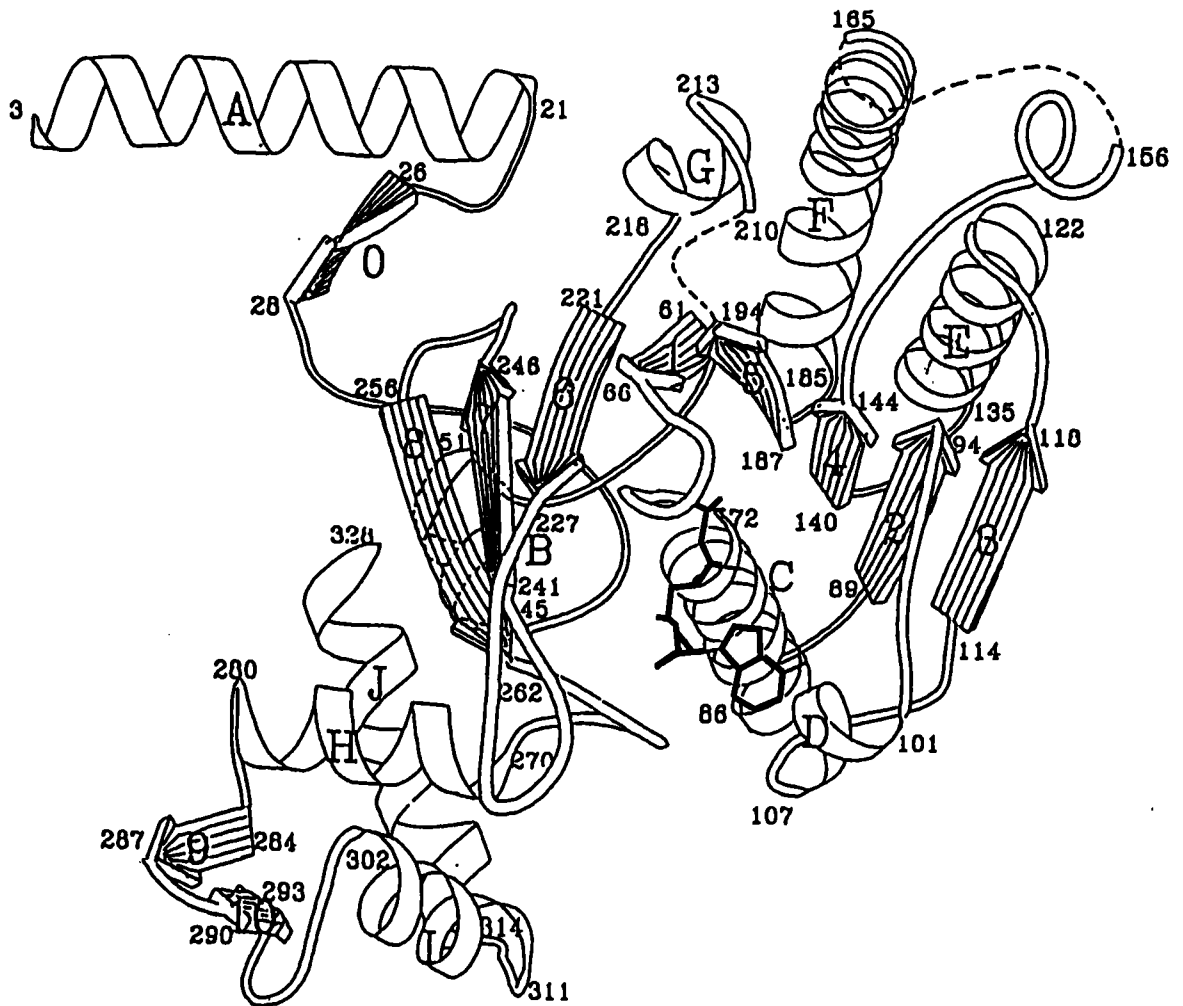
Figure 4. Crystal structure of the RecA monomer. Disordered loop L1 (156-165) and L2 (195-210) are indicated by dashed lines. ADP is shown in red. From Story, R. and Steitz, T. (1992). *Nature* **355**, 318-325.

Figure 5.

Figure 5. Space filling model of a RecA trimer showing the position of disordered loops L1 and L2 along the inner surface of the RecA filament. This view depicts the inner surface of one half of a turn of the helical RecA oligomer. Main chain α- carbons are shown in white or yellow for alternating RecA monomers. Side chain atoms for residues 67-69 and 226-227 are shown in green. Residues which flank disordered loops L1 (Glu156 and Gly165) and L2 (Ile195 and Thr210) are shown in blue and labeled 1 and 2 respectively. ADP is shown in red. From Konola, J. *et al.* (1994) *J. Mol. Biol.* **237**, 20-34.

binding motif, coordinates Mg^{+2} through a water molecule. Glu96 is the suggested catalytic residue within RecA, which activates a water molecule for in-line nucleophilic attack on the γ-phosphate during ATP hydrolysis. Additionally, Gln194, which immediately precedes disordered loop L2, is implicated in the allosteric regulation of ssDNA binding by RecA (Story & Steitz, 1992; Chapter III).

Monomers of RecA within the crystal are arranged in a helical filament with 6 monomers per turn of the helix. However, the pitch of the helix within the crystal (82Å) is slightly compressed relative to nucleoptrotein filaments formed in the presence of ATPγS (95Å) (Egelman & Stasiak, 1986; Stasiak *et al.*, 1981). The arrangement of monomers into a helical filament within the crystal has allowed identification of key domains that make up the subunit interface. In one region of the interface, Lys216, Phe217 and Arg222 all project outward towards the neighboring monomer (Figure 6) and both genetic and biochemical studies have shown that these positions are critical for RecA function (Skiba & Knight, 1994; Logan *et al.*, 1997; Skiba *et al.*, 1999). Other areas within RecA, which include Lys6 and Arg28, have been implicated in monomer-monomer interactions. Mutations at these positions severely disrupt filament formation giving rise to small oligomeric species including monomers, dimers and trimers (Eldin *et al.*, 2000).

Since RecA plays such a pivotal role in the process of recombination in *E. coli*, much time and effort was put into searching for eukaryotic homologs. In

Figure 6.
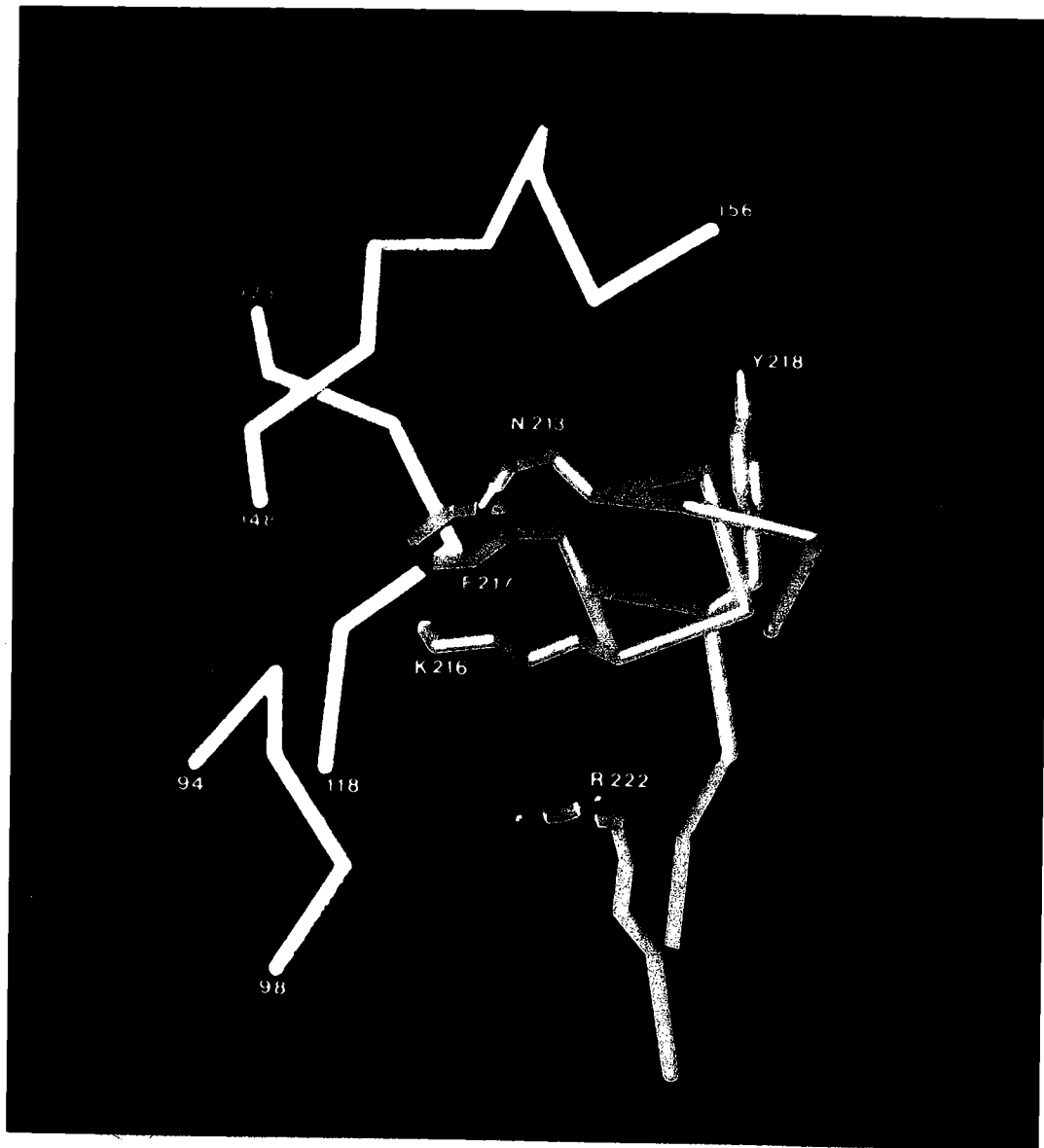
Figure 6. Position of residues at the subunit interface of RecA. Residues Asn213, Lys216, Phe217, Tyr218 and Arg222 are colored according to atom type: carbon-yellow, nitrogen-blue, oxygen-red. Lys216, Phe217 and Arg222 are critical for oligomerization. The surface of the opposing monomer is white and shows an α- carbon trace of residues 94-98, 118-123 and 148-156. From Skiba, M. *et al.* (1994). *J Biol Chem* **269**, 3823-3828.

Saccharomyces cerevisiae, genes of the *RAD52* epistasis group, *RAD50, RAD51, RAD52, RAD54, RAD55, RAD57, RAD59, MRE11* and *XRS2* were initially identified by their sensitivity to ionizing radiation (Petes *et al.*, 1991). Subsequently, they were shown to be sensitive to the DNA damaging agent MMS and to be defective in meiotic recombination. These genes have been implicated in an array of recombination events including mitotic and meiotic recombination as well as double strand break repair. Consistent with a role in meiotic recombination, mammalian Rad51 is expressed at high levels in the testes and ovaries (Bezzubova *et al.*, 1993; Morita *et al.*, 1993; Shinohara *et al.*, 1993) and is localized within distinct subnuclear foci during prophase I of meiosis (Barlow *et al.*, 1997), the stage at which crossing over occurs. These foci can also be induced in mitotic cells following the generation of DSBs by exposure to ionizing radiation (Haaf *et al.*, 1995). Additionally, *rad51* and *rad52* mutants accumulate DSBs (Shinohara *et al.*, 1992), further suggesting a role for Rad51 in double strand break repair.

In 1992, identification of *S. cerevisiae* Rad51 (*Sc*Rad51) as a RecA homolog led to the subsequent isolation and characterization of RecA-like recombination proteins in higher eukaryotes including *Xenopus laevis* (Maeshima *et al.*, 1995) chicken (Bezzubova *et al.*, 1993), mouse (Morita *et al.*, 1993; Shinohara *et al.*, 1993) and human (Shinohara *et al.*, 1993). This suggests an overall conservation of the processes of recombination from bacteria to humans. Sequence alignment of the *E. coli* RecA, *Sc*Rad51 and human Rad51 (hRAD51) proteins reveals that the proteins share significant homology within a 207 amino acid "core domain"

Figure 7.

A.

Escherichia coli RecA

1 33   240   352

Saccharomyces cerevisiae Rad51p

1 74   154   374 400

Homo sapiens RAD51

1 17   96   314 339

B.

RecA
E. coli

51%

59%

RAD51
H. sapiens

83%

Rad51p
S. cerevisiae
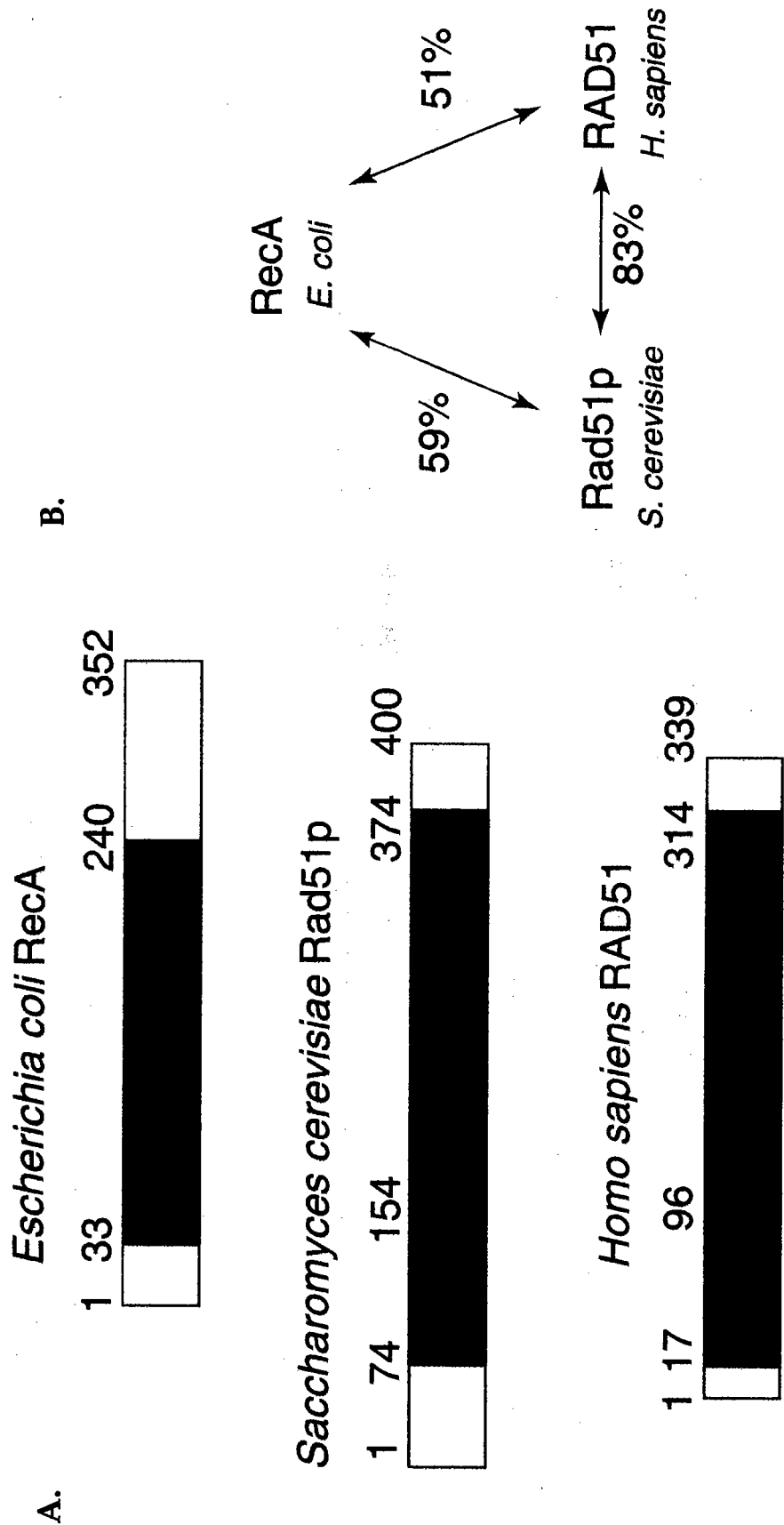
Figure 7. Comparison of the homology between *E. coli* RecA, yeast Rad51 (*Sc*Rad51) and human Rad51 (hRad51). **(A)** Schematic of the domain structures of these proteins. The "central core" domain is shown in red. Sequences conserved between Rad51 proteins are shown in blue. Non-homologous sequences are shown in white. **(B)** The percentage of homology between the proteins within the core domain. Both identical and similar amino acids are indicated. From Baumann, P. and West, S. (1998). *TIBS* **23**, 247-251.

Figure 8.

	Walker A	Walker B
RecA	$_{66}$GPESSGKT$_{73}$	$_{140}$LIVVD$_{144}$
scRad51	$_{185}$GEFRTGKT$_{192}$	$_{276}$LIVVD$_{280}$
hRad51	$_{127}$GEFRTGKT$_{134}$	$_{218}$LLIVD$_{222}$

RecA	Proposed Function	scRad51	hRad51
K72	ATP hydrolysis	K191	K133
E96	Activates H_2O molecule during ATP hydrolysis	E221	E163
D144	Coordinates Mg^{+2} ion	D280	D222
Q194	γ-phosphate sensor	Q326	Q268
G211/212	critical structural elements	G246/247	G288/289
F217	mediates cross-subunit allosteric information	H253	H294

Figure 8. Comparison of the conserved sequences between RecA, *Sc*Rad51 and hRad51. Conserved sequences between RecA *Sc*Rad51 and hRad51 include the Walker A and B nucleotide binding motifs **(A)** and catalytic residues **(B)**. From [1]Story, R., *et al.* (1993) *Science* **259**, 1892-1896, [2]Shinohara, A., *et al.* (1992). *Cell* **69**, 457-470 and [3]Yoshimura, Y., *et al.* (1993) *Nuc Ac Res* **21**, 1665.

(Baumann & West, 1998; Shinohara *et al.*, 1993; Yoshimura *et al.*, 1993) (Figure 7A). This suggests that functions common to all three proteins, such as ATP binding and hydrolysis as well as DNA binding are defined by determinants that lie within this region. Both Rad51 proteins contain an N-terminal extension not found in RecA, while RecA possesses a C-terminal domain not present in its eukaryotic homologs. Presumably, these divergent domains define functions specific to the particular protein, such as species specific protein-protein interactions. The yeast and human Rad51 proteins show 59% and 51% overall homology with the RecA protein, respectively. *Sc*Rad51 and hRad51 share an 83% overall homology (Figure 7B). The Walker A and B nucleotide binding motifs of all three proteins are highly conserved, along with other important catalytic and structural residues (Figure 8). Lys72, the invariant lysine within the P-loop element, corresponds to Lys191 and Lys133 in yeast and human Rad51, respectively. Similarly, ATP binding site catalytic residues Glu96 and Asp144, as well as Gln194, the "γ-phosphate sensor" are conserved in both yeast (Glu221, Asp280, Gln236) and human Rad51 proteins (Glu163, Asp222, Gln268). In addition to a significant degree of sequence homology, all three proteins form extended nucleoprotein filaments on DNA which show remarkable similarities. Using electron microscopy, RecA was shown to form a right-handed nucleoprotein filament on dsDNA with a pitch of 92Å. There are 6.2 monomers per turn of the protein helix which bind with a stoichiometry of 1 monomer per 3 base pairs. Additionally, RecA was shown to unwind and extend the dsDNA duplex, resulting in an increased axial rise per base pair from 3.4Å found in B-form DNA to 5.1Å when bound by RecA (Egelman & Stasiak, 1986; Stasiak *et al.*,

1981). In the presence of ATP, yeast Rad51 polymerizes onto dsDNA forming RecA-like nucleoprotein filaments also with 6.2 monomers/turn which bind with the same stoichiometry seen in RecA-dsDNA filaments. The pitch of the filaments (99Å) is slightly higher than that seen with RecA. Binding of ScRad51also extends the DNA to the same extent as in RecA (Ogawa *et al.*, 1993c). Likewise, filaments of hRad51 formed on dsDNA show conserved structural properties with RecA and yeast Rad51 nucleoprotein filaments (Benson *et al.*, 1994).

Both the yeast and human Rad51 proteins also share functional homologies with RecA. Like RecA, ScRad51 and hRad51 have been shown to bind and hydrolyze ATP in a ssDNA-dependent manner (Baumann *et al.*, 1996; Gupta *et al.*, 1997; Sung, 1994), bind to single and double-stranded DNA (Benson *et al.*, 1994; Gupta *et al.*, 1997; Shinohara *et al.*, 1992) and promote strand annealing as well as homologous pairing and strand exchange (Baumann *et al.*, 1996; Sung, 1994). Despite the apparent sequence, structural and functional similarities between RecA, ScRad51 and hRad51, genetic and biochemical studies have revealed that there are significant differences between the proteins. While ΔrecA bacteria and ΔRAD51 yeast are viable, disruption of RAD51 in mouse cells results in embryonic lethality suggesting an essential role in genome maintenance (Tsuzuki *et al.*, 1996). Additionally, despite their high degree of sequence homology, overexpression of human Rad51 is unable to rescue a ΔRAD51 deletion in yeast cells, suggesting profound mechanistic differences between the proteins (Shinohara *et al.*, 1993). Furthermore, although RecA binds to both

single and double-stranded DNA, it exhibits a much higher affinity for ssDNA (McEntee et al., 1981). It has been reported that the Rad51 proteins have comparable affinities for both single and double-stranded DNA (Baumann et al., 1996; Benson et al., 1994; Gupta et al., 1997; Sung, 1994), although a comprehensive biochemical comparison has not been reported for either hRad51 or ScRad51. The rates at which these proteins hydrolyze ATP are also dramatically different. RecA hydrolyzes ATP with a turnover rate of 30 min^{-1} (Kowalczykowski, 1991), while both ScRad51 and hRad51 hydrolyze ATP at a significantly reduced rate, k_{cat}= 0.7 min^{-1} (Sung, 1994) and 0.16 min^{-1} (Baumann et al., 1996; Gupta et al., 1997), respectively. Furthermore, all three proteins catalyze strand exchange, however there are important differences among the three. RecA catalyzes the *in vitro* strand exchange reaction efficiently in the absence of other cofactors, although the presence of SSB potentiates its action (Roman & Kowalczykowski, 1986). Both yeast and human Rad51, however, require the assistance of other proteins, such as RPA (Sugiyama et al., 1997; Sung & Robberson, 1995) Rad52 (Benson et al., 1998; New et al., 1998; Shinohara & Ogawa, 1997) or Rad54 (Petukhova et al., 1998) for certain DNA substrates. A particularly striking difference between RecA and yeast Rad51 was reported by Sung and coworkers (Sung, 1994). They examined the effect of a mutation in the invariant lysine within the P-loop motif within yeast Rad51 (Lys191Arg). The analogous mutation within RecA (Lys72Arg) confers a completely *rec*⁻, UV sensitive phenotype (Konola et al., 1994). In the *in vitro* strand exchange reaction, the Lys72Arg mutant protein supports limited strand exchange, catalyzing the

formation of joint molecules, but it does not support the conversion of these intermediates to products (Rehrauer & Kowalczykowski, 1993). In contrast, the yeast Lys191Arg mutant is functional *in vivo*, and is able to rescue the sensitivity of a Δ*RAD51* strain to the DNA damaging agent MMS when overexpressed (Sung & Stratton, 1996). Additionally, the Lys191Arg mutant protein shows no defect in its strand exchange abilities; i.e. it supports the formation of joint molecules as well as their conversion into nicked circular and linear ssDNA products. RecA also catalyzes strand exchange with a 5'→3' polarity, exactly the opposite of that reported for both yeast (Sung & Robberson, 1995) and human Rad51 (Baumann & West, 1997).

Extensive genetic and biochemical studies have shown that Rad51 mediated recombination in eukaryotes is dependent on multiple protein-protein interactions (Figure 9). In yeast, specific physical interactions have been demonstrated between Rad51 and many other proteins including RPA, Rad52 (Shinohara *et al.*, 1992), Rad54 (Clever *et al.*, 1997) and Rad55 (Johnson & Symington, 1995). Additional interactions between other members of this group have also been reported. Rad52 self associates (Hays *et al.*, 1995a) and interacts with RPA (Hays *et al.*, 1995b). Rad55 forms a heterodimer with Rad57 (Johnson & Symington, 1995). Many of the same interactions have been observed within the human system, as hRad51 has been shown to specifically interact with hRad52 (Shen *et al.*, 1996), hRad54 (Golub, 1997) and hRPA (Golub *et al.*, 1998). The human equivalents of *Sc*Rad55 and *Sc*Rad57 have not yet been identified. Human Rad52 and human RPA also interact with one another (Park *et al.*, 1996).

Figure 9.
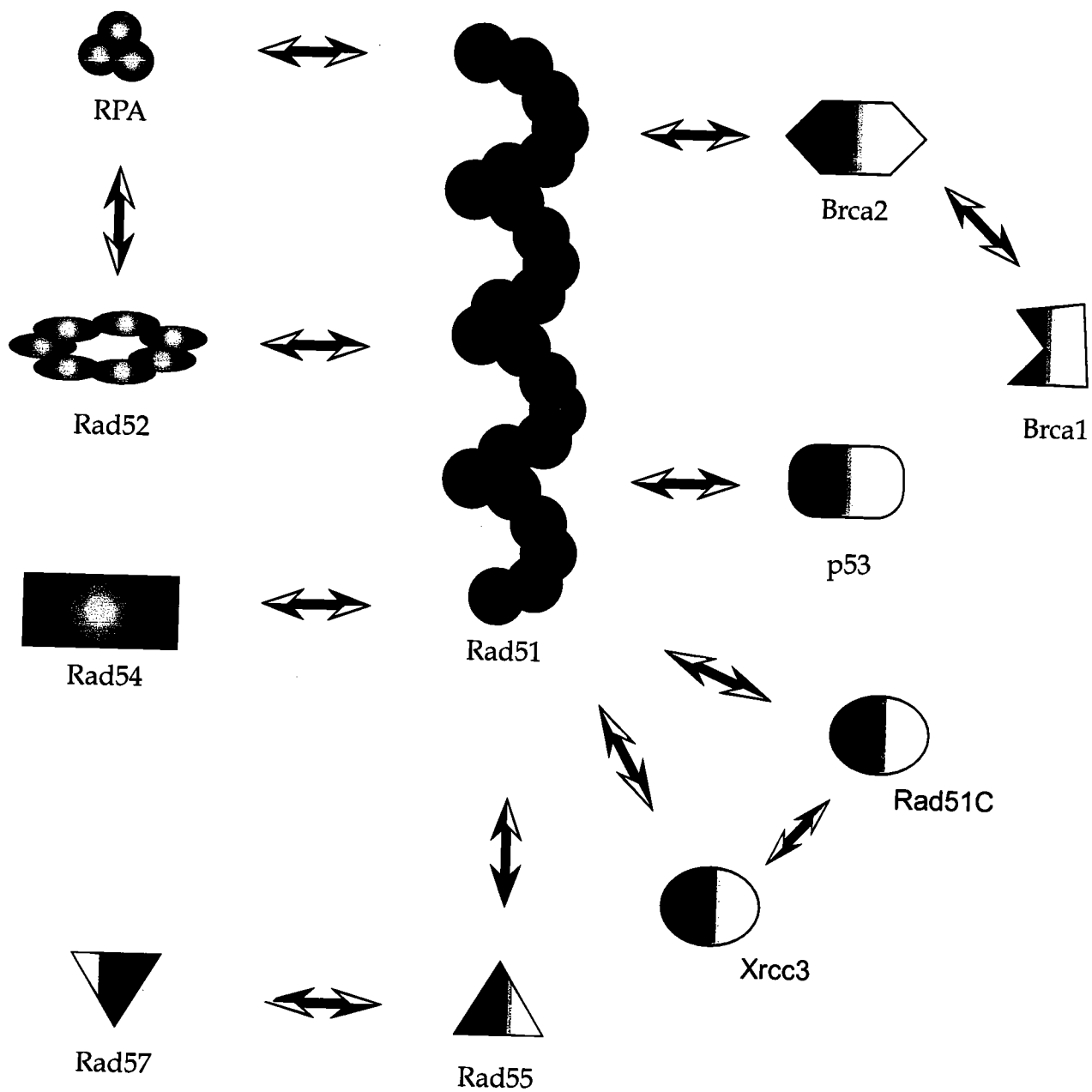
Figure 9. Physical interactions between Rad51 and other factors. Interactions demonstrated in both yeast and human systems are designated in yellow. Those seen only in yeast are represented in green, and human interactions are pink.

Several other interactions attesting to the increased level of complexity within mammalian systems have also been identified. Rad51 has been shown to interact specifically with BRCA2 (Sharan *et al.*, 1997). An interaction between hRad51 and BRCA1 has also been demonstrated using two-hybrid analysis (Scully *et al.*, 1997). Since BRCA1 and BRCA2 have been shown to form a complex (Chen *et al.*, 1998), it is unclear whether the interaction between hRad51 and BRCA1 is direct, or if it occurs indirectly through BRCA2. Rad51 is also specifically phosphorylated by c-Abl (Yuan *et al.*, 1998). Further, a Rad51-p53 interaction has been characterized (Sturzbecher *et al.*, 1996). These interactions provide specific evidence linking Rad51 to DNA damage check points and cell cycle control within the cell.

The specific role of each of these proteins and their involvement in the recombination process is currently a topic of intense study within the field. The array of protein-protein interactions that are involved in the recombination process suggests that these proteins either function together as part of a large multiprotein "recombinosome" or, more likely, that the temporal formation of smaller, specific protein complexes may drive the recombination reaction. Current biochemical characterization of each of these eukaryotic proteins has provided some insight into their specific roles during recombination.

Both yeast and human Rad51 have been shown to promote the strand exchange reaction, although with very low efficiency (Benson *et al.*, 1998; New *et al.*, 1998; Petukhova *et al.*, 1998). Joint molecule formation by Rad51 occurs at a

stoichiometry of 1 monomer per 3 nucleotides of ssDNA. Increasing or decreasing this ratio, even slightly, severely inhibits the reaction (Baumann & West, 1997). The fact that these proteins catalyze strand exchange so inefficiently suggests that either the *in vitro* system designed to look at these properties is sub-optimal, or that a required factor is missing. Since both yeast and human Rad51 have been shown to interact with many other proteins, the latter explanation is more likely. In fact, hRPA has been shown to stimulate the strand exchange reaction *in vitro*, by helping to remove secondary structure from the ssDNA (Baumann & West, 1997). Similar roles for *Sc*RPA (Alani *et al.*, 1998), as well as its bacterial homolog SSB (Kowalczykowski & Krupp, 1987) have been proposed. RPA and SSB may also function by binding the displaced single-strand during strand exchange, thereby preventing re-initiation (Ullsperger & Cox, 1995). Similarly, the presence of yeast or human Rad52 in the strand exchange reaction leads to a significant stimulation of joint molecule formation by Rad51 (Benson *et al.*, 1998; New *et al.*, 1998; Petukhova *et al.*, 1998). Incubation of Rad52 with ssDNA prior to the addition of Rad51 leads to the greatest level of stimulation, in both the yeast and human systems (Benson *et al.*, 1998; New *et al.*, 1998; Petukhova *et al.*, 1998). Consistent with these results, hRad51 and hRad52 have been shown to colocalize (Benson *et al.*, 1998) and Rad51 foci do not form in the absence of Rad52 (Benson *et al.*, 1998). Several mechanisms by which Rad52 may stimulate homologous pairing and strand exchange have been suggested (Benson *et al.*, 1998; New *et al.*, 1998; Petukhova *et al.*, 1998). Rad52 may act by helping to recruit Rad51 to the ssDNA, thereby allowing it to discriminate between single and double-stranded DNA. Likewise, Rad52 may function by

assisting in the assembly of a continuous Rad51 nucleoprotein filament, or by increasing the cooperativity of Rad51. Further characterization of the biochemistry of Rad52 and its interactions with Rad51 and other proteins will more clearly define its role in the process of recombination.

Although homologs of yeast Rad55 and Rad57 have not yet been identified in humans, a potential role for the ScRad55/57 heterodimer has been suggested. It has been shown that mutations in either RAD55 or RAD57 disrupt Rad51 focus formation in yeast (Gasior et al., 1998). Additionally, overexpression of Rad51 can suppress the X-ray sensitivity defects of a rad55 or rad57 mutant (Johnson & Symington, 1995). This suggests that Rad55/57 may function by recruiting Rad51 to the site of its action or potentiation of nucleoprotein filament formation, analogous to the functions of the E. coli RecF, RecO and RecR proteins (Johnson & Symington, 1995). It has also been suggested that Rad55/Rad57 may function in the same way as the RuvAB complex in E. coli (Hays et al., 1995a; Johnson & Symington, 1995).

A possible role for Rad54 in recombination is suggested by its homology to the Swi2/Snf2 family of DNA-dependent ATPases (Petukhova et al., 1998). This homology reveals that Rad54 contains the 7 sequence motifs characteristic of DNA helicases. hRad54 has been shown to complement a ΔRAD54 deletion in S. cerevisiae, suggesting a common function for the two proteins. This is the first demonstration in which a human protein complements the analogous yeast deletion in this system. Although a helicase activity has yet to be demonstrated

for either human or yeast Rad51, it has been shown that Rad54 stimulates the *in vitro* strand exchange reaction using linear single-stranded DNA and supercoiled substrates (Petukhova *et al.*, 1998). In this reaction, Rad51 alone is unable to promote the formation of D-loops, which are intermediates in this reaction. However, D-loops are efficiently formed in the presence of Rad54. These data suggests that Rad54 may indeed function as a helicase or a chromatin remodeler, providing the Rad51 nucleoprotein filament access to DNA in a higher order chromatin structure.

In humans, five Rad51 paralogs have been identified: Xrcc2, Xrcc3, Rad51B, Rad51C and Rad51D. Each of these proteins exhibits a unique set of interactions with one or more of the other paralogs, with both Xrcc3 and Rad51C interacting directly with hRad51 (Schild *et al.*, 2000). These proteins have been knocked out in chicken cell lines and each shows an increased sensitivity to DNA damage (Takata *et al.*, 2000). This suggests that these proteins function as part of a protein complex within a common pathway. It is not clear whether interactions between paralogs are mutually exclusive or if they assemble into a large complex that functions during repair and recombination. The identification of these interactions, along with those previously described between hRad51 and other factors, attests to the complexity of these pathways. Furthermore, it is likely that additional factors that play critical roles remain to be identified. The specific functions of each of the factors currently identified remains unclear. Further biochemical characterization of the functions of each of these proteins will provide significant insight into these complex processes. As the function of each

individual factor is more clearly defined, it will be possible to begin to reconstruct the temporal assembly of these multiple protein complexes, eventually leading to an efficient *in vitro* system with which to study hRad51 mediated DNA repair and recombination processes.

Chapter II

Materials and Methods

Materials

Labeled NTPs and dNTPs were from NEN. PEI cellulose chromatography plates were from J.T. Baker, Inc. Restriction enzymes, T4 DNA ligase, T4 polynucleotide kinase and Klenow DNA polymerase I large fragment were from New England Biolabs. Sequenase version 2.0 was from USB. Nitrocellulose filters were from Schleicher and Schuell. Superbroth and 2X YT media was purchased from Bio101, Inc., IPTG and ampicillin from Bioworld, a general protease inhibitor cocktail [40x contains 4-(2-aminoethyl)-benzenesulfonyl fluoride (8 mM), EDTA (4 mM), bestatin (0.5 mM), E64 (5.6 mM), leupeptin (4 mM), and aprotonin (0.3 mM)], lysozyme, ATPγS, ATP, phosphoenolpyruvate (PEP), pyruvate kinase, ssDNA cellulose, heparin agarose, ATP agarose, IPTG and mitomycin C were from Sigma. Ceramic hydroxyapatite was from BioRad. Oligonucleotides (biotinylated and non-biotinylated) were made using an ABI 392 DNA/RNA synthesizer. 5′-biotin phosphoramidite was from Glen Research. QuickChange mutagenesis kit was from Stratagene. LexA protein was a generous gift from Dr. John Little and Donald Shepley (Department of Biochemistry, University of Arizona). Biotinylated cuvettes were from Affinity Sensors. PD10 and Superose 6 columns were from Pharmacia.

Plasmids and DNA substrates

Wild type and all mutant *recA* genes are carried on plasmids in which *recA* expression is regulated by p*tac* (Skiba & Knight, 1994). Wild type RAD51 is carried on the pET15B (Novagen) in which hRad51 expression is regulated by the T7 promoter. The hRAD51 gene was cloned from a human testis cDNA library into pET15B by Dr. Sam Ganesan, using a method similar to that described by Benson *et al.* (Benson *et al.*, 1994). Substrates for strand exchange assays and electron microscopy (single-stranded circular and double-stranded φX174 DNAs) were from New England Biolabs, and phage M13 RV-1 single-stranded circular DNA was prepared as described (Zagursky & Berman, 1984).

Buffers

PBS-Tween buffer contains 10 mM Na_2HPO_4/NaH_2PO_4 (pH 7.4), 138 mM NaCl, 27 mM KCl and 0.05% Tween20. PBS-Tween-Mg buffer contains PBS-Tween buffer and 5 mM $MgCl_2$. R-buffer contains 20 mM Tris-HCl (pH 7.5), 5% glycerol, 5 mM β-ME and 0.1 mM EDTA. R-filtration buffer is R-buffer containing 30 mM NH_4Cl and 15 mM $MgCl_2$. ATP binding buffer contains 20 mM Tris-HCl (pH 7.5), 20 mM KCl, 10 mM $MgCl_2$, and 0.5 mM EDTA. TAE buffer contains 40 mM Tris-Acetate and 1 mM EDTA.

Mutagenesis

Mutations were introduced at position 194 using a modification of a previously described cassette mutagenesis procedure (Skiba & Knight, 1994).

Two 81 base oligonucleotides corresponding to the top and bottom strands encoding residues Thr186 to Asn213 were synthesized such that codon 194 read NNG/C and all other bases were the wild type *recA* sequence. Oligonucleotides were annealed and the resulting cassette was ligated into AflIII/MluI-digested pTRecA332, a derivative of pTRecA322 (Nastri & Knight, 1994) containing a unique AflIII site at position 187 and a unique MluI site at position 214. Plasmids were transformed into a Δ*recA* strain, DE1663ʹ (Nastri & Knight, 1994), and colonies selected on LB-ampicillin plates. Amino acid substitutions were determined by DNA sequence analysis.

Alanine scanning mutagenesis was performed using the QuickChange Mutagenesis kit with instructions supplied by the manufacturer. Several changes in the manufacturers protocol were made. A maximum of 7 base changes were made in the construction of each mutant. The length of the mutagenic oligonucleotides was increased, as was the number of cycles performed per reaction (increased to 25-30 cycles). These changes resulted in an increased efficiency of mutagenesis.

Recombinational DNA Repair Activity *in vivo*

The recombinational DNA repair activity of each mutant protein was determined using two genetic screens as described previously (Nastri & Knight, 1994) 1) cell survival in the presence of mitomycin C and 2) cell survival following exposure to different doses of UV light. Cell survival in the presence of the mutagenic agent mitomycin C was assayed by spotting 2 μl of a 1:40

diluted overnight culture of DE1663' carrying a copy of either the wild type, mutant RecA or negative control plasmid onto LB-Ampicillin plates containing either 0.3 or 0.6 µg/ml of mitomycin C. Plates were incubated overnight at 37°C and cell growth was assessed on a scale of 0-4, with a score of 0 being equivalent to the survival of the negative control and 4 maintaining wild-type like survival. For UV survival assays, a 1:40 diluted overnight culture of DE1663' bacteria carrying a copy of either the wild type, mutant RecA or negative control plasmid were streaked across LB-ampicillin plates. The plates were divided into 7 time zones (0-60 seconds) in 10 second intervals. Cells were exposed to $1.52 \, J/m^2/sec$ or $0.67 \, J/m^2/sec$ of UV light for the indicated amount of time. Plates were wrapped with aluminum foil and incubated overnight at 37°C and cell growth was assessed on a scale of 0-4, as described above.

Determination of the Size of Mutant RecA Protein Oligomers

The oligomeric distribution of wild type and mutant RecA proteins was determined using gel filtration chromatography as described previously (Logan *et al.*, 1997). Overnight cultures (5 ml) grown in 2xYT/ampicillin were used to inoculate 500 mls of 1/2x Superbroth/ampicillin. Cultures were grown at 37°C to $OD_{600} \approx 0.8$, IPTG was added to a final concentration of 1 mM and incubation was continued for an additional 3 hrs. Cells were harvested, resuspended in 10 ml of ice cold buffer (25% sucrose/0.25 M Tris, pH 7.5), quick frozen in liquid nitrogen and stored at -70 °C. Cell paste was thawed, diluted in half with dH_2O, lysozyme was added to a final concentration of 0.2 mg/ml and the mixture

stirred slowly on ice for 60 min. β-mercaptoethanol and EDTA were added to final concentrations of 0.5 and 2.0 mM, respectively, and the mixture stirred on ice for an additional 30 min. Brij-58 (3% stock in 50 mM Tris, pH 7.5) was added to a final concentration of 0.5%, followed by NaCl to a final concentration of 1.5 M, with continued stirring for 30 min after each addition. The mixture was centrifuged (20K rpm, 90 min), total protein was precipitated from the supernatant with 0.32 g/ml ammonium sulfate and collected by centrifugation (12K rpm, 30 min). The pellet was dissolved in R-buffer (20 mM Tris-HCl, pH 7.5, 5% glycerol, 5 mM β-mercaptoethanol, 0.1 mM EDTA) containing 50 mM NH_4Cl, dialyzed against the same, loaded onto a DE-52 column (25 ml bed volume) equilibrated in R-buffer/50 mM NH_4Cl and the protein was eluted with R-buffer/350 mM NH_4Cl. Protein was precipitated and centrifuged as above, resuspended in 2.5 ml of R-filtration buffer (R-buffer containing 30 mM NH_4Cl/15 mM $MgCl_2$) and was desalted using a PD-10 column (Sephadex G25, Pharmacia) equilibrated in the same buffer. RecA protein concentrations were determined using the Bio-Rad protein assay kit and by densitomitry using RecA standards with the BioRad FluorS MultiImager. A 30 μM sample of RecA was incubated with DNase (30 U) at room temperature for 5 min in R-filtration buffer containing 10 mM $CaCl_2$ in the presence or absence of ATPγS or ATP (0.5 mM) and loaded onto an Superose 6 column (21 ml bed volume; Pharmacia) equilibrated in R-filtration buffer with or without 0.5 mM ATPγS or ATP. The first 6 ml were collected as one fraction, and 200 μl fractions were collected subsequently. A 10 μl aliquot of every other fraction was loaded onto a 10%

SDS-polyacrylamide gel, stained with Coomassie Brilliant Blue and gels were scanned (BioRad FluorS MultiImager) to determine the percentage of RecA present in each fraction. The size of the RecA oligomers were estimated by comparison to protein standards of known molecular weight.

Purification of Wild Type and Gln194Mutant RecA Proteins

Wild type and mutant proteins (Gln194Ala, Gln194Glu and Gln194Asn) were purified using a previously described method (Konola *et al.*, 1995). Overnight cultures (400 ml) grown in 2xYT/ampicillin were used to inoculate 12L of 1/2x Superbroth/ampicillin. Cultures were grown at 37°C to $OD_{600} \approx 0.8$, IPTG was added to a final concentration of 1 mM and incubation was continued for an additional 3 hrs. Cells were harvested, resuspended in 100 ml of ice cold buffer (25% sucrose/0.25 M Tris, pH 7.5), quick frozen in liquid nitrogen and stored at -70 °C. Cell paste was thawed, diluted in half with dH_2O, lysozyme was added to a final concentration of 0.2 mg/ml and the mixture stirred slowly on ice for 60 min. β-mercaptoethanol and EDTA were added to final concentrations of 0.5 and 2.0 mM, respectively, and the mixture stirred on ice for an additional 30 min. Brij-58 (3% stock in 50 mM Tris, pH 7.5) was added to a final concentration of 0.5% with continued stirring for 30 min after addition. Soluble proteins were recovered following centrifugation (12,500 x g) and PEI was added to 1% (v/v). Proteins were eluted stepwise from PEI pellets with RecA eluting in the 300 mM $(NH_4)_2SO_4$ fraction. Proteins in the RecA-containing fraction were precipitated by addition of saturating $(NH_4)_2SO_4$. The resulting pellet was dissolved in R-

buffer/50 mM NH_4Cl and dialyzed against the same. Protein was loaded onto a

DE-52 column (25 ml bed volume) equilibrated in the same buffer and proteins

were eluted with a R/350 mM NH4Cl. The "bump" fraction, which contained

RecA protein, was precipitated by addition of $(NH_4)_2SO_4$. The resulting protein

pellet was dissolved in 2.5 ml of R-filtration buffer (+15 mM $MgCl_2$) and desalted

using a PD-10 column. The sample was loaded onto a Sephacryl S-1000 gel

filtration column (1.5 x 120 cm) equilibrated in R- filtration buffer with 15 mM

$MgCl_2$. Wild type RecA and the mutant proteins elute in pure form in the void

volume of this column. Fractions containing RecA were pooled and protein

precipitated as above. The precipitate was dissolved in R-buffer (200 - 400 ul)

and dialyzed extensively against the same. Glycerol was added to a final

concentration of 25% and samples (20 ul) were quick-frozen and stored at -70 °C.

Proteins were determined to be > 95% pure as judged by Coomassie stained gels.

The concentration of wild type RecA and mutant proteins was determined

spectrophotometrically using an extinction coefficient of $\varepsilon_{280} = 0.59$ mg^{-1}ml (21).

No exonuclease activity was detected in any of these preparations, even at

elevated concentrations of RecA (50 μM) in the nuclease assay. None of these

mutations has any deleterious effect on the overall folded structure or thermal

stability of the protein. Wild type RecA and each mutant protein showed

identical circular dichroism profiles and measurements of θ_{222}nm as a function of

temperature (5 - 90 °C) gave a $T_m = 53 \pm 1$ °C for all 4 proteins (data not shown).

Purification of Phe217Tyr Mutant RecA Protein

Phe217Tyr mutant RecA was purified essentially as described above for wt RecA. Purification on S-1000 alone was not sufficient to separate out contaminating proteins, therefore, following gel filtration chromatography on S-1000, fractions containing Phe217Tyr were pooled and precipitated with $(NH_4)_2SO_4$. The resulting pellet was resuspended in ATP binding buffer, and desalted using a PD-10 column equilibrated in the same buffer. The resulting fraction was incubated with ATP-agarose for 1 hour. The resin was washed extensively with ATP binding buffer, and pure Phe217Tyr was eluted with ATP binding buffer containing 2 mM ATP. Fractions containing Phe217Tyr were run over a Mono-Q column to remove any residual nuclease activity. Protein was precipitated with $(NH_4)_2SO_4$ and dissolved in R-buffer (200 - 400 ul) and dialyzed extensively against the same. Glycerol was added to a final concentration of 25% and samples (10 µl) were quick frozen and stored at -70 °C. Proteins were determined to be > 95% pure as judged by Coomassie stained gels.

hRad51 Protein purification (Figure 10)

E. coli strain BLR(DE3)/pLysS carrying the hRad51-plasmid was grown in 1/2x Superbroth (12 L) containing 100 µg/ml ampicillin. At OD_{600} = 0.75, IPTG was added to a final concentration of 5 mM, growth was continued for 3.5 hours and cells were harvested and resuspended in 100 ml of buffer (250 mM Tris, pH 7.5/25% sucrose) plus 2x protease inhibitor cocktail. Cells were lysed in the presence of 0.2 mg/ml lysozyme, 5 mM β-ME, and 0.1 mM EDTA, followed by

addition of Brij-58 to 0.5% (w/v) (See above for RecA). Soluble proteins (Fraction I, Figure 10) were recovered following centrifugation (12,500 x g) and PEI was added to 1% (w/v). Proteins were eluted stepwise from PEI pellets with hRad51 eluting in the 350 mM $(NH_4)_2SO_4$ fraction (Fraction II). Fraction II was passed through a phosphocellulose column equilibrated in R-buffer/350 mM $(NH_4)_2SO_4$, and proteins were precipitated by addition of saturating $(NH_4)_2SO_4$ (Fraction III). The resulting pellet was dissolved and desalted in R-buffer/50 mM $(NH_4)_2SO_4$ and protein was loaded onto a ssDNA cellulose column equilibrated with the same buffer. hRad51 was eluted with R-buffer/350 mM $(NH_4)_2SO_4$. Fractions containing hRad51 were pooled and precipitated with saturating $(NH_4)_2SO_4$. The resulting pellet was dissolved and desalted in R-buffer/50 mM $(NH_4)_2SO_4$ (Fraction IV), protein was loaded onto a CHT column equilibrated in the same buffer and eluted with a gradient of 50 - 600 mM KH_2PO_4/K_2HPO_4 (pH 6.8). Fractions containing hRad51 were precipitated as above and the resulting pellet was dissolved and desalted in R-buffer/50 mM $(NH_4)_2SO_4$ (Fraction V). Protein was loaded onto a heparin agarose column equilibrated in the same buffer and eluted with a gradient of 50-750 mM $(NH_4)_2SO_4$. Fractions containing purified hRad51 were concentrated and stored in R-buffer/50 mM $(NH_4)_2SO_4$/25% glycerol (Fraction VI). The yield was ≈ 2 mg hRad51 with a purity of >95% as judged by Coomassie-stained gels analyzed using a Biorad Fluor-S Multimager. Identity of the protein as hRad51 was

Figure 10.
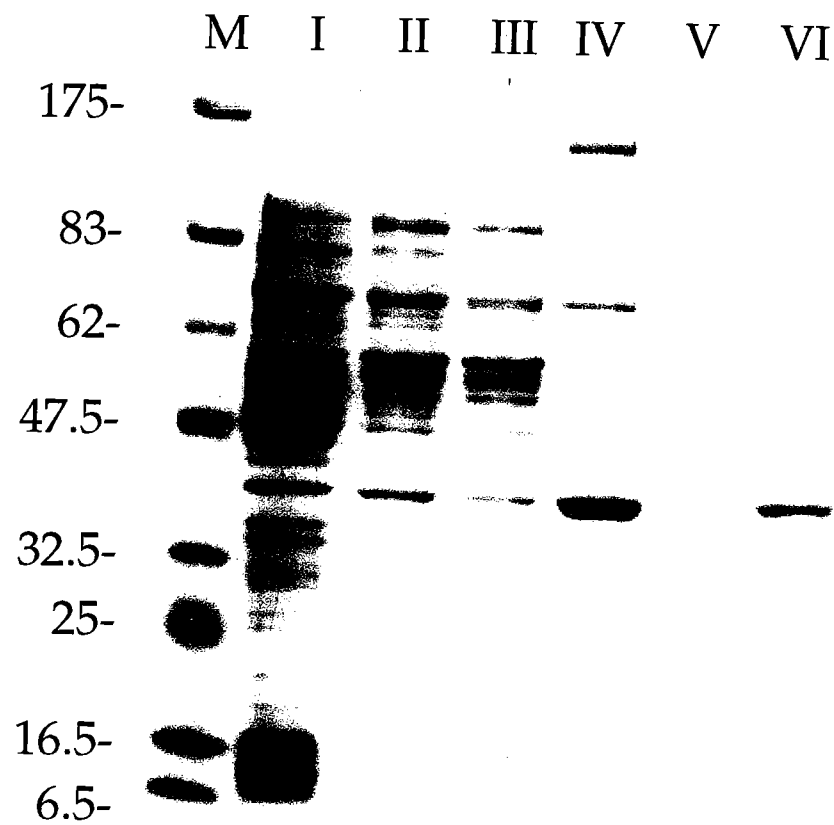
Figure 10. Purification of hRad51. SDS gel showing purity at different stages in the procedure as described in Materials and Methods. M = molecular weight markers; I = crude cell extract; fraction eluted from PEI (II), phosphocellulose (III), ssDNA cellulose (IV), CHT (V) and heparin agarose (VI). Purified hRad51 was judged to be >95% pure.

confirmed by MALDI-TOF analysis. The hRad51 protein preparation did not contain any contaminating nuclease activity (data not shown).

RecA-mediated LexA cleavage

RecA-mediated cleavage of the LexA repressor was measured using 3 different assays. LexA cleavage *in vivo* was measured as previously described (Nastri & Knight, 1994). Strain DE1663´ carries the *lacZ* and *Y* genes under control of the *recA* operator/promoter. Since *recA* expression is regulated by the LexA repressor, measurement of β-galactosidase activity is directly proportional to the extent of RecA-mediated LexA cleavage. β-galactosidase activity was measured by spotting 1 µl of an overnight culture containing a copy of either the wild type, mutant RecA or negative control plasmid onto MacConkey-lactose plates containing either no mitomycin C or 0.05 µg/ml of mitomycin C, which is a sublethal dose sufficient for induction of the SOS response. Plates were incubated overnight at 37° and β-galactosidase activity was assessed as either inducible (activated only in the presence of DNA damage), constituitive (turned on in both the presence and absence of DNA damage, or coprotease⁻ (off in both the presence and absence of DNA damage). The ability of purified wild type and mutant RecA proteins to mediate the autocleavage of the LexA repressor *in vitro* was assessed (i) in the presence of ssDNA as previously described (Konola *et al.*, 1994) and (ii) in the presence of high salt using the following modifications of a previously described method (DiCapua *et al.*, 1990). For high salt activation of LexA cleavage, reaction buffer contained 50 mM K_2HPO_4/KH_2PO_4 (pH 7.0), 10

mM Mg(OAc)$_2$, 0.6 M NaOAc, 5 mM ATPγS, and 5% glycerol. Reactions (60 μl) were performed at 37°C and contained RecA protein (0.5 mg/ml) which had been preincubated with 5 mM ATPγS. LexA protein was added to a final concentration of 1.0 mg/ml. During the time course samples (8 μl) were removed and EDTA was added to 100 mM. Intact LexA and cleavage products were resolved on a 15% SDS-polyacrylamide gel, stained with Coomassie Brilliant Blue and quantitated using scanning densitometry (Konola et al., 1995).

ATPase Activity

Hydrolysis of ATP was measured under 3 different conditions in the presence of (i) ssDNA, (ii) dsDNA or (iii) 1.8 M NaCl. The ssDNA-dependent ATPase activity was measured as previously described (Konola et al., 1995; Weinstock et al., 1981). The dsDNA-dependent ATPase activity was measured essentially as described (Weinstock et al., 1981). Reaction mixtures contained 20 mM Na-maleate (pH 6.2), 10 mM MgCl$_2$, 1 mM DTT, 25 μM dsDNA (concentration of bases), 0.5 mM [α-P^{32}] ATP (150 μCi/ml) and 2 μM purified RecA protein. These were incubated at 37°C for the indicated times and 1 μl aliquots were spotted onto PEI cellulose. High salt activation of ATP hydrolysis was measured essentially as described (Pugh & Cox, 1988). Reaction mixtures contained 50 mM Tris-HCl (pH 7.1) 17.5 mM Mg(OAc)$_2$, 5 mM [α-^{32}P] ATP (150 uCi/ml), 1.8 M NaCl, 2% (v/v) glycerol, 0.1 mM EDTA, 1 mM DTT and 5 uM purified RecA protein. These were incubated at 37°C and 1 μl samples were diluted 10 fold in water prior to spotting onto PEI cellulose. PEI plates were chromatographed in

0.5M LiCl/1 M Formic acid and percent ATP hydrolysis was quantitated using a

Molecular Dynamics Phosphor-Imager and Imagequant software (v5.6). Units of

V_i/E are min^{-1}. Data shown in Figure 24 are derived from initial rates of ATP

hydrolysis determined using various ATP concentrations (1 – 500 µM) and fit to

the Hill equation, $v = \dfrac{V_{max} S^{n(app)}}{K' + S^{n(app)}}$, using KaleidaGraph 3.08 ™ (Synergy Software,

Reading, PA.). Using PEI cellulose chromatography as described above, we

calculated turnover numbers (V_i/E) of 0.6 and 20.0 mol ATP hydrolyzed•min^{-1}

•mol enzyme^{-1} in the presence of ssDNA for hRad51 and RecA, respectively,

values which are consistent with published accounts (Gupta et al., 1997; Kelley &

Knight, 1997; Weinstock et al., 1981)

ssDNA Nitrocellulose Filter Binding Assay

Nitrocellulose filter binding assays were performed using a variation of a

described procedure (McEntee et al., 1981) and an apparatus similar to that

described by Wong and Lohman (Wong & Lohman, 1993). Filters were prepared

by soaking in 0.4 M KOH for 10 min followed by several washes with ddH$_2$0

until the pH approximated 7.0. Filters were equilibrated in binding buffer for at

least 1 hour prior to use. Reaction mixtures (50 µl) contained binding buffer (20

mM Tris-HCl (pH 7.5), 10 mM MgCl$_2$, 1 mM DTT, 0.5 mM EDTA, 20 mM NaCl),

40 µM 5′ end-labeled ssDNA (concentration of bases) and where indicated, 0.5

mM ATPγS. Reactions were started with the addition of the indicated amounts

of protein and incubated at 37°C for 15 minutes. Samples were applied to the

filter under suction and the filters washed with 2.0 ml of binding buffer containing 150 mM NaCl. Filters were air dried and bound DNA was quantitated by analyzing dried filters with a Molecular Dynamics PhosphorImager and Imagequant software (v5.6).

dsDNA Nitrocellulose Filter Binding Assay

Nitrocellulose filter binding assays were performed using a variation of a previously described procedure (Wong & Lohman, 1993). Filters were pre-equilibrated in binding buffer [20 mM sodium maleate (pH 6.2) 10 mM $MgCl_2$, 1 mM DTT, 0.5 mM EDTA] for at least 1 hour. Reaction mixtures contained 20 µM end-labeled dsDNA (concentration of bases), purified RecA protein and where indicated, 0.5 mM ATPγS. Incubations were performed at 37°C for 15 minutes, samples were applied to the filter under suction and washed with 2.0 ml of binding buffer. Double-stranded DNA binding was quantitated by analyzing dried filters with a Molecular Dynamics PhosphorImager and Imagequant software (v5.6).

ATP Crosslinking

Reaction mixtures (30 µl) contained 20 mM Tris-HCl (pH 7.5), 20 mM KCl, 10 mM $MgCl_2$, 0.5 mM EDTA, 5 µM purified RecA protein and the indicated amounts of [α-^{32}P] ATP (200 µCi/mmol). Mixtures were placed on ice, 4 cm from an 8 watt Hg-vapor lamp (Sylvania G8T5) and irradiated for 45 min. Crosslinked products were resolved on a 10% SDS-polyacrylamide gel and

analyzed using a Molecular Dynamics PhosphorImager and Imagequant software (v5.6).

DNA strand exchange

DNA strand exchange activity was measured as follows. Reactions (120 µl) were performed in buffer containing 25 mM TrisOAc (pH 7.5), 10 mM MgOAc, 1 mM dithiothreitol and 5% (w/v) glycerol. RecA protein (6.7 µM) was incubated with both single-stranded (10 µM) and XhoI-linearized double-stranded ϕX174 DNA (20 µM) in reaction buffer for 10 min at 37°C. Reactions were started by simultaneous addition of dATP (3 mM) and SSB (2 µM). Samples (9 µl) were removed at the indicated times and added to stop solution such that the final concentrations of SDS, glycerol and EDTA were 1% (w/v), 5% (w/v) and 10 mM, respectively. Samples were electrophoresed on a 0.8% agarose gel in TAE buffer (3 V cm^{-1}, 2.5 hrs.) and DNAs were visualized by staining with ethidium bromide. Gels were displayed using a FluorS MultiImager (Bio-Rad).

Electron microscopy

Samples were prepared for electron microscopy by incubating wild type or mutant RecA protein at 4.0 µM in the absence of DNA, or 0.8 µM in the presence of 3.0 µM RV-1 single-stranded circular DNA. All reactions containing DNA included *E. coli* SSB (0.03 µM) and were pre-incubated at 37°C for 5 min. Reaction buffer included 25 mM triethanolamine-HCl (pH 7.5), 50 mM KCl, 5 mM MgCl$_2$ and 1 mM ATPγS. Upon addition of RecA reactions were incubated

for 15 min at 37 °C. Reactions were spread onto thin carbon films on holey carbon grids (400 mesh) and stained with 1% uranyl acetate. Samples were visualized by transmission electron microscopy using either a Philips CM10 or a Philips EM400 microscope.

IAsys affinity biosensor ssDNA binding

Reactions were initiated with addition of protein to a cuvette containing immobilized ssDNA (see Chapters IV and V), and were performed at 37°C in PBS-Tween-Mg buffer in the absence or presence of 2 mM ATPγS or 5 mM ATP. Reactions in the presence of ATP also included an ATP regenerating system (2 mM PEP and 2.6 units/ml pyruvate kinase). Protein was preincubated for 1 minute at 37°C (with NTP when appropriate) prior to addition to the cuvette. Binding was measured for 3 minutes (hRad51) or 30 minutes (RecA). A number of binding experiments were performed over various times and showed that these times were required in order to calculate a true equilibrium binding value. Following binding, the cuvette was rapidly washed 3 times with the indicated buffer and dissociation of the protein from ssDNA was measured for 3 minutes (hRad51) or 10 minutes (RecA). The immobilized DNA surface was regenerated by addition of 3 M $MgCl_2$ for 2 minutes to strip protein, then washed and re-equilibrated in PBS-Tween-Mg buffer containing NTP where indicated. PBS-Tween-Mg served as our standard buffer, however the effect of lower ionic strength was tested using a low salt buffer (20 mM NaCl). Additionally, the effect of different concentrations of Mg^{2+} on binding was also measured in PBS-Tween

buffer. Binding is measured in "arc seconds", which corresponds to the accumulation of mass within the optical window at the binding surface, and "extent" refers to the calculated maximum binding at equilibrium for any given protein concentration. Binding data were analyzed using the Fastfit software supplied with the instrument. Control experiments showed that neither hRad51 nor RecA gave any background signal when added to the streptavidin treated cuvette surface in the absence of ssDNA (not shown).

Gel shift assay

Reactions (15 ml) were performed in PBS-Tween-Mg^{+2} buffer with 2 mM ATPγS where indicated and varying concentrations of either RecA or hRad51. Reactions were started with the addition of 10 μM (bases) 5´ end-labeled 86mer and incubated for 30 minutes at 37 °C. Samples were loaded onto a 1.2% agarose gel and electrophoresed in 1x TBE buffer (Sambrook, 1989). Gels were displayed and analyzed using a Molecular Imager FX and QuantityOne software (Biorad).

Chapter III

Allosteric Regulation of RecA Protein Function
is Mediated by Gln194

Introduction

The *E.coli* RecA protein is a multifunctional enzyme which plays a central role in the processes of recombinational DNA repair, homologous genetic recombination, and the cellular SOS response to DNA damage (Kowalczykowski *et al.*, 1994; Roca & Cox, 1997; West, 1992). Each of these activities exhibits a common initial or activating step, formation of a RecA-ATP-ssDNA nucleoprotein filament (Craig & Roberts, 1980; Little *et al.*, 1980; Radding, 1989). The binding of RecA to ssDNA is regulated in a classic allosteric fashion, whereby the binding of ATP induces a high affinity DNA binding state of the protein (Menetski & Kowalczykowski, 1985b; Silver & Fersht, 1982). In the presence of ADP, or in the absence of cofactor, RecA exhibits a low affinity (> 20 μM) for ssDNA (Menetski & Kowalczykowski, 1985b).

The crystal structure of the helical RecA protein filament has been solved in both the absence and presence of ADP (Story & Steitz, 1992; Story *et al.*, 1992) and displays a helical pitch (82.7 Å) which is intermediate between the inactive

nucleotide-free form ($\approx$ 70 Å) and the active ATP-bound form ($\approx$ 95 Å) as determined by electron microscopy (Egelman, 1993). Despite this, the ATP binding site shows a remarkable conservation of structure compared to several other nucleotide binding proteins (e.g. ras p21, EF-Tu and adenlyate kinase), and Story and Steitz were able to model specific determinants of both ATP binding and hydrolysis in the RecA structure (Story & Steitz, 1992; Story et al., 1992). In addition, the structure provided valuable insight into a possible allosteric mechanism for ATP-induced high affinity binding to ssDNA. The carboxyamide side chain of Gln194 extends into the ATP binding site and would be in very close proximity to the γ-phosphate of bound ATP (Figure 11). Gln194 immediately precedes one of two disordered loops in the structure (L2, residues 195-209) which were proposed to be part of the DNA binding sites (Story & Steitz, 1992; Story et al., 1992). Recent work has, in fact, provided strong evidence that L2 comprises all or a large part of the ssDNA binding site within RecA (Gardner et al., 1995; Malkov & Camerini-Otero, 1995). Story and Steitz (Story & Steitz, 1992) proposed that upon ATP binding Gln194 interacts with the nucleotide γ-phosphate thereby causing L2 to assume a conformation with high affinity for ssDNA. Upon ATP hydrolysis this interaction would be lost, returning L2 to a low affinity DNA binding conformation. In this study, we show that mutations at Gln194 prohibit the formation of a high affinity ssDNA binding state when ATP is bound. In addition, mutations at Gln194 block the high-salt activation of RecA function. These results indicate that Gln194 is an important "on-off" switch required for the general activation of RecA function.

Figure 11.
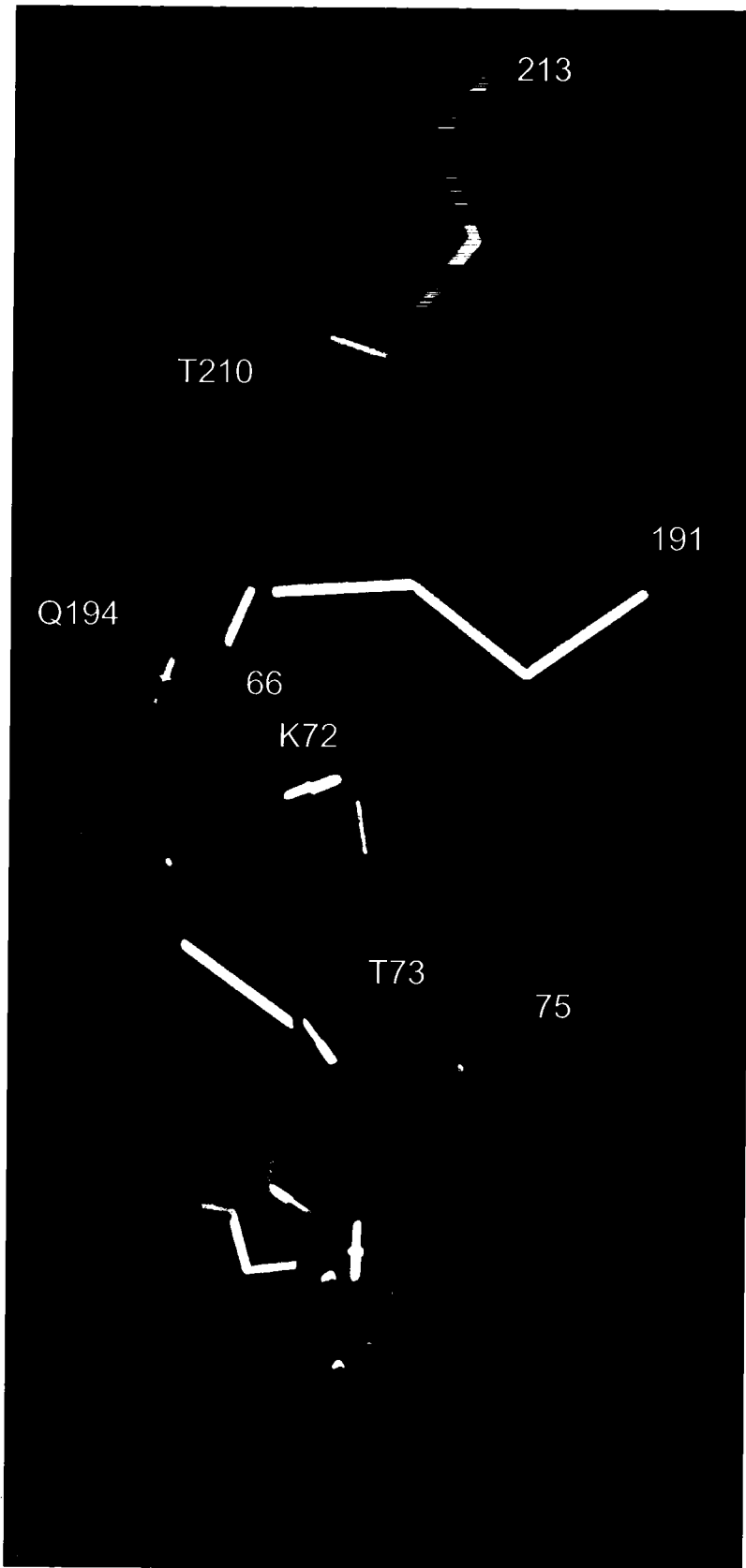
Figure 11. Position of Gln194 in the RecA ATP binding site. The structure of the RecA-ADP complex (Story & Steitz, 1992) shows the amide nitrogen of Gln194 to be approximately 6.9 Å from the β-phosphate of ADP. Residues 195 - 209, not visible in the structure, correspond to region L2 which is likely to contain all or part of the primary DNA binding domain of RecA (see text). From the RecA-ADP structure Story and Steitz (Story & Steitz, 1992) modeled P-loop residues Lys72 to interact with the γ-phosphate of ATP and Thr73 with a Mg^{2+} which bridges the β- and γ-phosphates of ATP. Atom colors are: carbon = *yellow*, oxygen = *red*, nitrogen = *blue*, phosphorus = *orange*.

Results

RecA Activity *in vivo*

We obtained 16 of 19 possible substitutions at Gln194, including a conservative Asn, an isosteric Glu and an Ala. *In vivo* screens for recombinational DNA repair and LexA cleavage showed that these activities are completely dependent on the wild type Gln residue (data not shown). None of the 16 mutants showed any survival greater than the $\Delta recA$ control in the presence of mitomycin C or following exposure to UV, even under low dose conditions (0.3 µg/ml mitomycin C or 0.67 J/m^2/sec UV light). In addition, the *in vivo* LexA coprotease activity of each mutant was completely inhibited, a result which was confirmed by *in vitro* LexA cleavage assays (see below).

ssDNA binding

RecA exhibits two distinct binding affinities for ssDNA, a low affinity in the absence of any nucleotide cofactor or the presence of ADP, and a high affinity in the presence of cofactor (Menetski & Kowalczykowski, 1985b; Silver & Fersht, 1982). We show that in the absence of nucleotide wild type RecA protein binds to ssDNA with an apparent $K_D \approx 20$ µM (Figure 12A). Each mutant protein tested, Gln194Ala, Gln194Glu, and Gln194Asn exhibits an apparent affinity comparable to that demonstrated by wt RecA, although the Gln194Asn protein appears to have a slightly reduced binding capacity (Figure 12A). In the presence of ATPγS,
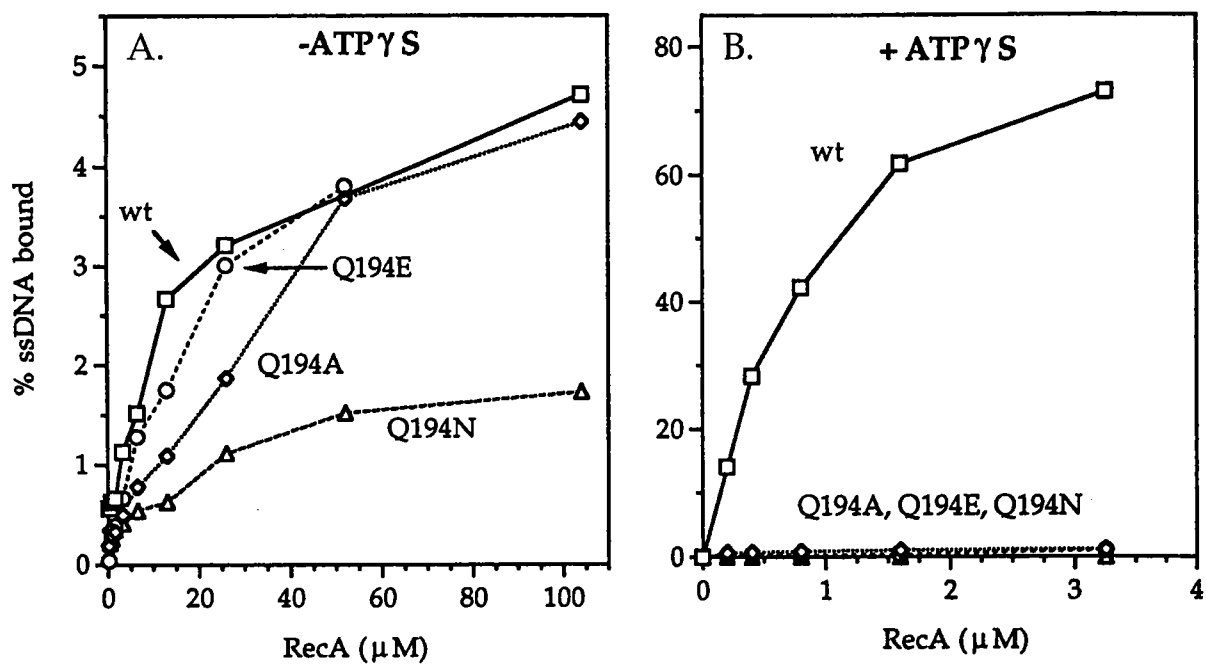
Figure 12.

Figure 12. Single-stranded DNA binding by wt and mutant RecA proteins.
Percent DNA bound as a function of protein concentration was measured for
wild type RecA and the Gln194Ala, Gln194Glu and Gln194Asn mutant proteins
in the absence **(A)** or presence **(B)** of 0.5 mM ATPγS. The nitrocellulose binding
assay is described in Materials and Methods.

however, a dramatic increase is seen in the affinity of wild type RecA for ssDNA compared to the mutant proteins (Figure 12B). Wild type RecA binds the ssDNA substrate with an apparent $K_D \approx 1 \mu M$, whereas none of the 3 mutant proteins show any change in affinity for ssDNA in the presence of nucleotide cofactor. These results indicate that the mutations at position 194 render the proteins unable to undergo the ATP-induced transition required for high affinity ssDNA binding.

ATP binding

An essential control in this study was to test the ability of the mutant proteins to bind ATP. Using a UV crosslinking procedure we show that ATP binding by each of the 3 mutant proteins (Gln194Ala, Gln194Glu and Gln194Asn) is very similar to that of wild type RecA (Figure 13). Proteins that had been heat denatured prior to UV exposure show no crosslinking. These results show that the mutant proteins maintain their ability to bind ATP, and that the inability of the mutant proteins to assume a high affinity ssDNA binding state is not simply due to a defect in ATP binding.

ATP-induced effects on the oligomeric distribution of RecA

In solution RecA protein exists as a heterogeneous population of oligomers, ranging in size from monomers, dimers, and hexamer-sized rings to larger filaments and bundles of filaments (Brenner *et al.*, 1988; Heuser & Griffith, 1989; Wilson & Benight, 1990). In the presence of ATP this distribution is shifted such that bundles of filaments are disrupted and the average filament length is shorter

Figure 13.
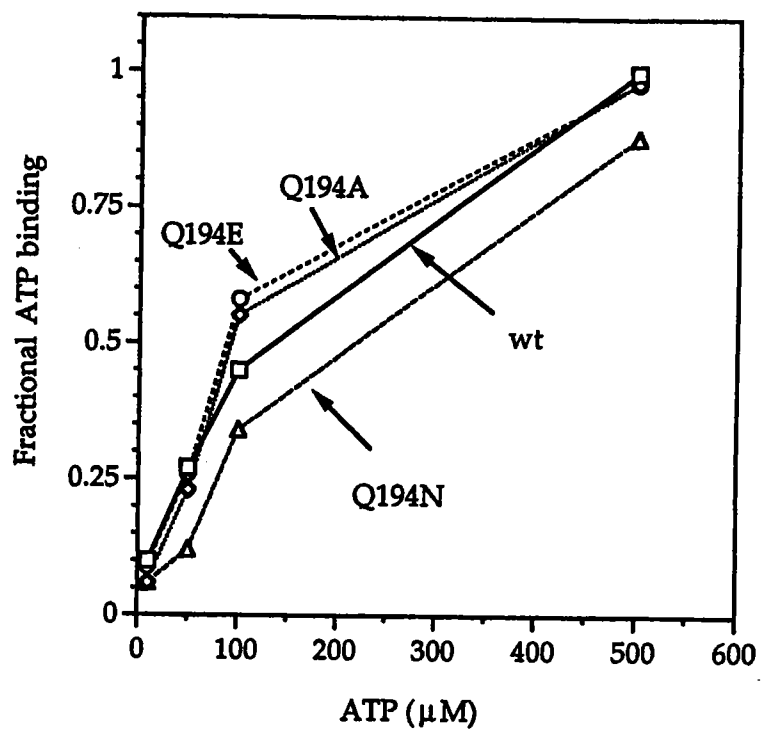
Figure 13. **ATP binding by wt and mutant RecA proteins.** ATP binding to wild type RecA and the Gln194Ala, Gln194Glu and Gln194Asn mutant proteins was measured using a UV crosslinking procedure as described in Materials and Methods. Fractional binding is the ratio of ATP bound/ATP bound to wild type RecA at an ATP concentration of 500 μM.

(Brenner *et al.*, 1988; Heuser & Griffith, 1989; Wilson & Benight, 1990). We used a recently developed gel filtration assay (Logan *et al.*, 1997) to assess any effect that mutations at position 194 may have on the oligomeric properties of RecA, as well as the effect of ATP on the oligomeric distribution. Our results show that Gln194 mutant proteins do not show a defect in oligomerization and importantly, that each mutant protein maintains an ATP-induced shift in the oligomeric distribution similar to that observed for wild type RecA (Figure 14). Addition of ATPγS shifts the peak representing long RecA filaments and bundles to a smaller size (Figure 14) (Logan *et al.*, 1997). These results again show that each mutant RecA protein is capable of binding ATP and that conformational changes associated with the ATP-induced shift in the distribution of RecA oligomers are maintained and, therefore, not transmitted through Gln194.

ATPase activity

The ATPase activity of RecA protein is stimulated upon binding to either ssDNA or dsDNA (Weinstock *et al.*, 1981). In the absence of DNA wild type RecA exhibits a low level ATPase activity at pH 7.5 ($V_i/E = 0.2$ min^{-1}) whereas in the presence of a ssDNA cofactor activity increases significantly ($V_i/E = 17.4$ min^{-1}) (Figure 15). While the basal rate of ATP turnover for the mutant proteins is similar to that of wild type RecA ($V_i/E = 0.2$ min^{-1}; Figure 15A), no ssDNA-dependent increase in activity is observed (Figure 15B). At pH 6.2 the catalytic efficiency of RecA

Figure 14.

Figure 14. Gel filtration profiles of (A) wild type RecA and the (B) Gln194Ala, (C) Gln194Glu and (D) Gln194Asn mutant proteins. Runs were performed on a Superose 6 gel filtration column (Pharmacia/LKB; 21 ml bed volume) in the absence (open boxes) or presence (filled boxes) of 0.5 mM ATPγS. The RecA protein concentration in the load was approximately 26 μM (1 mg/ml). Peaks eluting early in the profile correspond to longer filaments of RecA or bundles of filaments (19). The peak centered near 15.5 to 16 ml approximates the size of a RecA hexamer. In the presence of ATPγS larger molecular weight oligomers are shifted to smaller sizes. Molecular weight markers are thyroglobulin (650 kDa), apoferritin (450 kDa), β-amylase (206 kDa), bovine serum albumin (68 kDa) and cytochrome C (12.5 kDa).

Figure 15.
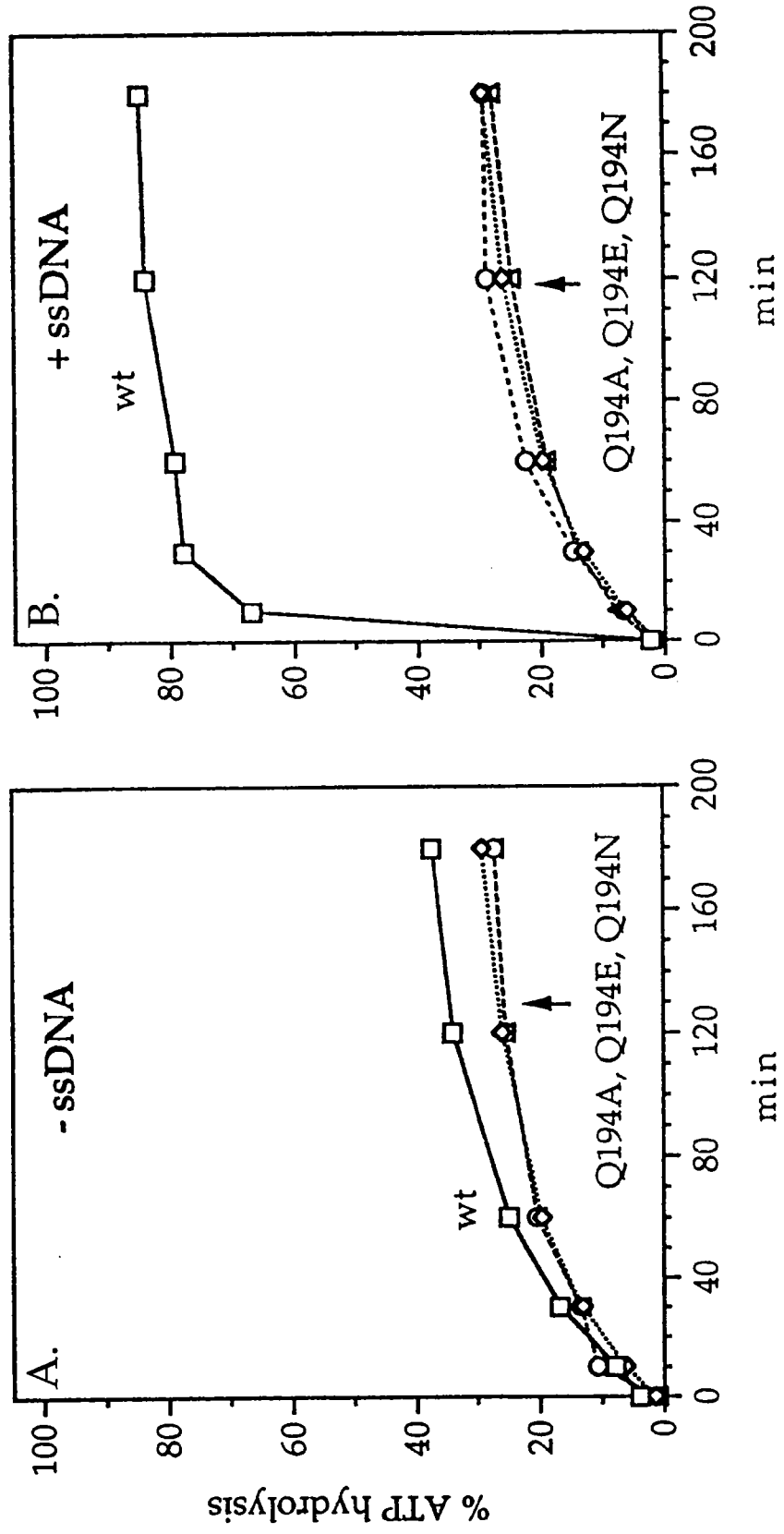
Figure 15. Single-stranded DNA-dependent ATP hydrolysis. ATP hydrolysis catalyzed by wild type RecA and the Gln194Ala, Gln194Glu and Gln194Asn mutant proteins at pH 7.5 was determined in the absence **(A)** or presence **(B)** of ssDNA as described in Materials and Methods.

increases approximately 30-fold in the presence of dsDNA (Weinstock *et al.*, 1981). Each of the Gln194 mutant proteins maintains a wild-type level of DNA-independent ATPase activity at pH 6.2 ($V_i/E = 0.5$). However, an increase in the presence of dsDNA was seen only with wild type RecA (data not shown). Control experiments showed that wild type and mutant proteins bound equivalent low levels of dsDNA in the absence of ATPγS, yet only wild type RecA displayed a significant ATP-dependent increase in dsDNA binding (data not shown). These results demonstrate that mutations at Gln194 block the DNA-dependent activation of ATPase activity but do not affect the basal level of DNA-independent ATP turnover.

LexA Coprotease Activity

In the presence of both nucleotide and ssDNA cofactors RecA mediates the autoproteolysis of the LexA repressor (Little *et al.*, 1980). While wild type RecA catalyzes a significant level of LexA autoproteolysis (95% cleaved/40 min) this activity is completely lacking in each of the 3 mutant proteins (Figure 16).

High Salt Activation of RecA Activities

In the absence of any DNA cofactor, but in presence of high salt, wild type RecA protein is activated for both ATP hydrolysis (Pugh & Cox, 1988) and LexA cleavage (DiCapua *et al.*, 1990). Because mutations at Gln194 prohibit high affinity DNA binding required for both of these activities we determined whether the Gln194Ala, Gln194Glu and Gln194Asn mutations also affected high salt activation of RecA function. We found that although the ATPase activity of

wild type RecA was greatly stimulated in the presence of 1.8 M NaCl ($V_i/E = 23$)

the 3 mutant proteins showed only very low activity under these conditions

(Figure 17). Similarly, in the presence of 0.6 M NaOAc wild type RecA catalyzed

a significant level of LexA autoproteolysis (50% cleaved/40 min) yet this activity

was lacking in each mutant protein (data not shown).

Figure 16.
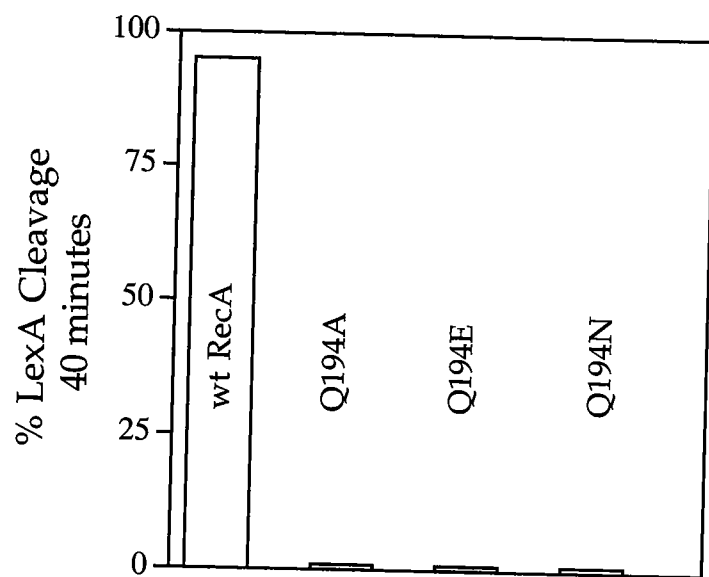
Figure 16. RecA-mediated Lex A cleavage by wt RecA, Gln194Ala, Gln194Glu and Gln194Asn mutant proteins. Graph shows the amount of LexA cleavage after 40 minutes of incubation with the indicated purified protein in the presence of ssDNA as described in Materials and Methods.

Figure 17.
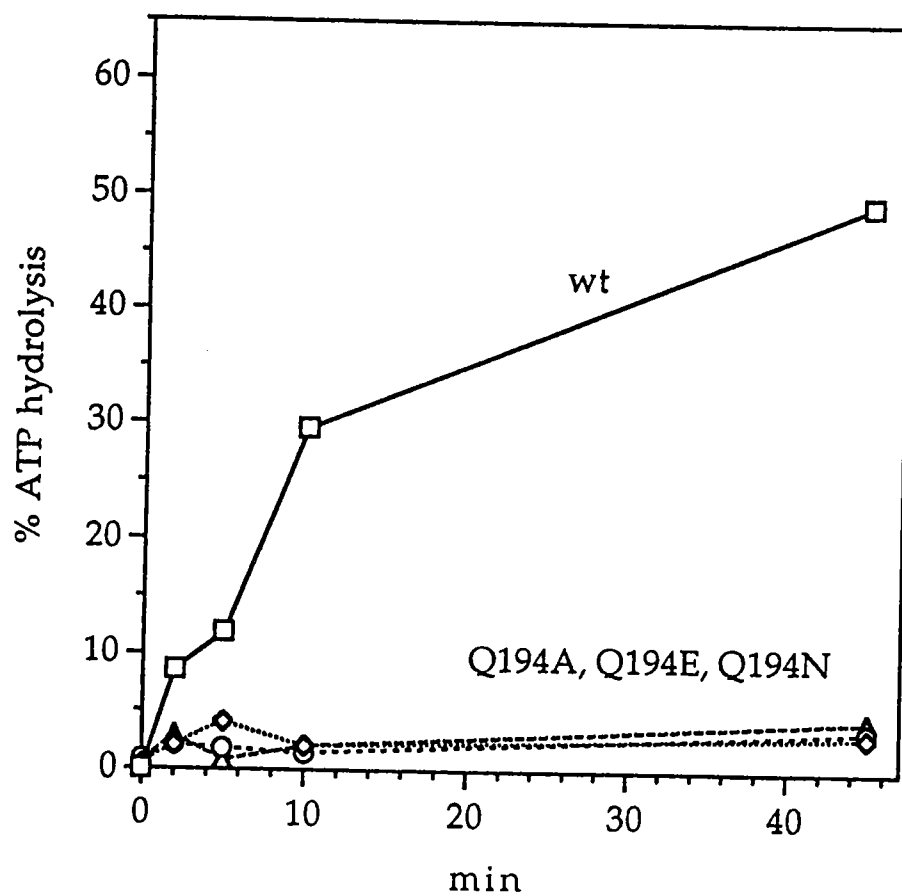
Figure 17. High salt activation of RecA ATPase function. ATP hydrolysis catalyzed by wild type RecA and the Gln194Ala, Gln194Glu and Gln194Asn mutant proteins in the presence of 1.8 M NaCl was determined as described in Materials and Methods.

Discussion

NTP-induced conformational change is a common theme for activation of enzyme function. Studies of a number of NTP binding proteins, including G-protein complexes (Lambright *et al.*, 1994; Milburn *et al.*, 1990), the myosin motor domain (Fisher *et al.*, 1995; Lambright *et al.*, 1994; Milburn *et al.*, 1990), the kinesin and ncd microtubule motor proteins (Sablin *et al.*, 1996) and the $ADP \bullet AlF_4^-$-stabilized nitrogenase complex (Schindelin *et al.*, 1997) have identified specific protein-nucleotide interactions which mediate conformational changes leading to activation of protein function. Additionally, the position of residues in the ATP binding site of the PcrA helicase from *B. stearothermophilus* shows a striking similarity to those in RecA (Subramanya *et al.*, 1996). For example, in addition to residues proposed to be involved in Mg^{2+} binding (Asp223 in PcrA, Asp144 in RecA) and the catalysis of ATP hydrolysis (Glu224 in PcrA, Glu96 in RecA), Gln254 occupies a position in PcrA very similar to Gln194 in RecA. Subramanya *et al.* (Subramanya *et al.*, 1996) propose that ATP-induced effects on the DNA binding affinity by neighboring regions are mediated by Gln254.

Our data show that Gln194 is essential for RecA function, possibly serving as an NTP-binding site "γ-phosphate sensor" within the protein. Any mutation at this position disrupts only the ATP-induced increase in RecA activities and not the basal level functions or properties of the protein. For example, the low level DNA-independent ATP hydrolysis seen with wild type RecA is maintained for

each of the Gln194 mutant proteins indicating that Gln194 is not an important component of the intrinsic RecA ATPase catalytic mechanism. In addition, Gln194 does not appear to be an important determinant of ATP binding as Asn, Glu and Ala mutations show binding profiles similar to wild type RecA. We also show that each of the three mutant proteins maintains a low-affinity binding to ssDNA in the absence of ATP similar to wild type RecA and therefore, Gln194 is not a determinant of this DNA binding property. We cannot necessarily exclude the possibility that Gln194 interacts with DNA in the activated RecA/ATP/DNA complex. Using synthetic peptides corresponding to residues 193 - 212, which includes the entire L2 region, Voloshin, et al. (Voloshin et al., 1996) identified position 203 as an important determinant of DNA binding. Studies using peptides with substitutions at Gln194 could assist in defining a potential role for this residue in DNA binding.

Furthermore, these results demonstrate that the wild type Gln194 side chain is necessary for the general activation of RecA function and supports the suggestion by Pugh and Cox (Pugh & Cox, 1988) that salt activation of RecA is "functionally mimicking the ionic interaction of the protein with DNA". In the presence of ATP and elevated salt concentrations, if 3 to 4 anions bind to the same sites within RecA as do phosphate groups on the DNA backbone (Leahy & Radding, 1986; Pugh & Cox, 1988), our data shows that Gln194 mediates the ATP-induced occupancy of these sites giving rise to an activated RecA/ATP/DNA (or RecA/ATP/salt) complex. In future studies it would be interesting to determine the ion occupancy of the Gln194 mutant proteins.

Although our data demonstrate the importance of Gln194 in transmitting allosteric information within the RecA protein structure it certainly does not exclude other residues, perhaps within the L2 DNA binding region, as also participating in ATP-induced allosteric effects. We note that specific ATP-induced changes in the oligomeric structure of RecA are not blocked by mutations at Gln194 (Figure 14). Therefore, other residues must play important roles in mediating nucleotide-induced changes in RecA structure and/or function as the protein progresses through the catalytic cycle.

Chapter IV

Phe217 Regulates the Transfer of Allosteric Information Across the Subunit Interface of the RecA Protein Filament

Introduction

The bacterial RecA protein is a multifunctional enzyme that plays a central role in recombinational DNA repair, homologous genetic recombination and induction of the cellular SOS response (Eggleston & West, 1996; Roca & Cox, 1997). Each of these activities requires a common initial step, formation of a RecA-ATP-ssDNA nucleoprotein filament (Eggleston & West, 1996; Radding, 1989; Roca & Cox, 1997). Studies of related DNA repair and recombination proteins including UvsX from bacteriophage T4 (Griffith & Formosa, 1985; Story et al., 1992) and both yeast and human Rad51 (Benson et al., 1994; Ogawa et al., 1993c) show that such an oligomeric filament is a common structure found in RecA homologs among a wide variety of prokaryotic and eukaryotic organisms. RecA function is regulated in a classic allosteric fashion, whereby the binding of ATP greatly enhances the protein's affinity for ssDNA binding and activates it for its catalytic activities (Menetski & Kowalczykowski, 1985b; Silver & Fersht, 1982). Recent work suggests that this effect of ATP on DNA affinity is a result of an increase in the cooperative assembly of the protein itself rather than an

increase in the intrinsic affinity for DNA (De Zutter & Knight, 1999). Analysis of the RecA crystal structure shows that 55 of the 303 residues in the structure participate in monomer-monomer interactions (Story *et al.*, 1992). Our studies of different areas of the subunit interface have addressed two fundamental questions: (*i*) which of the intersubunit contacts observed in the structure are actually important for RecA function and oligomer stability and (*ii*) which specific residues are important for the transmission of allosteric information across the protein's oligomeric interface. Our initial studies focused on a region defined by residues 213-222, which shows 5 side chains that make specific contacts with positions in the neighboring subunit. Through mutational analyses and the use of engineered disulfides (Logan *et al.*, 1997; Skiba & Knight, 1994; Skiba *et al.*, 1999) we have demonstrated the importance of one particular residue within this region, Phe217, for maintenance of both the structural and functional integrity of the protein. While a Phe217Tyr mutation maintains wild type recombination activities *in vivo*, all other substitutions severely inhibit RecA function (Skiba & Knight, 1994). In the present study we compare various biochemical properties of wild type RecA and the Phe217Tyr mutant protein. These data identify Phe217 as a key residue within the RecA subunit interface required for the transmission of ATP-mediated allosteric information throughout the oligomeric structure of the protein.

Results

Electron microscopy

Negative stained samples of both wild type RecA and the Phe217Tyr mutant are shown in Figure 18. In the absence of both ATP and DNA the wild type protein forms short filaments (Figure 18A) whereas the mutant forms no detectable oligomeric structures (Figure 18D). In the presence of DNA and ATPγS both proteins form well defined nucleoprotein filaments (Figure 18C and F). However, in the absence of DNA the mutant shows a dramatic increase in filament length with addition of ATPγS (Figure 18E), whereas the length of wild type filaments clearly decreases (Figure 18B). Results for wild type RecA are consistent with previous electron microscopic and hydrodynamic analyses (Brenner *et al.*, 1988; Wilson & Benight, 1990) whereas the ATP-dependent increase in polymer length for the Phe217Tyr mutant is the first demonstration of such an occurrence for any mutant RecA protein. Gel filtration analyses of both proteins shows an ATP-dependent decrease in the oligomeric size of wild type RecA, while a small but significant percentage of the Phe217Tyr mutant protein increases in size in the presence of ATPγS (data not shown). Together, these data suggest that position 217 plays a key role in regulating polymerization of the RecA protein filament. To provide a quantitative understanding of the effect of the Tyr substitution on RecA polymerization we performed a series of biosensor DNA binding studies.

Figure 18.
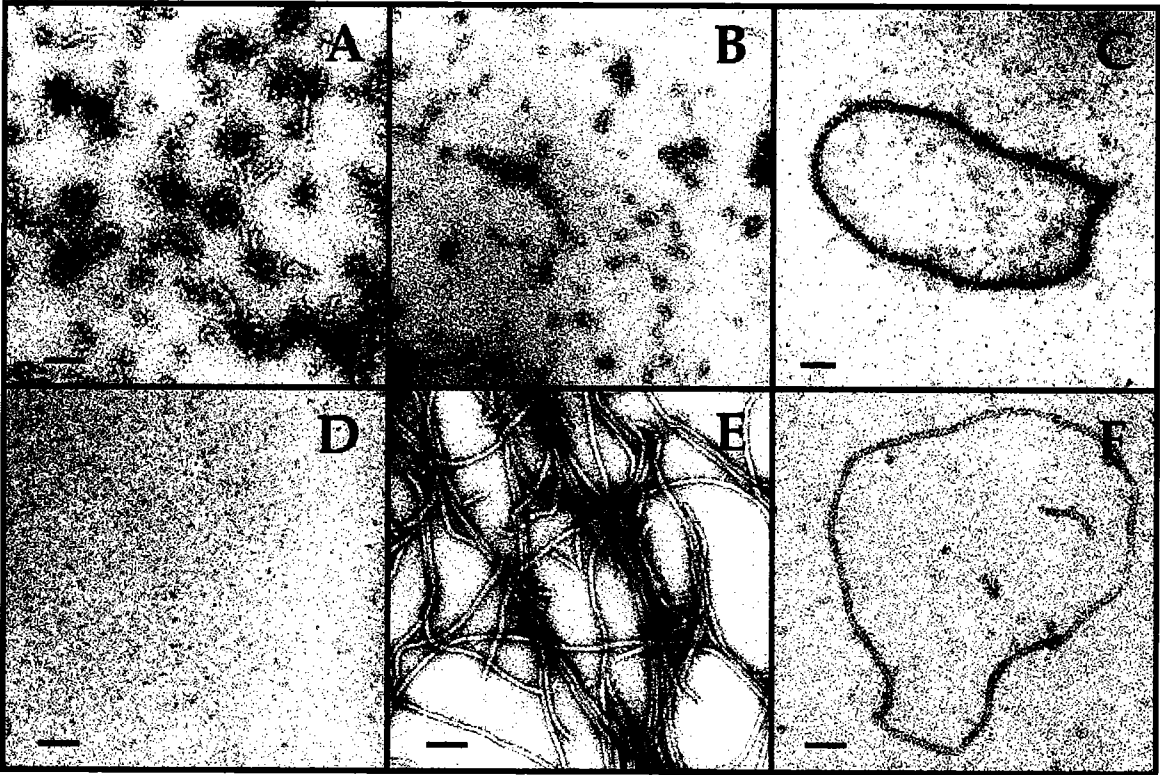
Figure 18. Negative stained electron micrographs of protein and protein-ssDNA complexes. Wild type RecA (A-C) and the Phe217Tyr protein (D-F) were incubated as described in Methods in the absence of ATPγS and ssDNA (A, D), in the presence of ATPγS (B, E) or in the presence of both ATPγS and φX174 single-stranded circular DNA (C, F). Black bar in each panel equals 0.1 μm.

DNA binding: equilibrium parameters

Binding of both wild type RecA and the Phe217Tyr mutant to ssDNA was measured using an IAsys biosensor. We have demonstrated that this technique provides a reliable and quantitative measurement of the DNA binding properties of both RecA and the human Rad51 protein (Chapter V)(De Zutter & Knight, 1999). A cartoon depicting the immobilized ssDNA binding surface is shown in Figure 19A. The surface was constructed as follows (Figure 19B). Saturating amounts of streptavidin were added to a biotin-coated cuvette and incubated for $\approx$ 4 min (Figure 19B, step 1). After a brief wash with PBS-Tween buffer (Figure 19B, step 2), a 5′-biotinylated 86 base oligonucleotide was added (Figure 19B, step 3) and incubated until equilibrium binding was observed ($\approx$ 2 min). This was followed by a brief wash with PBS-Tween buffer (Figure 19B, step 4). The final concentration of ssDNA in the working volume of the cuvette was 67 nM (concentration of bases). Binding time courses for wild type RecA and the mutant protein in the presence of ATPγS are shown in Figure 20. Both proteins showed similar low levels of DNA binding in the absence of ATPγS (not shown). From these curves the extent of binding (binding response at equilibrium) was calculated for each protein concentration. Data were fit to the form of the Hill equation shown below.

$$\text{(extent bound) } b = \frac{B_{max} S^{n(app)}}{K' + S^{n(app)}}$$

B_{max} is the maximum amount of protein-DNA complex at equilibrium (reported as the maximum extent of binding in arc seconds), S is protein concentration (free) and K' is a complex constant comprising interaction factors which reflect successive binding and dissociation steps along the cooperative binding pathway (Segel, 1975). Free protein concentration (S) was calculated by subtracting the amount of protein-DNA complex from total protein. The amount of complex was determined using a conversion of 600 arc seconds = 1 ng protein/mm^2, with a useable surface area in the biotinylated cuvette of 4 mm^2. Assuming that RecA polymer assembly progresses by addition of monomers to the growing chain (Menetski & Kowalczykowski, 1985a), we have interpreted the Hill coefficient (n_{app}) as the minimum number of interacting monomers during growth of the nucleoprotein filament which give rise to the observed cooperative binding parameters. . If $n_{app} > 1$, the system is considered to be cooperative (Segel, 1975). $S_{0.5}$, the protein concentration at the mid-point of the titration curve, is calculated as $S_{0.5} = \sqrt[n_{app}]{K'}$ (Segel, 1975). The sigmoidal curves in Figure 21 indicate cooperative binding of both proteins to ssDNA, with the mutant showing a dramatic transition from 10 – 90% binding over an extremely narrow range of protein concentration. Calculated values for B_{max}, K', n_{app} and $S_{0.5}$, appear in Table I. Values for wild type RecA are consistent with those determined previously (De Zutter & Knight, 1999; Menetski & Kowalczykowski, 1985a). The mutant protein shows a slight decrease in B_{max} and a 2.5-fold increase in affinity

Figure 19.

A.
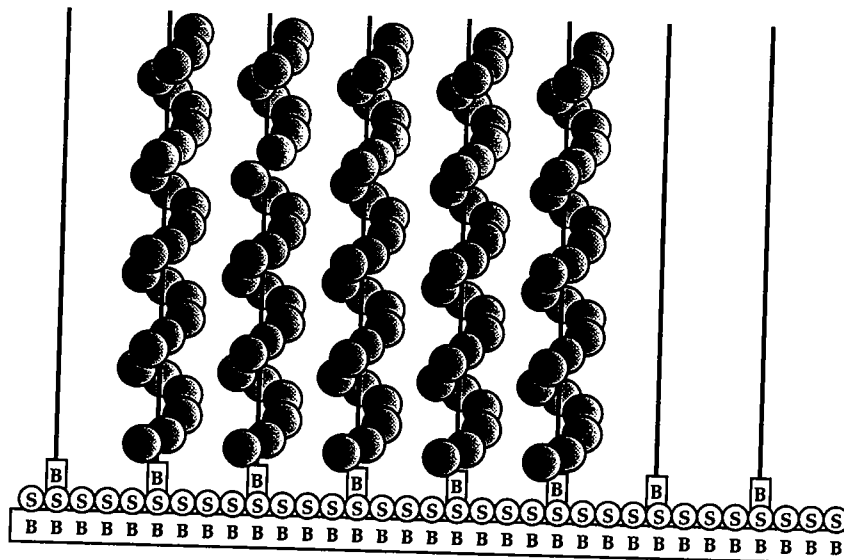
B.
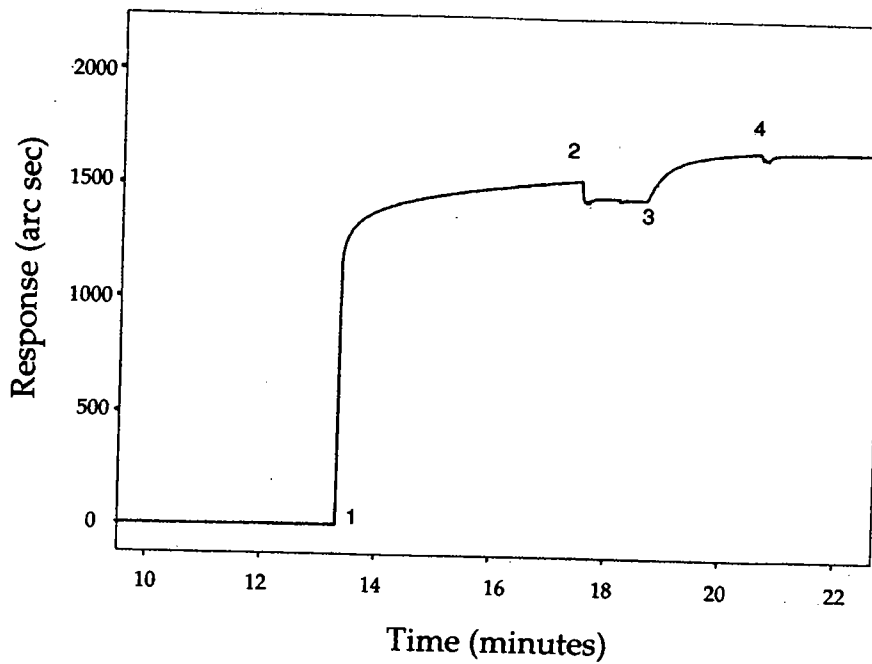
Figure 19. Construction of IAsys biosensor cuvette containing immobilized ssDNA. (A) Cartoon depicting the immobilized ssDNA binding surface of the cuvette. **(B)** Construction of the ssDNA binding surface. Using a cuvette with a biotin coated surface (Affinity Sensors), a saturating amount of streptavidin was added (1) followed by a brief wash with PBS-Tween buffer (2), addition of 5′-biotinylated oligonucleotide (3) and a final wash with PBS-Tween buffer (4). Details are provided in the text.

Figure 20.
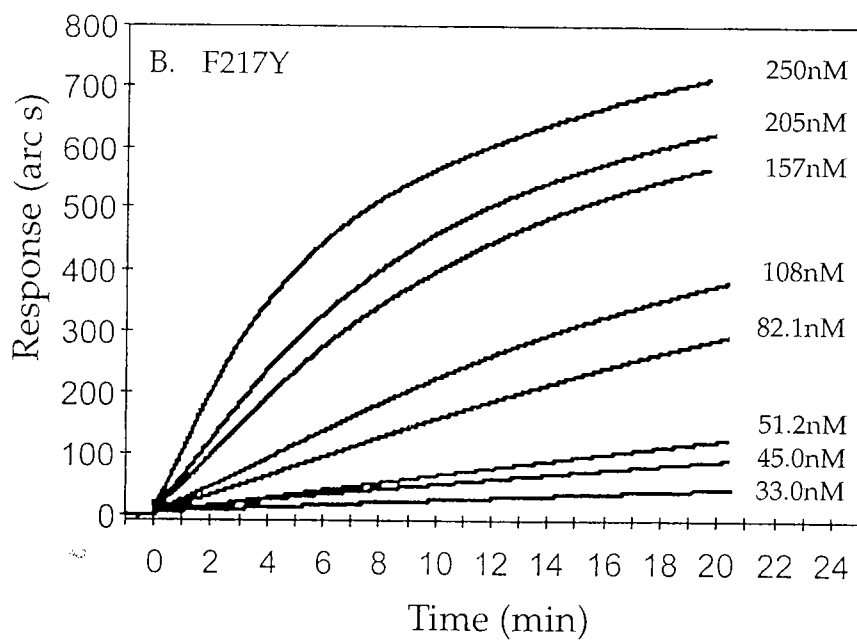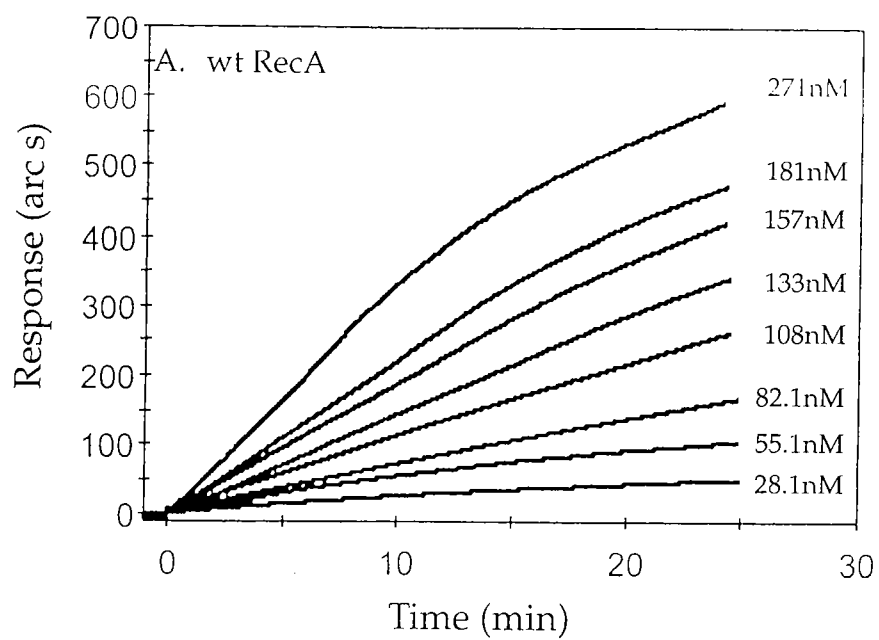
Figure 20. Biosensor DNA binding time courses for wt RecA _vs._ Phe217Tyr.
Reactions included the indicated concentrations of protein and 2 mM ATPγS, and
were incubated at 24 °C for approximately 25 minutes as described in Methods.
All time courses were repeated a minimum of 3 times.

Figure 21.
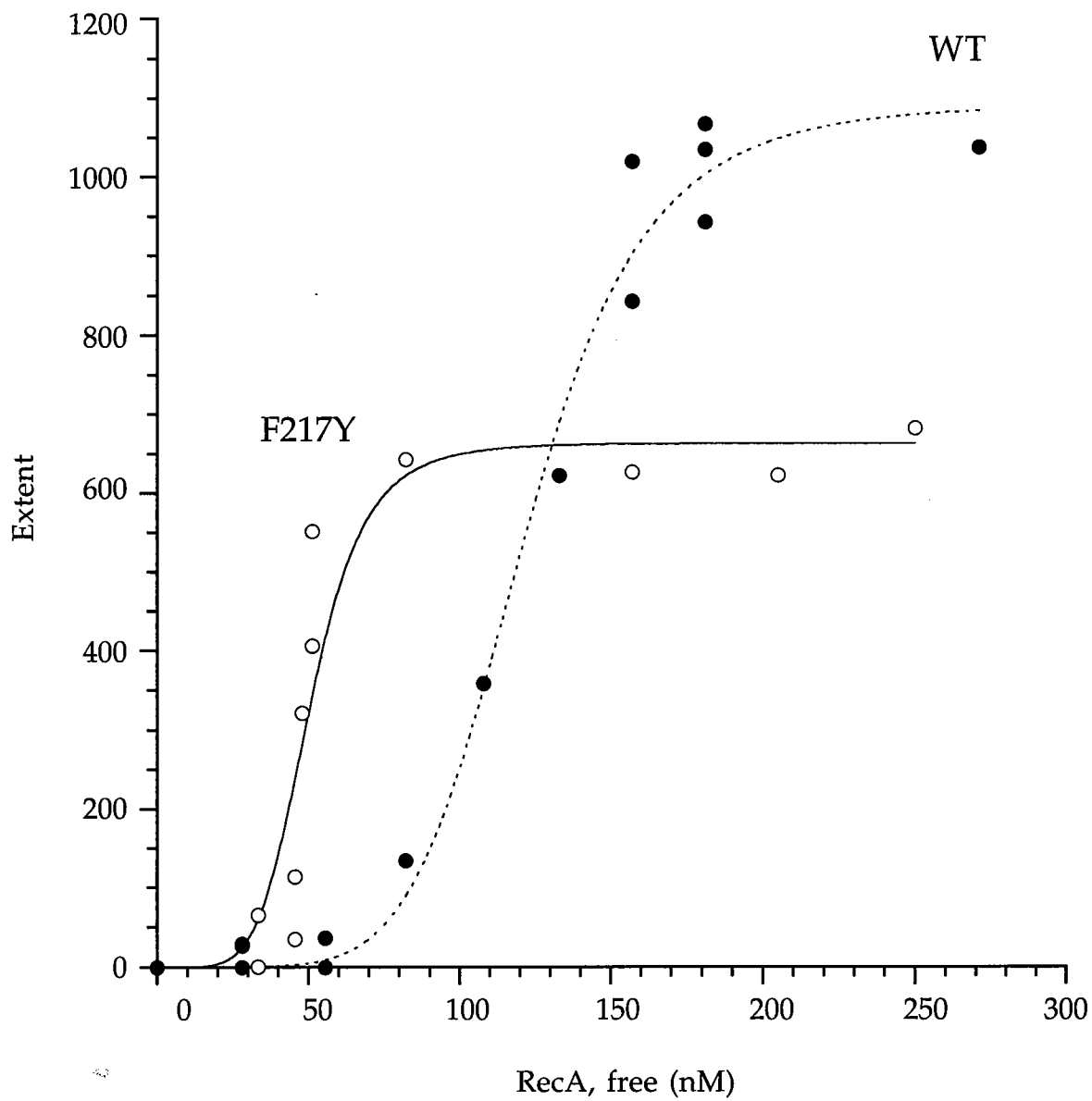
Figure 21. DNA binding by wt RecA and Phe217Tyr as a function of protein concentration. Extent data from time courses in Figure 20 were fitted to the Hill equation as described on page 87 to calculate B_{max}, n_{app}, K' and $S_{0.5}$. Values are listed in Table I on page 95. Extent is the calculated maximum binding at equilibrium in arc seconds for each protein concentration.

Table I

Equilibrium and Cooperative ssDNA Binding Parameters for Wild Type and Phe217Tyr RecA Proteins. Values for B_{max}, n_{app}, K' and $S_{0.5}$ are derived from averages of 3 sets of data as shown in Figure 21 using the Hill equation as described on page 87. Values for K and ω were calculated using a variation of Equation 2 in Kowalczykowski, *et al.* (1986) as described on page 96. Standard errors were calculated from 3 separate experiments and range from 5 – 25%.

	Wild type RecA	Phe217→Tyr
Hill analysis		
B_{max}	1120.0	765.0
n_{app}	5.8	5.8
K'	7.2×10^{-41}	2.5×10^{-43}
$S_{0.5}$ (nM)	120.0	45.2
McGhee/von Hippel analysis		
K (M^{-1})	1.1×10^5	1.0×10^3
ω	75.8	2.0×10^4
$(K\omega)^{-1}$ (nM)	120.0	50.0

($S_{0.5}$ = 120 and 45.2 nM for wild type and mutant, respectively). Additionally, n_{app} = 5.8 for wild type RecA and the mutant. This suggests that the DNA binding properties of the entire RecA filament are defined by the interaction of the initial 6 monomers for both wild type and mutant proteins. Therefore, when the data is analyzed using this standard form of the Hill equation the Phe217Tyr substitution seems to impose no significant change in the DNA binding properties of the protein. However, analysis of the binding data using a procedure that dissects out the intrinsic DNA binding affinity from cooperative protein-protein interactions (McGhee & von Hippel, 1974) reveals that the Phe217Tyr mutation has a dramatic effect on RecA polymerization.

DNA binding: determination of K and ω

To investigate potential changes in cooperative filament assembly resulting from the Phe217Tyr mutation we analyzed our data as previously described (De Zutter & Knight, 1999; McGhee & von Hippel, 1974) using the equation below.

$$L = \frac{v}{K(1-nv)\left[\dfrac{(2\omega-1)(1-nv)+v-\left\{(1-(n+1)v)^2+4\omega v(1-nv)\right\}^{1/2}}{2(\omega-1)(1-nv)}\right]^{n-1}\left[\dfrac{1-(n+1)v+\left\{(1-(n+1)v)^2+4\omega v(1-nv)\right\}^{1/2}}{2(1-nv)}\right]^2}$$

In this expression, L is the concentration of free ligand, n is the number of bases bound by a single RecA monomer (binding site size), v is the binding density of RecA on DNA (fractional maximum extent of binding/n), K is the

intrinsic binding constant of a single RecA monomer for DNA and ω is the cooperativity parameter. ω is defined as the relative affinity of an incoming ligand for a singly contiguous site *vs.* an isolated site (Kowalczykowski *et al.*, 1981; McGhee & von Hippel, 1974). In a non-cooperative system, $\omega = 1$. A value of $n = 3$ was used as the binding site size (Roca & Cox, 1997; Zlotnick *et al.*, 1993). This expression accommodates two aspects of a widely accepted model for RecA filament assembly onto ssDNA, it proceeds by (*i*) directional binding to an established site (Register & Griffith, 1985) and by (*ii*) addition of protein monomers to the growing filament (Menetski & Kowalczykowski, 1985a). Best fits for K and ω were obtained by iterative non-linear regression analysis using the software package KaleidaGraph™ 3.08d (Synergy Software, Reading, PA.). The product $(K\omega)^{-1}$ is equivalent to $S_{0.5}$ in the Hill eqation. Values for K, ω and $(K\omega)^{-1}$ are shown in Table I. As expected $(K\omega)^{-1}$ approximates the values of $S_{0.5}$ for both the wild type and mutant proteins. However, the analysis reveals a dramatic increase in the cooperative nature of filament assembly for the mutant protein. The Phe217Tyr substitution increases ω by more than 250-fold ($\omega = 75.8$ and 20,000 for the wild type and Phe217Tyr proteins, respectively).

RecA filaments have been shown to pack in a side-by-side manner in the absence of DNA to create ordered bundles (Stasiak & Egelman, 1994). Since biosensor measurements simply record the accumulation of mass within the optical window, experiments were designed to ask whether our measurements

Figure 22.
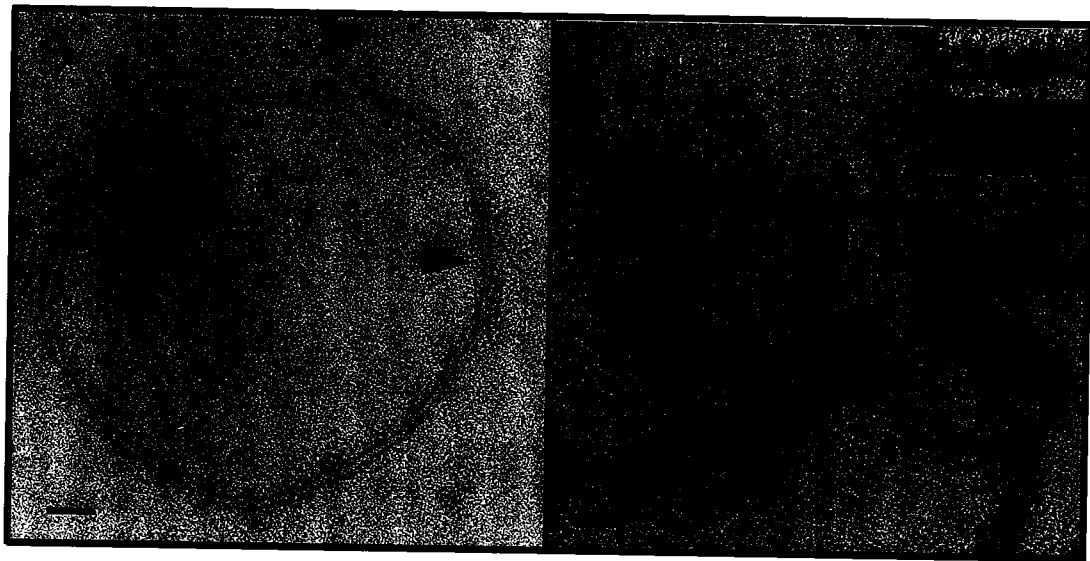
Figure 22. **Negative stained electron micrographs of protein-DNA complexes in the presence of a slight excess of protein.** 2.0 µM wild type RecA (A) or the Phe217Tyr protein **(B)** was incubated with 0.5 µM φX174 single-stranded circular DNA in the presence of 1.0 mM ATPγS and 0.03 µM *E. coli* SSB as described in Methods. In addition to circular nucleoprotein filaments, occasional short filaments of free protein are seen for wild type RecA (arrow in A) whereas frequent long filaments of free protein are observed for the mutant (arrows in B). The inset in B shows a magnification (approximately 3.5-fold) of a free protein filament (top) and a section of the circular nucleoprotein filament (bottom) for the Phe217Tyr mutant. Black bar in both panels equals 0.1 µm.

were also recording fortuitous interactions between free protein filaments and RecA-ATPγS-ssDNA complexes. Electron microscopic analyses were carried outusing excess protein relative to ssDNA (protein monomers: DNA bases = 4:1). The results showed normal nucleoprotein filament formation for both wild type RecA (Figure 22A) and the mutant protein (Figure 22B). For wild type RecA occasional short filaments of free protein were seen (arrow in Figure 22A), whereas a much larger percentage of the unbound mutant protein formed elongated filaments (arrows in Figure 22B). Differences in the helical pattern of free protein *vs.* nucleoprotein filaments (inset in Figure 22B) reflect the fact that when bound to DNA the pitch of the RecA filament is ≈ 95 Å, whereas in the absence of DNA it is ≈ 65 Å (Egelman, 1993). There was no appearance of free RecA protein bundling in a side-by-side manner with protein already in complex with DNA. Therefore, our biosensor measurements are recording only the growth of single RecA filaments on the immobilized ssDNA substrate.

Strand exchange

DNA strand exchange assays were performed using single-stranded circular and homologous linear duplex ϕX174 DNAs. For both wild type RecA and the Phe217Tyr mutant initial joint molecules are seen as early as 30 seconds (Figure 23). However, the appearance of joint molecules with reduced mobility (intermediates in the branch migration phase of the reaction) is delayed for the mutant protein. Additionally, the mutant protein shows a significant delay in the appearance of final products (nicked double-stranded circular DNA). These results show that while the Phe217Tyr protein initiates strand exchange

Figure 23.

Wt RecA

F217Y

0 0.5 1 2 3 4 6 8 10 15 30 60

M

0 0.5 1 2 3 4 6 8 10 15 30 60

jm

nc
ds
ss
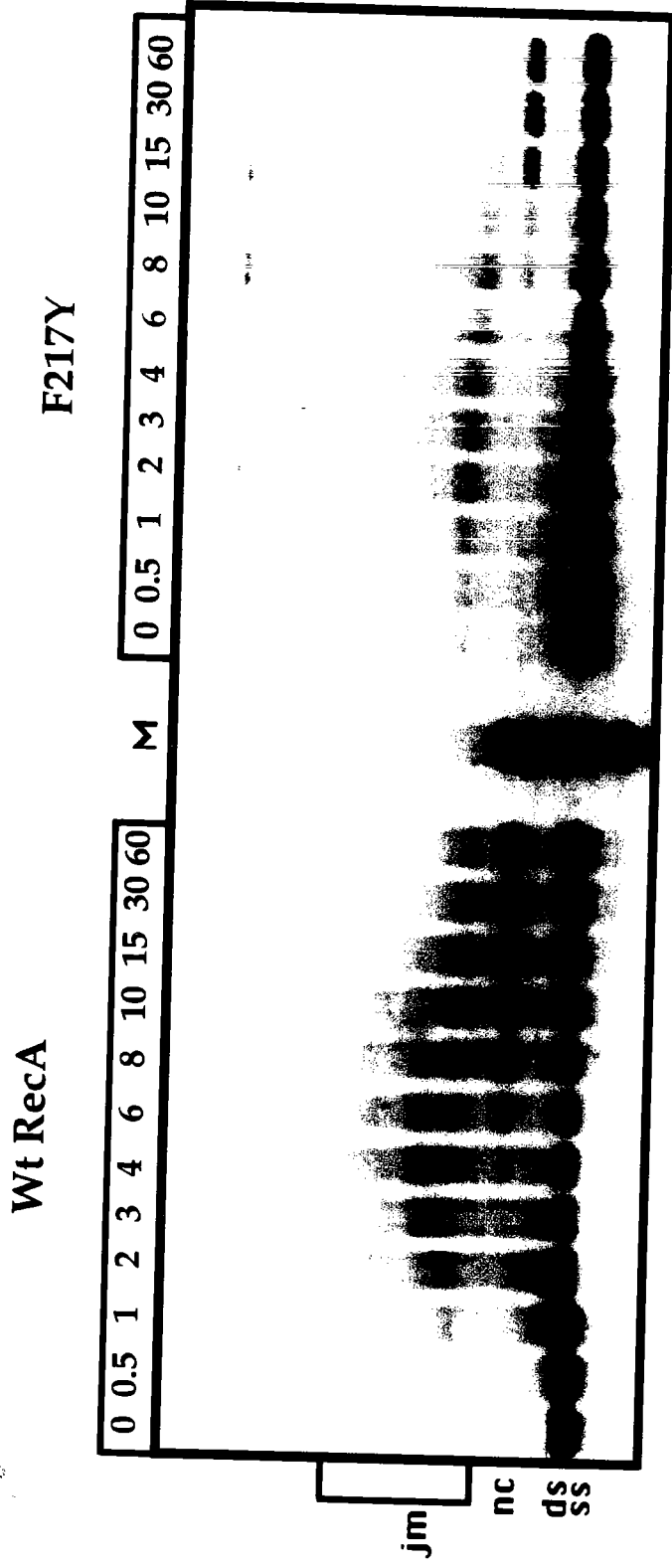
Figure 23. DNA strand exchange promoted by wt RecA and Phe217Tyr

Reactions included 6.7 μM protein, 10 μM φX174 single-stranded circular DNA (ss), 20 μM linearized φX174 double-stranded DNA (ds) and were incubated as described in Methods. Samples were removed at the indicated times (minutes, above each lane), added to stop buffer and were electrophoresed on a 0.8% agarose gel. DNAs were visualized by staining with ethidium bromide. Joint molecules (jm) are intermediates in the reaction that eventually resolve to the final product, nicked double-stranded circular DNA (nc), via RecA-catalyzed branch migration. M indicates DNA molecular weight markers.

efficiently, the progression of the reaction and resolution of intermediates is slowed relative to wild type RecA. Although the Phe217Tyr protein binds with higher affinity and cooperativity to ssDNA, there are several possible explanations for the observed decrease in strand exchange efficiency. The effective concentration of RecA in the reaction could be less for the mutant compared to wild type. Free protein filaments cannot bind directly to DNA and must first disassemble prior to their re-assembly on DNA (Morrical & Cox, 1985; Yu & Egelman, 1992). Given the propensity of the Phe217Tyr protein to form self-filaments in the presence of ATPγS (Figure 17E and Figure 22B), it may be that a certain population of this protein is not immediately available for catalysis of strand exchange. Also, the mutant protein may bind to dsDNA better than wild type, again lowering the concentration available for formation of active RecA-ssDNA filaments. Alternatively, the inherent catalytic ability of the mutant to carry out the branch migration phase of the reaction may be less than wild type RecA. Further studies have been designed to address these possibilities.

ATPase activity

We analyzed ssDNA-dependent ATP hydrolysis as a function of ATP concentration for both wild type and the Phe217Tyr mutant protein. As shown in Figure 24 the mutant protein has both a higher V_{max} and a higher affinity for ATP. Analysis of the data using the Hill equation shows that the mutant protein displays an approximate 1.2-fold increase in V_{max} and a 1.7-fold increase in affinity for ATP ($S_{0.5}$ = 36.6 and 62.2 µM for the mutant and wild type proteins,

respectively). Both proteins showed an equivalent basal level of ATP hydrolysis in the absence of ssDNA (V_i/E = 0.1 min^{-1}). Together with the DNA binding data, these results show that the Phe217Tyr mutation increases both cooperative protein-protein interactions and affinity for ATP.

Figure 24.
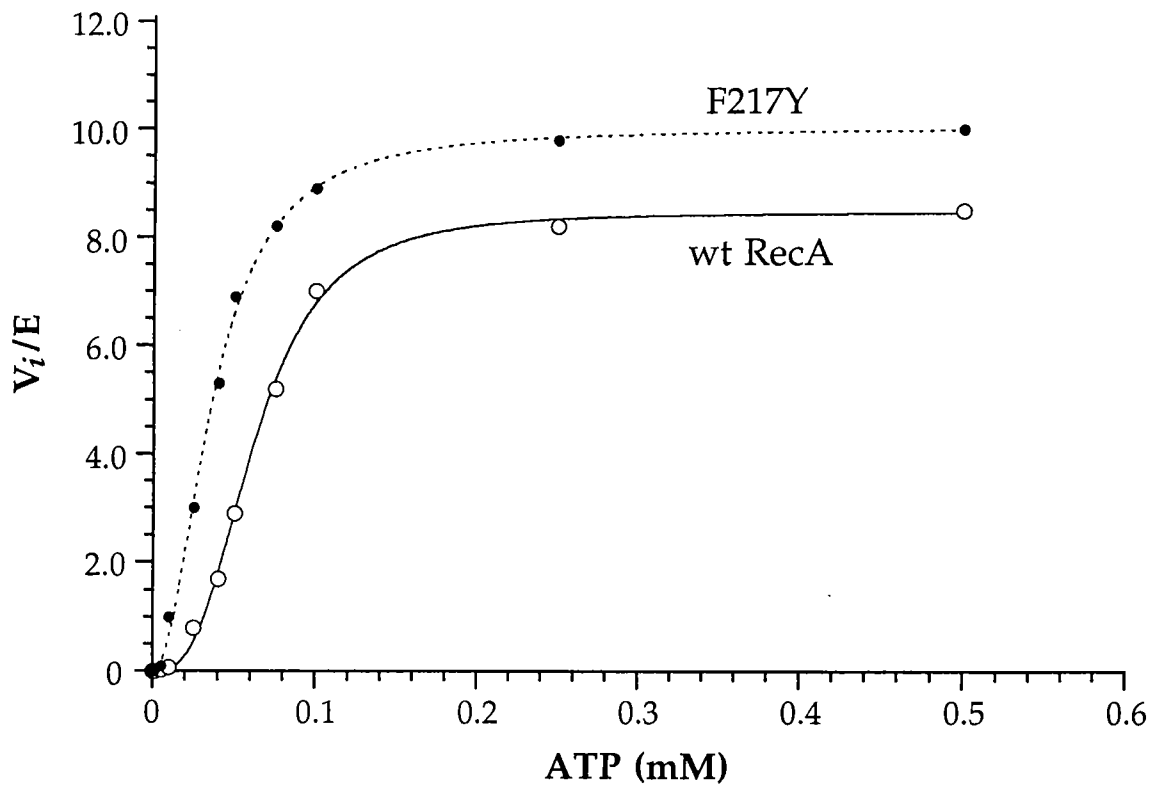
Figure 24. ATPase activity of both wild type RecA and the Phe217Tyr mutant protein as a function of ATP concentration. Reactions included 2 µM protein, 6 µM φX174 single-stranded circular DNA, the indicated concentrations of ATP and were incubated as described in Methods. Data were fit to the Hill equation as described in in the text.

Discussion

Substantial differences in subunit contacts between the active *vs.* inactive forms of RecA occur in a region of the structure other than that containing Phe217

Given that the helical pitch of free RecA filaments is ≈ 65 Å (the inactive form) and that of nucleoprotein filaments is ≈ 95 Å (the active form), differences in cross-subunit interactions likely exist between each of these two oligomeric states (Egelman, 1993). The data in this study show that ATP-mediated cooperative filament assembly is dramatically increased by virtue of a single, conservative mutation within one region of the RecA subunit interface. The fact that this increase occurs both in the presence and absence of DNA suggests that the positions of residues on either side of this region of the interface are similar whether RecA polymerizes on its own or on DNA. This idea is supported by two recent studies. First, in the region of the interface that includes Phe217, the efficiency of cross-subunit disulfide formation between specifically designed Cys substitutions was similar whether RecA was in the "active" or "inactive" form (Skiba *et al.*, 1999). Second, studies of another region of the RecA subunit interface (the N-terminal 28 residues in one monomer and residues 112 – 139 in the neighboring monomer) shows that certain mutations destabilize free RecA polymers to a far greater extent than nucleoprotein complexes (Eldin *et al.*, 2000). These results argue that significant differences in cross-subunit interactions

between free RecA oligomers *vs.* RecA nucleoprotein complexes occur in this latter area of the interface rather than in the region containing Phe217.

Mechanism of ATP-mediated information transfer across the RecA filament

The RecA crystal structure shows that Phe217 is close to positions in the neighboring monomer, specifically it is within van der Waals contact distance of the Thr150 and Ile155 side chains (Figure 25A and 24B). However, a Thr150Ser substitution imposes no defect in RecA function or structure, and Ile155 can tolerate a variety of polar and non-polar substitutions (Nastri & Knight, 1994). We, therefore, suggested that Phe or Tyr is required at position 217 because the side chain can form stable interactions with positions further within the neighboring monomer than is apparent in the structure (Skiba & Knight, 1994; Skiba *et al.*, 1999). Because a Tyr substitution at position 217 results in such a dramatic increase in ATP-dependent cooperative filament assembly, we propose that ATP-mediated allosteric information is transmitted across the RecA filament via the following mechanism. Gln194 serves as the γ-phosphate sensor within the ATP binding site (Kelley & Knight, 1997; Story & Steitz, 1992), and upon ATP binding its position is affected such that disordered loop 2 (L2, residues 195 - 209) assumes a structure that allows high affinity DNA binding (Voloshin *et al.,* 1996; Wang *et al.*, 1998). Phe217 is within a small helix (helix G) immediately downstream of the L2 region. Therefore, ATP-mediated conformational changes occurring within L2 will propagate through this helix and as a result, we propose that the Phe217 side chain inserts further into a pocket in the neighboring monomer. This insertion may be stabilized by hydrophobic interaction with

Figure 25A.
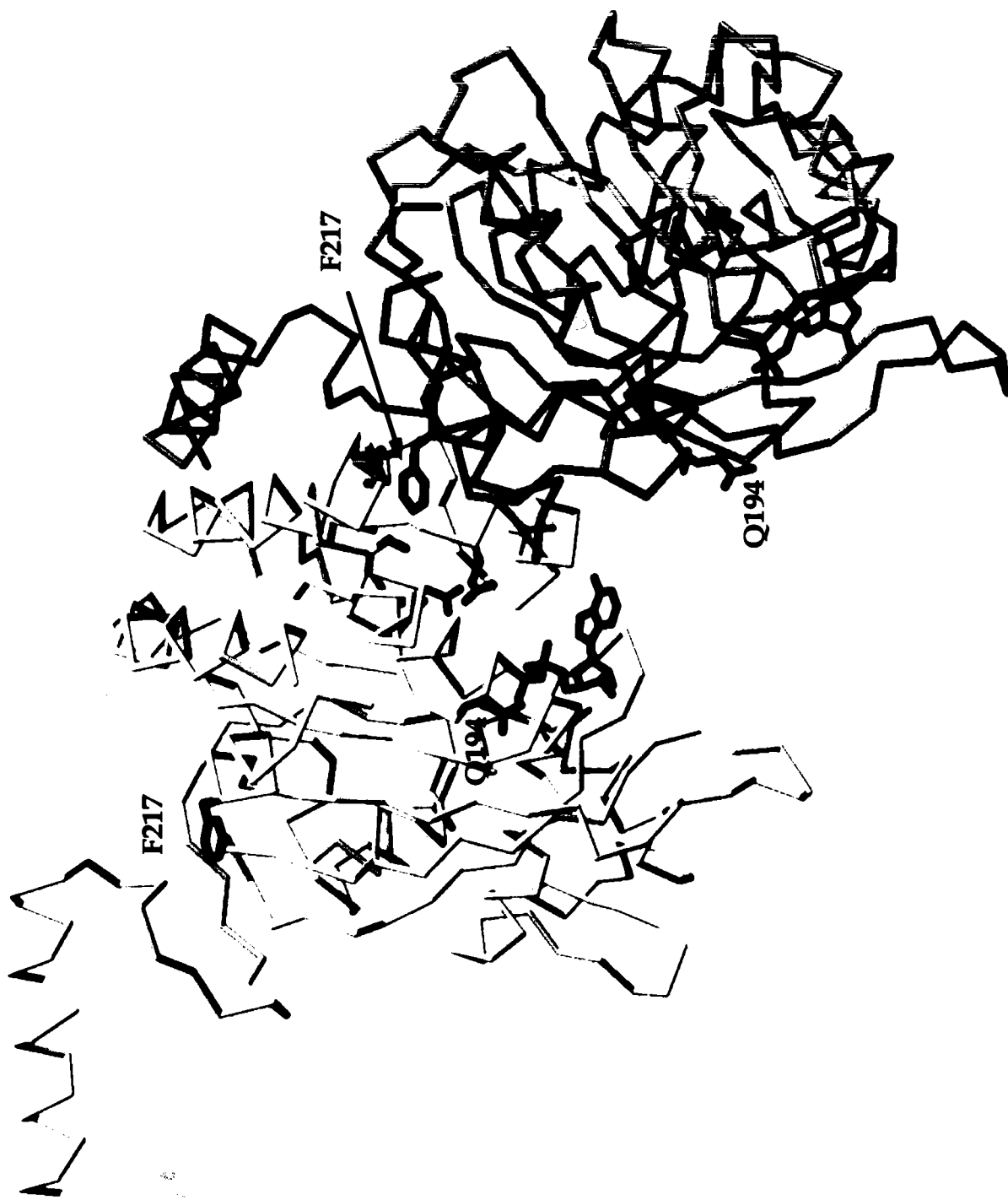
Figure 25B.
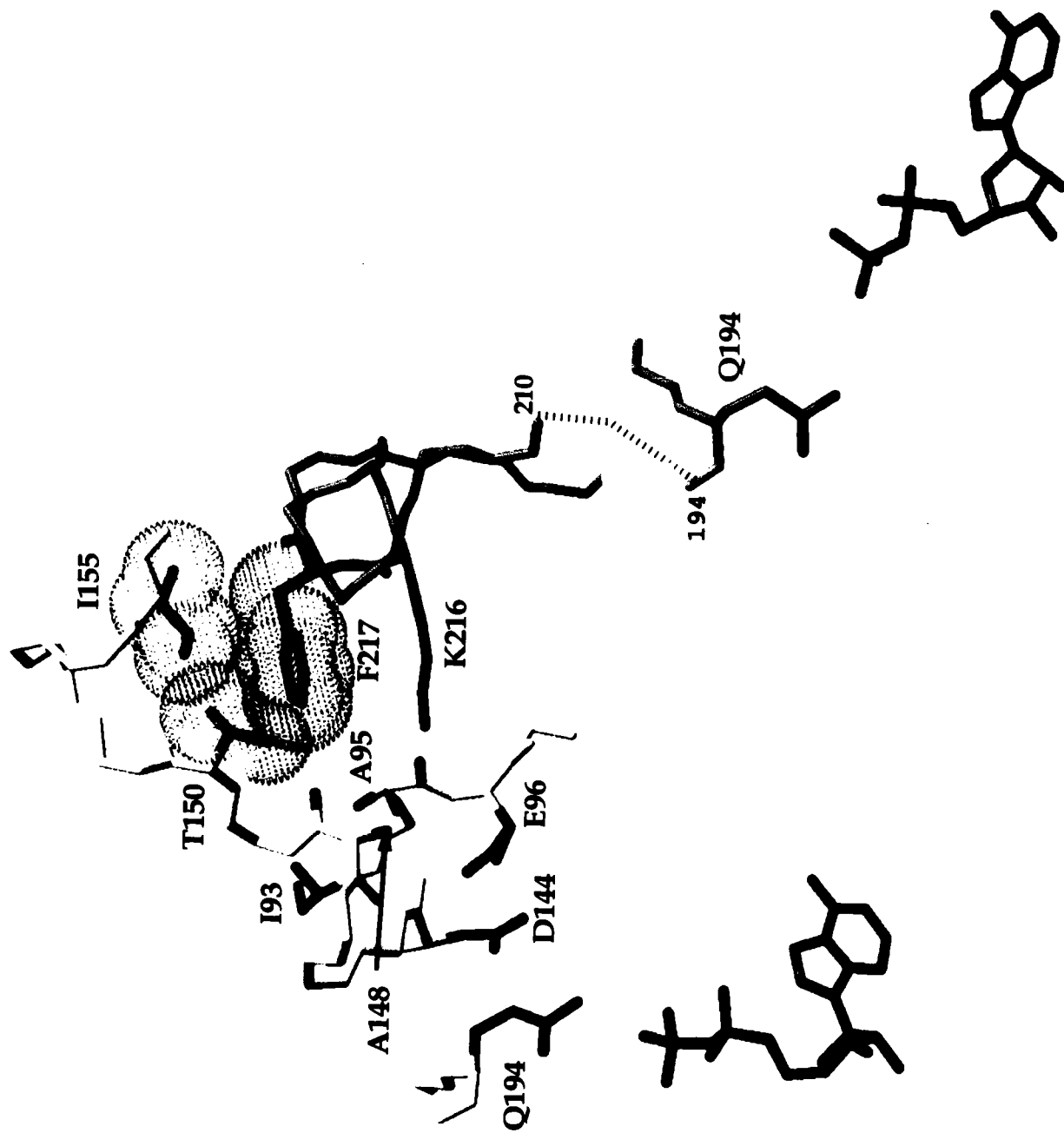
Figure 25C.
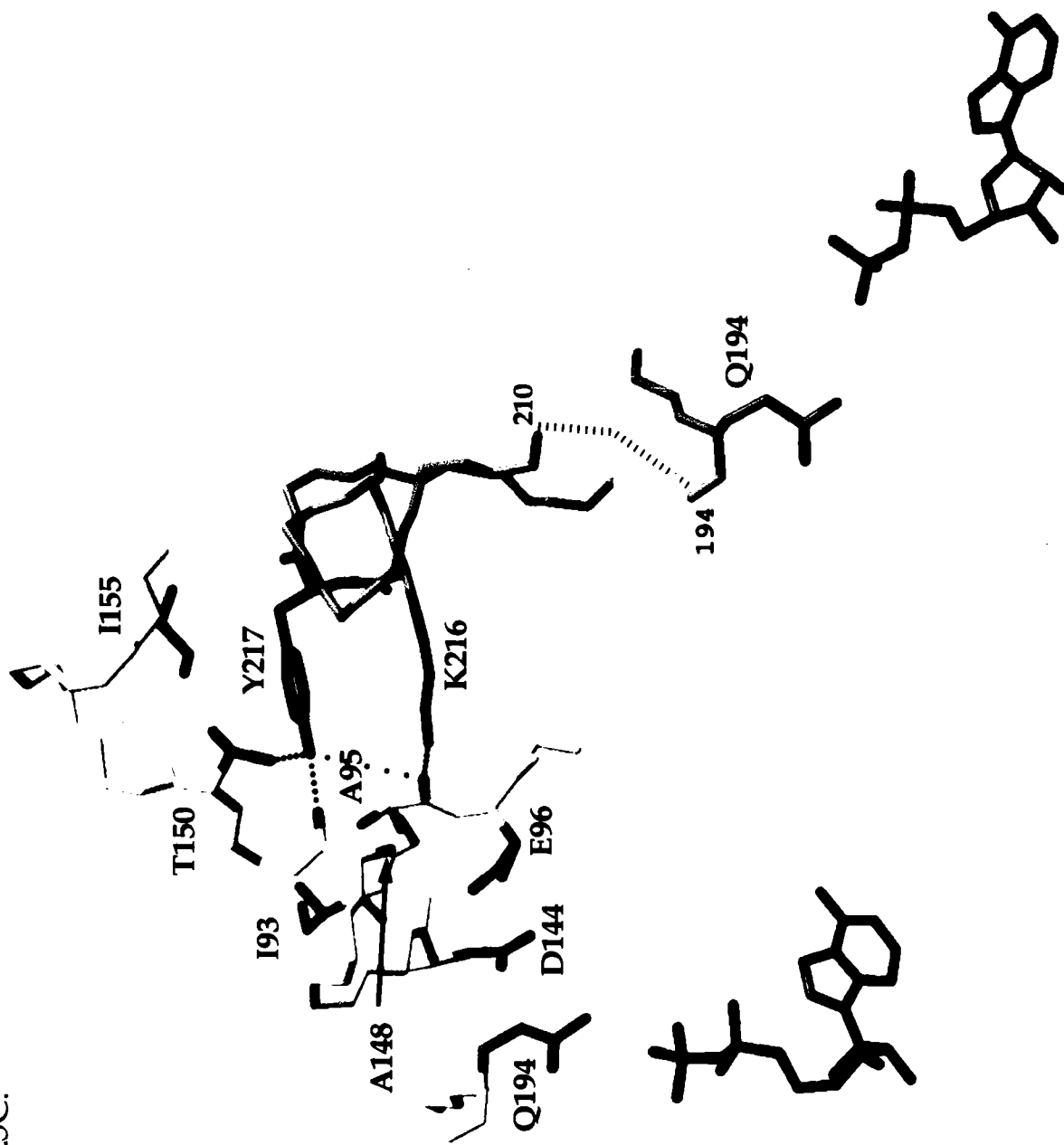
Figure 25. Structure of the RecA protein and specific interactions at the subunit interface. (A) An α-carbon trace of dimeric RecA taken from the crystal structure of the helical protein filament with the main chain of subunit 1 in yellow and subunit 2 in white. Gln194, Phe217 and ADP are shown in both subunits. In subunit 2 side chain carbons of Glu96, Asp144, Thr150 and Ile155 are dark gray, with side chain oxygens in red. **(B)** Detail of the region of the subunit interface involved in the proposed mechanism for ATP-mediated transfer of allosteric information. Phe217 is within van der Waals distance of Thr150 and Ile155 in the neighboring subunit. The model proposes that ATP binding in subunit 1 results in conformational changes that are propagated through the L2 region (residues 195-210; disordered in the current RecA structure) and into helix G (residues 212-219), thereby resulting in insertion of the Phe217 side chain further into a small pocket in subunit 2 (see text). Residues shown in subunit 1 include 191-194, 210-222 and ADP, and those in subunit 2 include 95-97, 144-155, 191-194 and ADP. **(C)** A Tyr has been modeled at position 217. Positions in the neighboring subunit within hydrogen bonding distance of the Tyr –OH include the main chain carbonyl oxygens of Ala95 and Ala148, and the –OH of Thr150. Also shown is Lys216 which may stabilize the position of either Phe or Tyr at position 217 through a cation-π interaction (see text). These images were created using the program Midas (U.C.S.F.).

several residues that lie within this pocket (Ile93, Ala95 and Ala148; Figures 25B, 25C, 26). By virtue of this insertion, cross-subunit interactions at the interface change in such a way that cooperative filament formation is enhanced. Upon ATP hydrolysis, Gln194 returns to its position in the inactive form of the enzyme resulting in low affinity DNA binding and a relaxation of cross-subunit interactions. The significant increase in cooperative filament assembly afforded by the Tyr substitution likely arises from its ability to form hydrogen bonds with positions in the neighboring monomer (see below).

Alternative cross-subunit contacts made by a Tyr side chain at position 217

Modeling a Tyr substitution at position 217 (Figure 25C) shows that the Tyr –OH is within hydrogen bonding distance of 3 positions in the neighboring monomer, the main chain carbonyl oxygens of Ala95, Ala148 and the side chain –OH of Thr150. The addition of one additional hydrogen bond, which contributes approximately 3-5 kcal of energy, could theoretically explain the more than 250 fold increase in ω for the Phe217Tyr mutant protein.

Also, the RecA structure shows that Lys216 lies immediately underneath Phe217, close enough to provide stabilization of the position of the Phe side chain via a cation-π interaction (Gallivan & Dougherty, 1999). The strength of a cation-π interaction in a Tyr/Lys pair increases if the Tyr –OH serves as a hydrogen bond donor (Mecozzi *et al.*, 1996), and given the proximity of residues in this region (Figure 25C), this may also contribute to the additional capability of filament formation by the mutant protein.

The molecular surface shown in Figure 26A provides an image of the pocket in the neighboring subunit into which residue 217 (either a Phe or Tyr) may insert. The open area in the neighboring subunit immediately in front of position 217 (Tyr217 is in green, Figure 26A) shows no steric constraints and again, stabilization of a transient insertion by the wild type Phe side chain may occur by interaction with hydrophobic residues in this pocket. Depending on the degree to which the mutant Tyr side chain inserts into this pocket several other positions appear as candidates for hydrogen bonding interactions, e.g. main chain nitrogens at Gly122 and Thr150. Additionally, regions of the polypeptide backbone at Thr121 and Gly122 may provide a planar surface with which the ring of a Phe or Tyr side chain could stack.

The RecA structure also shows that Phe217 lies very close to the ATP binding and catalytic site of the neighboring monomer (Figures 24 and 25B). Glu96 is proposed to activate a water molecule for an in-line attack of the γ-phosphate of ATP and Asp144 may stabilize binding of the active site Mg^{2+} (Story & Steitz, 1992). The idea that conformational changes in this region of the interface contribute to the cooperativity observed for ATP binding and hydrolysis (Mikawa, 1998; this study) is supported by our observation that both the affinity for ATP and the rate of ATP hydrolysis is increased by the Phe217Tyr mutation.

Figure 26-A.
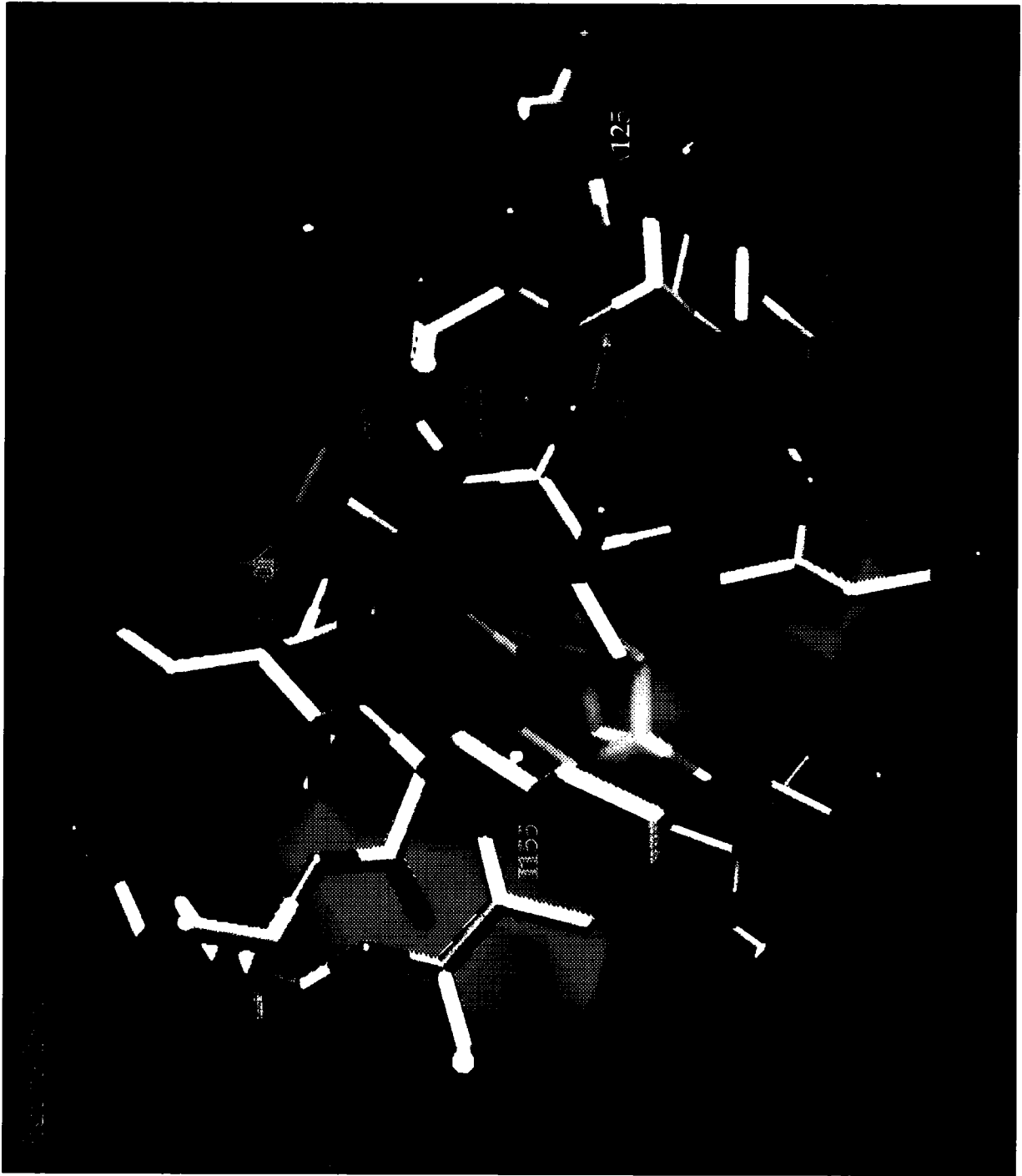
Figure 26. Molecular surface of the neighboring monomer with which residue 217 interacts. (A) The surface is colored by atom type (carbon = gray; oxygen = red; nitrogen = blue). In this view, looking from position 217 toward the neighboring monomer, the Tyr substitution at position 217 is seen to lie immediately across from a pocket in the adjacent subunit. (B) A top view of the pocket showing positions that may promote stable interactions with a Tyr side chain at position 217 (see text). Figures were created using the program GRASP.

Supporting evidence for this allosteric mechanism

The key roles played by each of the structural elements in this mechanism (*i*) Gln194, (*ii*) residues within and immediately flanking L2 and (*iii*) Phe217 are supported by previous studies. Each of 16 substitutions at position 194 gives rise to a *recA-* phenotype, and three mutant proteins, Gln194Asn, Gln194Glu or Gln194Ala are completely inhibited for all ATP-dependent activities (Kelley & Knight, 1997). Subsequent studies confirmed that the wild type Gln194 is essential for RecA function (Hörtnagel *et al.*, 1999). Studies of the L2 sequence support the idea that it makes up all, or a significant portion, of RecAs primary DNA binding site (Voloshin *et al.*, 1996). Upon ATP binding the L2 region undergoes a dramatic conformational shift from random coil to a β-structure (Voloshin *et al.*, 1996; Wang *et al.*, 1998). Additionally, both Gly211 and Gly212, which lie immediately next to L2 at the N-terminus of helix G, cannot tolerate any substitution (Hörtnagel *et al.*, 1999). Both residues are invariant among eubacterial RecA proteins (Roca, 1997; Story *et al.*, 1993) and it has been proposed that they may be involved directly in DNA binding or in mediating ATP-induced conformational changes (Story *et al.*, 1993). Our data strongly suggests that the flexibility of the polypeptide backbone at these positions is important for the propagation of conformational changes transmitted from the ATP binding site to the subunit interface at position 217. The mutational stringency at position 217, although strict, is less so than at Gln194. A Phe217Tyr substitution still permits wild type-like recombination function and a Cys substitution maintains partial activity (approximately 10 – 20% recombination function), while all other substitutions result in a *recA⁻* phenotype (Skiba & Knight, 1994; Skiba *et al.*, 1999).

All other side chains in this region that contact positions in the neighboring monomer (Asn213, Lys216, Tyr218 and Arg222) show a greater tolerance for mutation than does Phe217 (Skiba & Knight, 1994).

Implications for allosteric mechanisms in related enzymes: eukaryotic RecA homologues and DNA helicases

Published alignments comparing the bacterial RecA sequence with the yeast and human Rad51 and DMC1 proteins show that Gln194, Gly211 and Gly212 are conserved (Habu *et al.*, 1996; Shinohara *et al.*, 1992; Story *et al.*, 1993; Yoshimura *et al.*, 1993). This suggests that ATP may regulate allosteric events in these 4 eukaryotic proteins using a mechanism similar to that described here for RecA. However, residues in RecA helix G, including Phe217, are not conserved in either of the Rad51 or DMC1 proteins. As with RecA, binding of *S. cerevisiae* Rad51 to ssDNA is dependent on ATP (Namsaraev & Berg, 1998). Unexpectedly, however, the human Rad51 protein binds ssDNA cooperatively and with high affinity in the absence of ATP (De Zutter & Knight, 1999). Therefore, despite the fact that these residues play important roles in the allosteric mechanism of RecA, ATP-mediated allosteric events and key residues involved in propagating information across the protein filament may be quite different for human Rad51.

Functional and structural studies of helicase enzymes reveal distinct similarities with the RecA protein regarding the use of ATP as an allosteric effector (Egelman, 1998; Soultanas & Wigley, 2000). For example, Gln254 in the

B. stearothermophilus PcrA helicase corresponds to Gln194 in RecA (Subramanya *et al.*, 1996), and the PcrA structure shows that Gln254 is likely to be the switch that communicates ATP binding and hydrolytic events to a DNA binding site immediately downstream (residues 254-264) (Subramanya *et al.*, 1996). Likewise, Sawaya *et al.* (1999) propose that His465 serves as the γ-phosphate sensor in the NTP binding site of the bacteriophage T7 gene 4 protein and, like Gln194 in RecA, propagates conformational changes to the DNA binding motif H4. In fact, in all other DnaB helicase family members residue 465 is Gln (Sawaya *et al.*, 1999). The structure of this helicase domain of the T7 gene 4 protein shows a remarkable similarity to the helical filament structure of RecA (Sawaya *et al.*, 1999). However, a larger fragment of the gene 4 protein that is fully active as a helicase *in vitro*, crystallizes as a closed hexameric ring, which is thought to be the active form of the enzyme (Singleton *et al.*, 2000). Therefore, the subunit interface in hexamer helicase structures is very different from RecA and, although the mechanism by which ATP mediates DNA binding appears similar, it is unlikely that ATP regulates subunit interactions in helicases in a way related to that in RecA. While the helicase DnaB family may be derived from a *recA* gene duplication (Leipe *et al.*, 2000), RecA appears to have evolved to accommodate the fact that its functional form is a helical protein filament whose assembly and disassembly on DNA substrates is mediated by ATP-induced allosteric events.

Conservative point mutations within subunit interfaces that give rise to increases in cooperative behavior have been identified in several other systems.

For example, an Arg152Lys substitution creates a "hypercooperativity" mutant in *E. coli* phosphofructokinase (Auzat *et al.*, 1995). Similarly, a Thr72Val mutation in *S. inaequivalvis* hemoglobin results in an increase in cooperative oxygen binding (Royer *et al.*, 1996). Our studies of the Phe217Tyr mutant show a striking increase in cooperative assembly of a RecA protein filament. Together with previous mutational analysis our data identifies Phe217 as a critical component within the subunit interface that regulates the transmission of allosteric information throughout the protein filament. Further studies will identify specific conformational changes occurring within the neighboring subunit which potentiate the cooperative nature of monomer-monomer interactions as well as ATP binding and hydrolysis.

Acknowlegements

I would like to acknowledge Tony Forget for the work presented in this chapter on EM studies of both wt and Phe217Tyr RecA. Additionally, Karen Logan performed the strand exchange experiments presented for wt and Phe217Tyr RecA.

Chapter V

The hRad51 and RecA Proteins Show Significant Differences in Cooperative Binding to Single-Stranded DNA

Introduction

Formation of a nucleoprotein filament that is active for the initiation of DNA strand exchange is the hallmark of the bacterial RecA protein and its eukaryotic counterparts (Baumann et al., 1996; Benson et al., 1994; Eggleston & West, 1996; Kowalczykowski et al., 1994; Radding, 1989; Roca & Cox, 1997). Comparison of the hRad51, ScRad51 and bacterial RecA sequences shows strong similarities within a 207 amino acid core domain, while the N- and C-terminal regions show only sparse homology (Ogawa et al., 1993b; Shinohara et al., 1993; Yoshimura et al., 1993). The extended nucleoprotein filament structure formed by all 3 proteins displays remarkable similarities (Benson et al., 1994; Egelman, 1993; Ogawa, 1993c; Sung & Robberson, 1995) and both Rad51 proteins carry out a number of RecA-like activities in vitro, such as DNA-dependent ATP hydrolysis, DNA strand annealing and strand exchange (Baumann et al., 1996; Benson et al., 1994; Gupta et al., 1997; Sung, 1994). This suggests that there is an overall conservation of the processes of homologous recombination from bacteria to humans.

However, despite these similarities, there also appears to be fundamental mechanistic differences between these 3 proteins. The turnover number of Rad51 is approximately 30-fold less than that reported for RecA (Gupta *et al.*, 1997; Sung, 1994). In addition, although all three of these proteins catalyze homologous pairing and strand exchange, catalysis of strand exchange by RecA proceeds efficiently in the absence of other proteins (Kowalczykowski *et al.*, 1994), while both *Sc*Rad51 and hRad51 require the presence of other factors such as RPA and/or Rad52 (Baumann *et al.*, 1996; Benson *et al.*, 1998; New *et al.*, 1998; Shinohara & Ogawa, 1998; Sugiyama *et al.*, 1997; Sung, 1994; Sung, 1997), or Rad54 for certain substrates (Petukhova *et al.*, 1998). Sung and Stratton (Sung & Stratton, 1996) observed a rather remarkable difference between *Sc*Rad51 and RecA in that a Lys→Arg substitution in the consensus GK(S/T) "Walker A" motif of *Sc*Rad51 inhibited ATPase activity but still allowed completion of DNA strand exchange *in vitro*. This mutant also complemented the MMS sensitivity of a *RAD51*Δ strain. In RecA, however, the same Lys→Arg substitution allows initiation of strand exchange *in vitro*, but not completion of the reaction (Rehrauer & Kowalczykowski, 1993), and confers a completely U.V.-sensitive, *rec*⁻ phenotype (Konola *et al.*, 1994). Further, while Δ*recA* bacteria and *RAD51*Δ yeast are viable (Kowalczykowski *et al.*, 1994; Petes *et al.*, 1991), disruption of *RAD51* in mouse cells results in embryonic lethality (Lim & Hasty, 1996; Tsuzuki *et al.*, 1996), a result which may reflect the inherent complexity of Rad51 function in higher eukaryotes. Taken together, these results suggest that while the overall process of homologous recombination may be conserved, the molecular mechanisms by which it proceeds may show significant and important variations

among different classes of organisms. To more fully understand the processes mediated by the hRad51 protein, and to provide a more quantitative view of the underlying mechanistic differences between the hRad51 and RecA proteins, we have performed a series of experiments, which compare their binding to ssDNA. Our data show unexpected differences in both the equilibrium and kinetic binding properties of these proteins, which suggest a fundamentally different role for ATP as an energy source and allosteric effector in promoting hRad51 *vs.* RecA-mediated homologous recombination.

Results

hRad51 ssDNA binding: equilibrium parameters

DNA binding time courses were performed using a variety of hRad51 concentrations in either the absence or presence of a nucleotide cofactor. Figure 27 shows a representative series of time courses for hRad51 in the presence of ATPγS. Similar experiments were performed in the presence of ATP (with an ATP regenerating system) and in the absence of NTP, but for ease of comparison we show in Figure 27B binding curves for 60.4 nM hRad51 in the absence of NTP, or in presence of ATPγS. The addition of either ATP or ATPγS results in a slight decrease in both the rate and magnitude of binding. The extent of binding (binding response at equilibrium) was calculated for each concentration of protein from the curves in Figure 27A, and from similar curves obtained in the presence of ATP or in the absence of nucleotide cofactor. Data were fit to the form of the Hill equation shown below using KaleidaGraph™ 3.08d (Synergy Software, Reading, PA)

$$\text{(extent bound) } b = \frac{B_{max}S^{n(app)}}{K' + S^{n(app)}}$$

where B_{max} is the maximum amount of protein-DNA complex (reported as maximum extent of binding in arc sec), S is protein concentration (free) and K' is a complex constant comprising interaction factors which reflect successive

Figure 27.
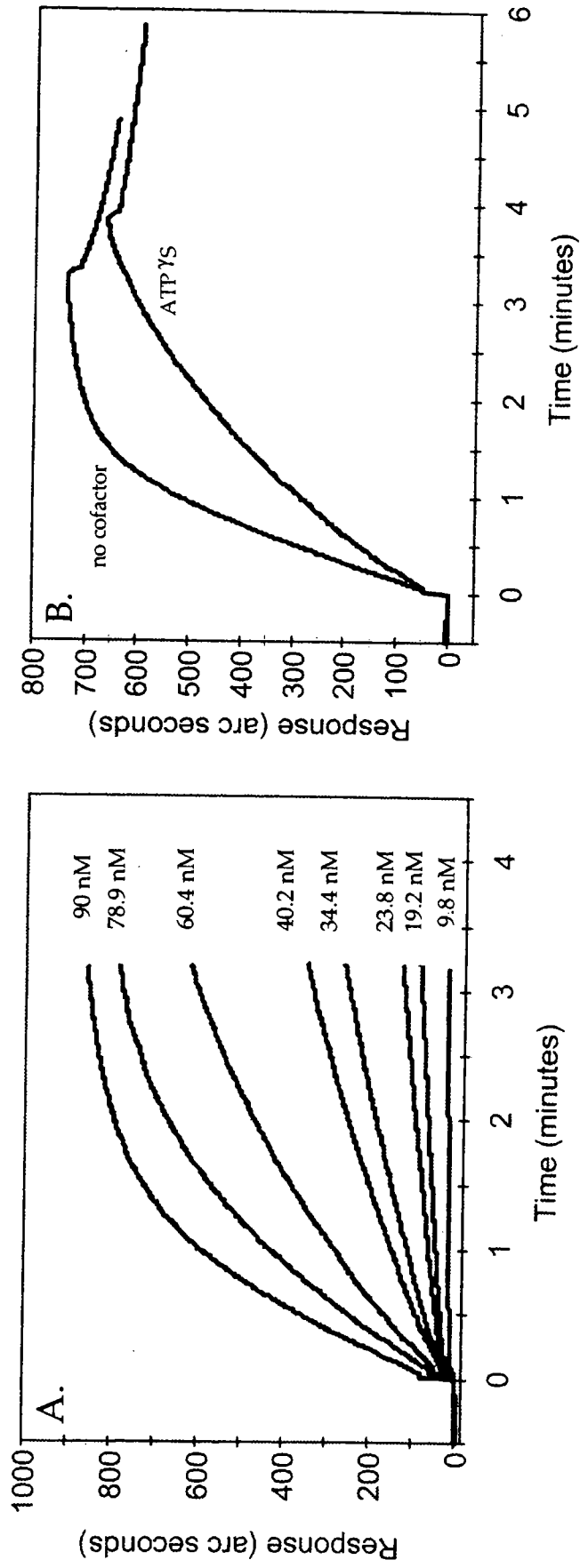
Figure 27. Biosensor hRad51-ssDNA binding time courses. (A) Time courses of ssDNA binding in the presence of ATPγS using various concentrations of hRad51 protein. Extent of binding as a function of time is measured in arc sec. **(B)** Binding time courses using 60.4 nM hRad51 in the absence or presence of ATPγS.

binding and dissociation steps along the cooperative binding pathway (Segel, 1975). The Hill coefficient (n_{app}) is interpreted as the number of binding sites in an allosteric protein that are recruited into the cooperative binding mechanism upon the first binding event (Segel, 1975). Here, n_{app} can be interpreted as the minimum number of interacting monomers during growth of the nucleoprotein filament which give rise to the observed cooperative binding parameters $S_{0.5}$, the protein concentration at the mid-point of the titration curve, is calculated as $S_{0.5} = \sqrt[n_{app}]{K'}$ (Segel, 1975) and is equivalent to the dissociation constant, K_D, in a noncooperative system.

The sigmoidal nature of the Hill plots in Figure 28 indicates cooperative binding of hRad51 to ssDNA in both the absence and presence of NTP. Calculated values for B_{max}, K', n_{app}, and $S_{0.5}$ are listed in Table II. These data show that, unlike RecA (see below), hRad51 does not require a nucleotide cofactor to bind cooperatively and with high affinity to ssDNA. In the absence of NTP, $S_{0.5} = 35.3$ nM and $n_{app} = 2.7$. In the presence of ATPγS, n_{app} increases 1.5 fold, from 2.7 to 4.3, indicating that the protein binds to ssDNA with greater cooperativity in the presence of this nucleotide cofactor. ATP does not show a significant change in n_{app}. Unexpectedly, we find that both ATP and ATPγS result in a slight decrease (< 2-fold) in the affinity of hRad51 for the ssDNA substrate ($S_{0.5} = 66$ nM). These results were reproducible over 4 different sets of experiments. High affinity binding of hRad51 to ssDNA in both the absence and

presence of NTP was also shown using a more conventional gel shift assay (data not shown). Interestingly, even this qualitative assay shows a slight decrease in the ssDNA binding affinity of hRad51 in the presence of ATPγS. Our results are consistent with other studies which have suggested that hRad51 does not require a nucleotide cofactor to bind ssDNA (Benson *et al*, 1994; Baumann *et al*, 1996; Gupta *et al*, 1997).

Figure 28.
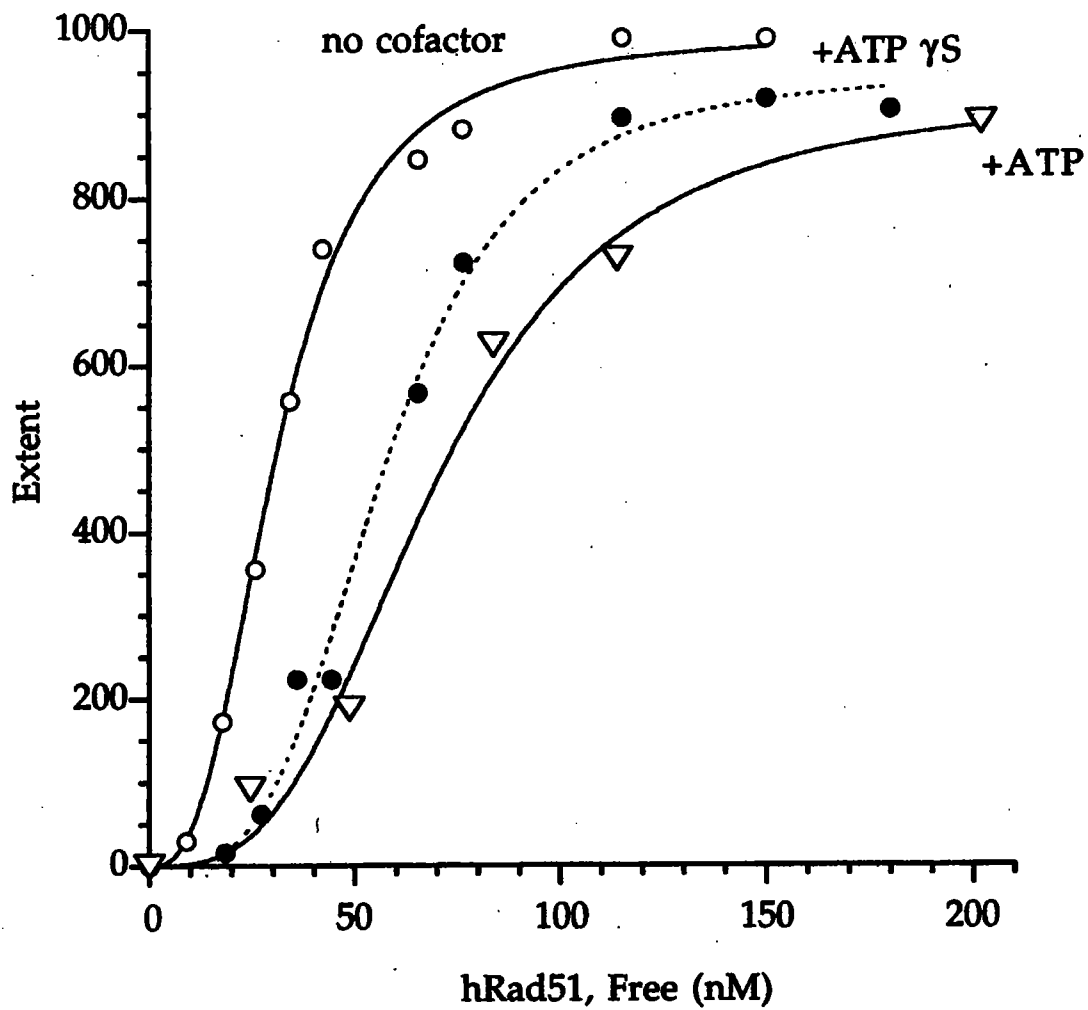
Figure 28. **Biosensor hRad51-ssDNA binding as a function of protein concentration.** Extent data from time courses in Figure 27 were fitted to the Hill equation as described on page 126 to calculate B_{max}, n_{app}, K', and $S_{0.5}$. Values are listed in Table II on page 133. Extent is the calculated maximum binding at equilibrium in arc seconds for each protein concentration.

Table II

Equilibrium ssDNA Binding Parameters for hRad51 and RecA. Values for B_{max}, n_{app}, K' and $S_{0.5}$ are derived from averages of 4 sets of data as shown in Figures 29 and 31 using the Hill equation as described in the text. Standard errors were calculated from 4 separate series of time courses. Errors are not shown for K' but are in the same range as those for the other parameters in the Table (from 5 – 30%).

	hRad51			RecA	
	(-)NTP	(+)ATP	(+)ATPγS	(-)NTP	(+)ATPγS
B_{max}	1108.3 ± 374	914.5 ± 180	1042.7 ± 250	216.4 ± 14.5	772.7 ± 33.3
n_{app}	2.74 ± 0.28	3.11 ± 0.31	4.28 ± 0.23	1.54 ± 0.36	5.33 ± 3.98
K'	3.81×10^{-21}	4.60×10^{-23}	1.95×10^{-31}	8.22×10^{-10}	7.59×10^{-39}
$S_{0.5}$ (nM)	35.3 ± 10.1	65.7 ± 8.2	66.8 ± 6.9	$1,260.6 \pm 252.1$	70.5 ± 20.5

We also performed hRad51 binding experiments in a low salt buffer [10 mM Na_2HPO_4/NaH_2PO_4 (pH 7.4), 20 mM NaCl, 5 mM $MgCl_2$, 0.05% Tween20] in the absence and presence of nucleotide cofactors and found no significant change in either the binding time courses or the calculated equilibrium binding parameters (data not shown). Additionally, experiments performed in PBS-Tween buffer with Mg^{+2} concentrations varying from 1–5 mM showed no significant differences in the calculated equilibrium binding parameters. Therefore, salt concentrations between 20 mM (low salt buffer) and 165 mM (PBS-Tween-Mg buffer) and Mg^{2+} concentrations between 1-5 mM show no significant differences in the affinity of hRad51 for this oligonucleotide substrate.

RecA ssDNA binding: equilibrium parameters

Figure 29A shows a representative series of RecA-ssDNA binding time courses in the presence of ATPγS. Again, similar experiments were performed in the absence of NTP but for ease of comparison we show binding time courses for 250 nM RecA in the absence and presence of ATPγS, and 15 μM RecA in the absence of ATPγS. The data in Figure 29B serve to emphasize the dramatic increase in ssDNA binding affinity induced by ATP or ATPγS, as has been previously described (Menetski & Kowalczykowski, 1985b; Silver & Fersht, 1982). Data were fit to the Hill equation as for hRad51 and the resulting plots are shown in Figure 30. Calculated values for B_{max}, K', n_{app} and $S_{0.5}$ are listed in Table II. In the absence of a nucleotide cofactor, the binding curve (Figure 30A) shows only a hint of

Figure 29.
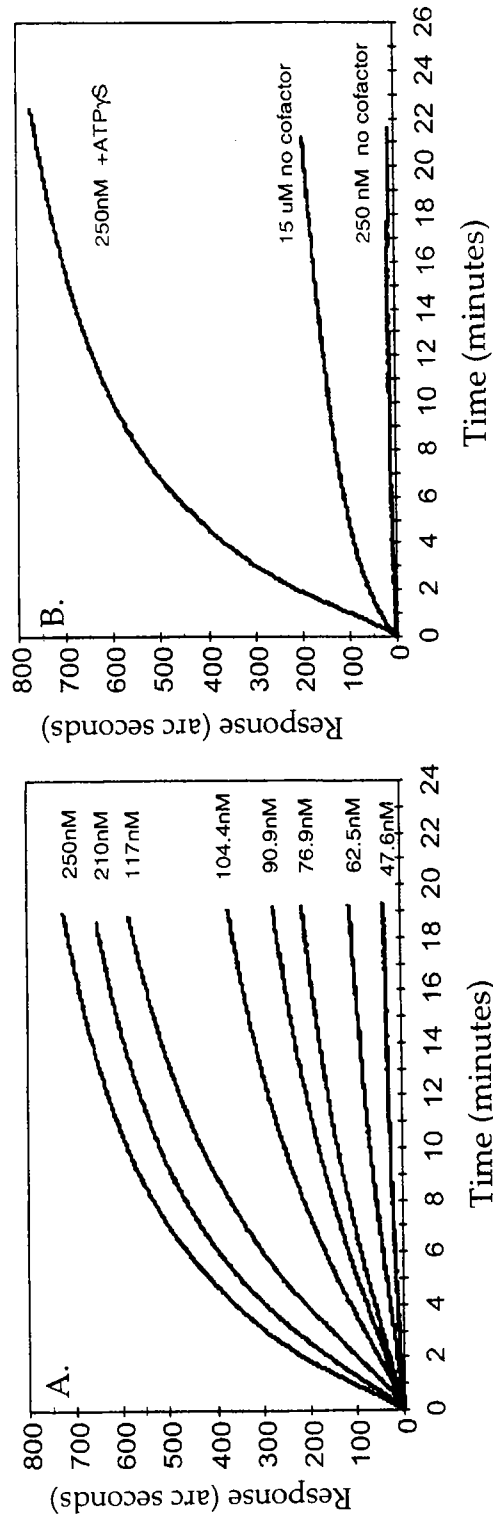
Figure 29. Biosensor RecA-ssDNA binding time courses. **A.** Binding time courses using various concentrations of RecA protein. Extent of binding as a function of time is measured in arc sec. **B.** Binding time courses using 250 nM RecA in the absence or presence of ATPγS. A time course using 15 μM RecA (-ATPγS) is included to emphasize the dramatic increase in affinity induced by ATPγS, and to show that curves in the absence of nucleotide cofactor do approach equilibrium, but over longer times than those in the presence of ATPγS.
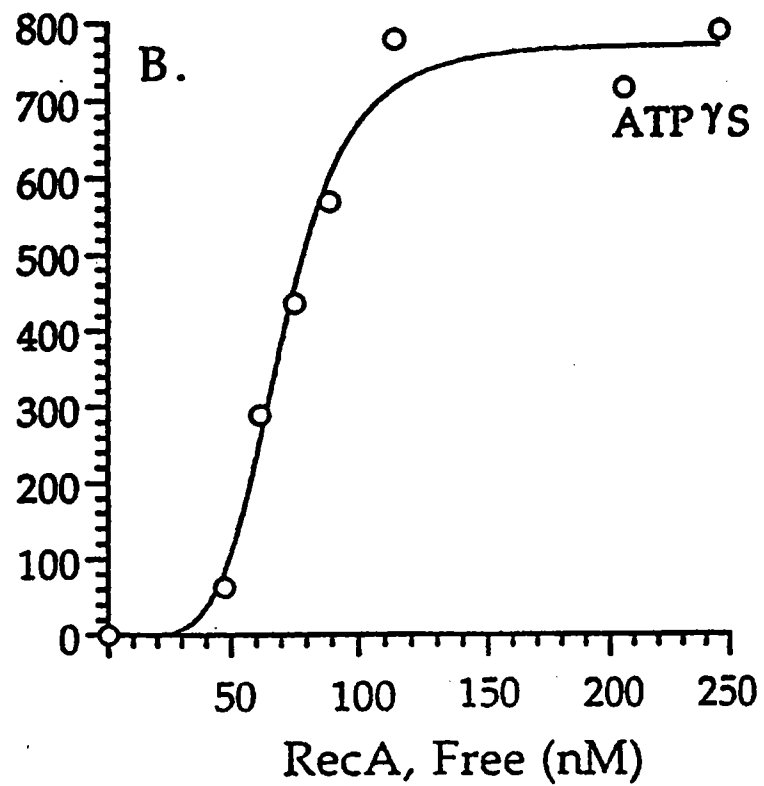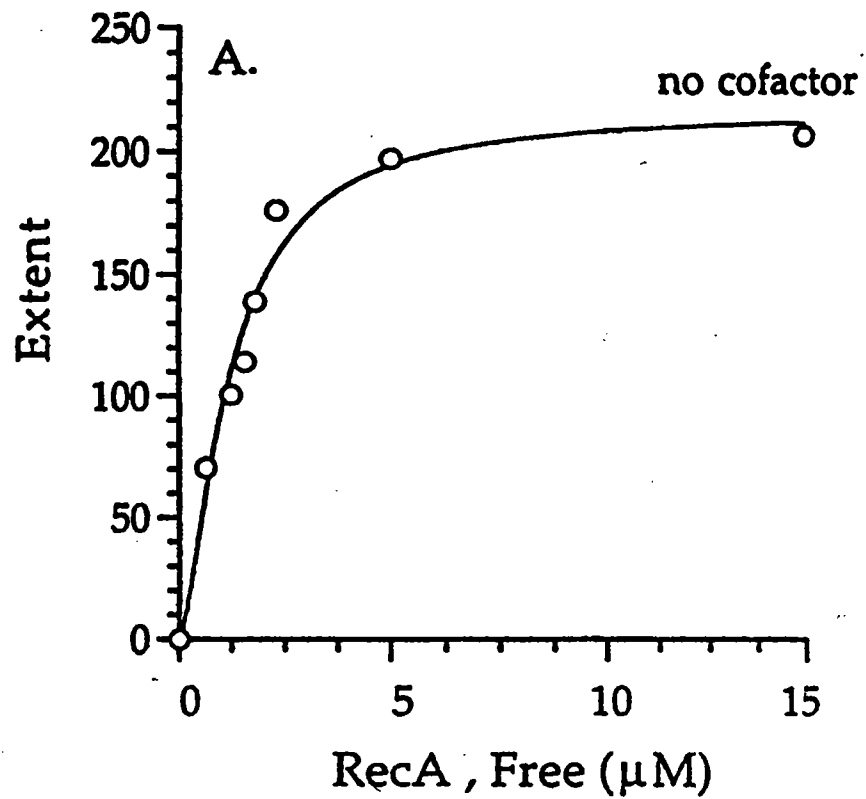
Figure 30.

Figure 30. **Biosensor RecA-ssDNA binding as a function of protein concentration.** Maximum extent of binding at each RecA concentration in the absence (**A**) or presence (**B**) of ATPγS was calculated and data fit to the Hill equation as described on page 126. Calculated values for B_{max}, K', n_{app}, and $S_{0.5}$ are listed in Table II on page 133. An ATPγS-induced increase in the cooperativity of binding is apparent from the increased sigmoidal character of the curve in B.

cooperativity (n_{app} = 1.5) and the protein binds with low affinity to ssDNA ($S_{0.5}$ = 1.26 µM). However, with the addition of ATPγS, there is a dramatic 18-fold increase in the affinity ($S_{0.5}$= 70.5 nM) and a 3.5-fold increase in the Hill coefficient (n_{app}= 5.33). As for hRad51, gel shift experiments corroborate the effects of a nucleotide cofactor on the affinity of RecA for ssDNA (data not shown). Additionally, filter binding data presented for wt RecA (Figure 12; Chapter III) and also reveals a dramatic increase in ssDNA binding when a nucleotide cofactor is introduced. From these data and from that shown in the next section, we estimated an apparent K_D of 20 µM and 1 µM in the presence and absence of ATPγS, respectively. Although this NTP-induced increase in ssDNA binding affinity has been well documented, we show in the next section that it appears to be accounted for almost entirely by an increase in the cooperative nature of nucleoprotein filament formation.

Determination of K and ω for hRad51 and RecA binding to ssDNA

We also analyzed our data using procedures similar to those described by Kowalczykowski (Kowalczykowski *et al.*, 1986). This type of analysis permits a separation of parameters that define the intrinsic ssDNA binding affinity from the cooperative nature of filament assembly (see below), and allows one to understand how a nucleotide cofactor affects each of these aspects of the binding event. The expression used to analyze the data generated was as follows,

$$L = \frac{v}{K(1-nv)\left[\frac{(2\omega-1)(1-nv)+v-\left\{(1-(n+1)v)^2+4\omega v(1-nv)\right\}^{1/2}}{2(\omega-1)(1-nv)}\right]^{n-1}\left[\frac{1-(n+1)v+\left\{(1-(n+1)v)^2+4\omega v(1-nv)\right\}^{1/2}}{2(1-nv)}\right]^2}$$

where L is the concentration of free ligand, n is the number of bases bound by ligand (binding site size), v is the binding density of the ligand on the DNA (mol ligand/mol base), K is the intrinsic binding constant of a single monomer for ssDNA and ω is the cooperativity parameter, defined as the relative affinity of an incoming ligand for a contiguous vs. an isolated site (Kowalczykowski et al., 1981; Kowalczykowski et al., 1986; McGhee & von Hippel, 1974). The model in Figure 31 shows initial binding of hRad51 and RecA to an isolated site with affinity K, and subsequent directional binding to a "singly contiguous" site with affinity Kω (McGhee & von Hippel, 1974). Best fits for K and ω were obtained by iterative, nonlinear regression analysis using the software package KaleidaGraph™ 3.08d (Synergy Software, Reading, PA). A value of $n = 3$ (Roca & Cox, 1997; Zlotnick et al., 1993) was used and v was defined as the fractional maximum extent of binding/n. We have assumed, as in earlier studies (Menetski & Kowalczykowski, 1985b), that nucleoprotein filament assembly proceeds by addition of protein monomers to the growing filament. The product $(K\omega)^{-1}$ is equivalent to $S_{0.5}$, the protein concentration at the midpoint of the titration curve.

Values for K, ω and $(K\omega)^{-1}$ are listed in Table III. In the absence of nucleotide, hRad51 exhibits a significantly greater intrinsic affinity (K $= 1.2 \times 10^6$ M^{-1}) than RecA (4.8×10^4 M^{-1}). In addition, the effect of nucleotide cofactors on the intrinsic affinity is very different for the two proteins. For hRad51, the intrinsic affinity is decreased approximately 10-fold in the presence of NTP (K$_{ATP\gamma S} = 1.4 \times$

Figure 31.

$$K \rightleftharpoons \qquad \qquad \rightleftharpoons K\omega$$
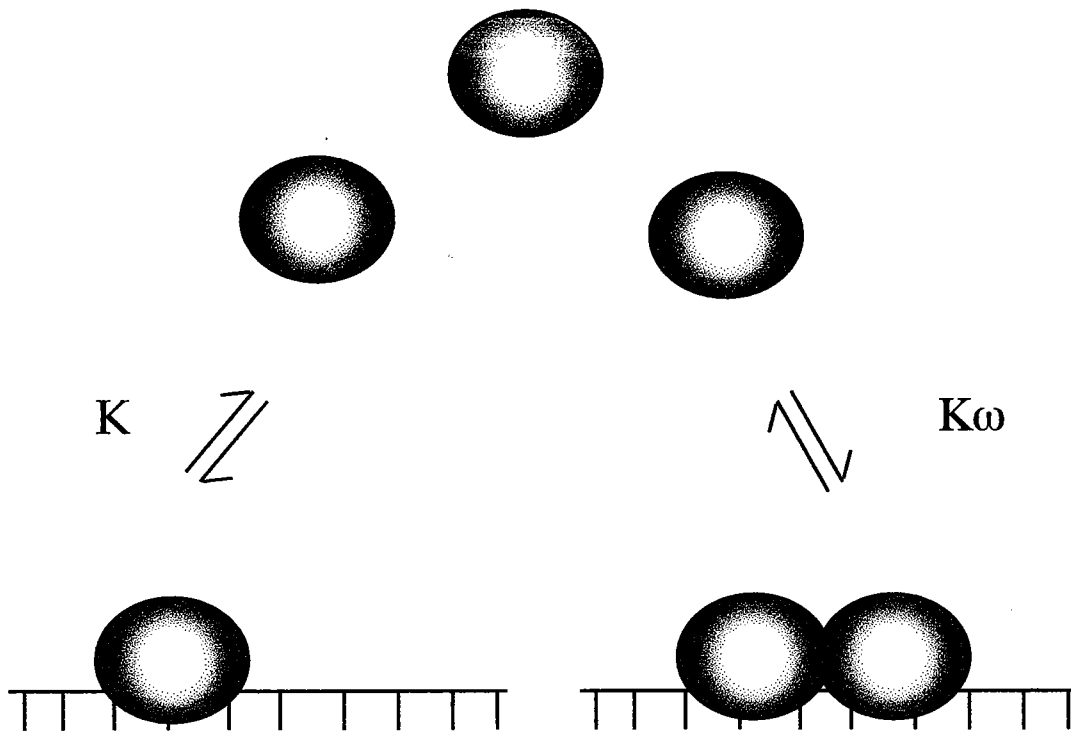
$$\text{hRad51} \quad (K\omega)^{-1}_{-ATP\gamma S} \;=\; 0.5x\,(K\omega)^{-1}_{+ATP\gamma S}$$

$$\text{RecA} \quad (K\omega)^{-1}_{-ATP\gamma S} \;=\; 20x(K\omega)^{-1}_{+ATP\gamma S}$$

Figure 31. Binding of either hRad51 or RecA monomers to a "singly contiguous" lattice of ssDNA. K is defined as the intrinsic affinity of a protein monomer for ssDNA and Kω is defined as the affinity of a protein monomer for the next position in an established site (see text and McGhee & von Hippel, 1974). The site size, or bases covered by a single protein monomer, is 3 (see text). Relative values of $(K\omega)^{-1}$ for both proteins are from Table III and are presented to emphasize the dramatic difference that nucleotide (ATPγS) has on the ssDNA binding affinity of hRad51 $vs.$ RecA.

10^5; $K_{ATP} = 1.7 \times 10^5$) whereas RecA shows a slight 1.7-fold increase ($K_{ATP\gamma S} = 8.4 \times 10^4$ M^{-1}). For both hRad51 and RecA, NTP cofactors increase the cooperative interaction between monomers during nucleoprotein filament assembly, but the effect is substantially greater for RecA. In the absence of a nucleotide cofactor, values of ω are 27 and 16 for hRad51 and RecA, respectively, whereas in the presence of NTP, ω increases 3 to 4-fold for hRad51 ($\omega_{ATP} = 83$; $\omega_{ATP\gamma S} = 107$) and greater than 11-fold for RecA ($\omega_{ATP\gamma S} = 182$). As expected, values of $(K\omega)^{-1}$ are in agreement with values of $S_{0.5}$ as determined from Hill plots in Figures 28 and 31. These data show that the slight NTP-induced decrease in the overall equilibrium binding affinity of hRad51 for ssDNA results from an approximate 10-fold decrease in the intrinsic affinity which is offset by a 3 to 4-fold increase in cooperativity. In contrast, the substantial NTP-induced increase in the equilibrium binding affinity of RecA for ssDNA [$(K\omega)^{-1} = 1.26$ μM and 66 nM in the absence and presence of ATPγS, respectively] is largely accounted for by the 11-fold increase in cooperativity. Therefore, NTP cofactors have a fundamentally different effect on the binding parameters of hRad51-ssDNA *vs.* RecA-ssDNA complex formation.

Table III

Cooperative ssDNA Binding Parameters for hRad51 and RecA. Values for K and ω were calculated using a variation of Equation 2 in Kowalczykowski *et al.* (1986) as described on page 139. Standard errors were calculated from 4 separate series of time courses. Errors are not shown for K and Kω but are in the same range as those for other parameters in the Table (from 5 – 30%).

	hRad51			RecA	
	(-)NTP	(+)ATP	(+)ATPγS	(-)NTP	(+)ATPγS
$K\ (M^{-1})$	1.26×10^6	1.70×10^5	1.44×10^5	4.83×10^4	8.36×10^4
ω	27.1 ± 9.2	82.6 ± 15.2	107.3 ± 25.8	16.4 ± 0.8	181.5 ± 48.5
$K\omega\ (M^{-1})$	3.41×10^7	1.40×10^7	1.55×10^7	7.92×10^5	1.52×10^7
$(K\omega)^{-1}$ (nM)	29.3 ± 8.5	71.2 ± 8.4	64.7 ± 6.9	$1,262.4 \pm 248$	65.8 ± 15.7

hRad51 and RecA ssDNA binding: kinetic parameters

Calculation of the association (k_a) and dissociation (k_d) rate constants for hRad51 and RecA binding to ssDNA further defines the mechanistic differences between these proteins. We used the following expression,

$$k_{on} = k_a \, [\text{protein}] + k_d$$

where k_{on} is the pseudo-first order rate for the interaction of protein and DNA at a given protein concentration. Values for k_a were obtained from the slope of a plot of k_{on} *vs.* protein concentration, and k_d was derived directly from biosensor dissociation data. The binding curves for both hRad51 and RecA fit well using a model of monophasic association and, hence, data is derived using this model. In the absence of NTP, k_a for hRad51 is approximately 400-fold greater than for RecA, while k_d is approximately equivalent for both proteins (Table IV). As expected from the effect of NTPs on the equilibrium binding parameters of both proteins, they have a far more dramatic effect on the kinetic parameters of RecA than hRad51. For hRad51, ATPγS induces a small, 2-fold decrease in both k_a and k_d, while ATP has no substantial effect on either k_a or k_d. This is consistent with our finding that ATP and ATPγS promote only small changes in the equilibrium binding constants $S_{0.5}$ and $(K\omega)^{-1}$ for hRad51 relative to ATPγS -induced changes in these parameters for RecA. In contrast to hRad51, ATPγS has a substantial effect on both k_a and k_d for RecA, increasing k_a approximately 47-fold and

decreasing k_d to the point where dissociation is undetectable during the time of the assay (Table IV). This latter result is consistent with previous studies of RecA showing that ATPγS has a substantial stabilizing effect on RecA/ssDNA complexes (McEntee *et al.*, 1981; Menetski & Kowalczykowski, 1985b). The dramatic difference between hRad51 and RecA is emphasized in Figure 32, which compares binding time courses for equal concentrations of both proteins (90 nM) in the presence of ATPγS.

hRad51 dsDNA binding

To determine the effect, if any, of a nucleotide cofactor on the binding of hRad51 to dsDNA, we performed a series of gel shift assays. Previous work has suggested that hRad51 exhibits a similar affinity for both single and double-stranded DNA substrates. We have shown that ATP is not required for binding to ssDNA, therefore we explored the possibility that ATP mediates binding to dsDNA. Using increasing concentrations of hRad51 in binding reactions with linearized dsDNA substrate, we show that the presence of a nucleotide cofactor in these experiments has no effect on the binding of hRad51 to dsDNA (Figure 33).

Figure 32.
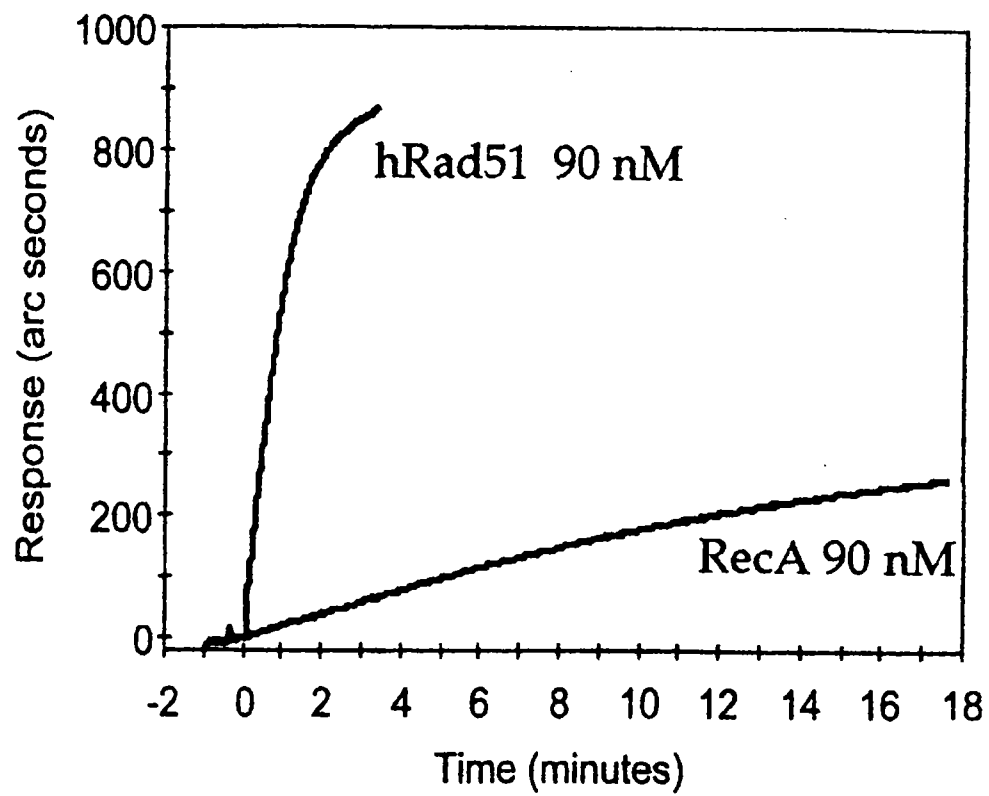
Figure 32. **Comparison of the binding time course between equivalent amounts of hRad51 and RecA proteins.** Extent of binding of either hRad51 or RecA (90.5 nM protein in the presence of ATPγS) is measured in arc sec, and demonstrates the significantly faster "on rate" for hRad51 (see Table IV).

Figure 33.

ATPγS   ATP   dATP   no cofactor

hRad51 (uM)

0 0.5 1 2 3 4 5 | 0 0.5 1 2 3 4 5 | 0 0.5 1 2 3 4 5 | 0 0.5 1 2 3 4 5
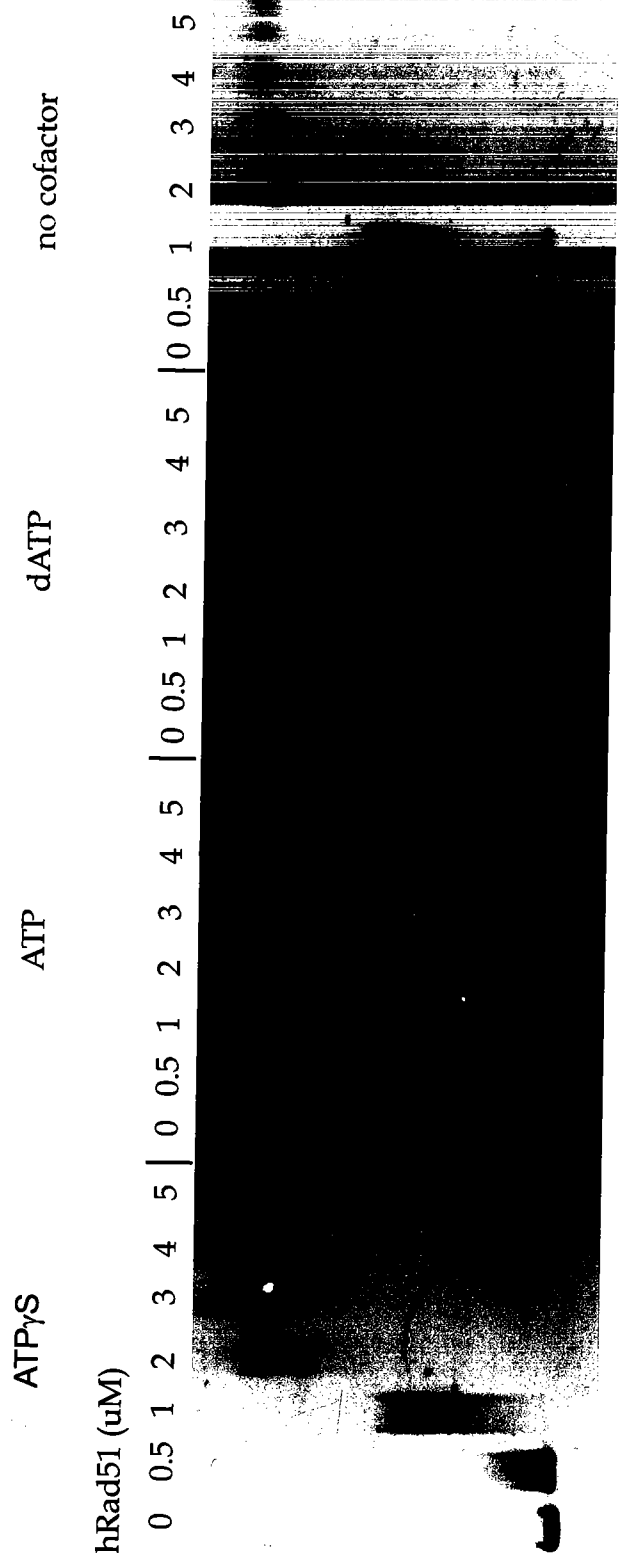
Figure 33. hRad51 binding to dsDNA. Various concentrations of wt hRad51 were incubated with linearized dsDNA for 30 minutes at 37°C in the presence or absence of nucleotide cofactor. Protein-DNA complexes were resolved using a 0.8% agarose gel and visualized by staining with EtBr.

Table IV

Kinetic Parameters for hRad51 and RecA Binding to ssDNA. Values for the association (k_a) and dissociation (k_d) rate constants were determined as described in the text (see Materials and Methods). Standard errors were calculated from 4 separate experiments and range from 10 – 40%. (n.d. = not detected).

	hRad51			RecA	
	(-)NTP	(+)ATP	(+)ATPγS	(-)NTP	(+)ATPγS
k_a (M^{-1} s^{-1})	9.1×10^{4}	7.3×10^{4}	4.2×10^{4}	2.1×10^{2}	9.8×10^{3}
k_d (s^{-1})	1.4×10^{-2}	2.2×10^{-2}	6.7×10^{-3}	8.3×10^{-3}	n.d.

Discussion

Despite considerable structural and functional similarities between the hRad51 and RecA proteins, we find significant differences in the equilibrium and kinetic parameters that define their ssDNA binding properties. Using an IAsys Affinity Biosensor, we have been able to dissect the effects that addition of nucleotide cofactor has on this critical first step in the process of homologous recombination and DNA repair. Biosensor technology affords a significant enhancement over other methods regarding the quantitative analyses of macromolecular interactions, and has proven useful in studies of protein-DNA interactions for a variety of systems (Bogdarina *et al.*, 1998; Cornille *et al.*, 1998; Myszka *et al.*, 1998; Michalopoulus *et al.*, 1999; Yoshioka *et al.*, 1999). The ease with which binding studies can be performed and the ability to use native DNA substrates has enabled us to provide new and unexpected insights into mechanistic considerations of hRad51 and RecA interactions with ssDNA. Importantly, the equilibrium binding parameters derived for RecA-ssDNA interactions in the absence of nucleotide cofactors are consistent with those derived from more commonly used methods, e.g. fluorescence quenching of εDNA (Menetski & Kowalczykowski, 1985b; Silver & Fersht, 1982; Silver & Fersht, 1983) and filter binding (Kelley & Knight, 1997; McEntee *et al.*, 1981), thereby supporting the reliability of the data in this study.

The fact that ATP or ATPγS induces a high affinity DNA binding form of RecA has been well known for some time (Menetski & Kowalczykowski, 1985b; Silver & Fersht, 1982). Our data is consistent with these findings, showing a low

affinity binding for ssDNA in the absence of cofactor ($S_{0.5}$ and $(K\omega)^{-1} = 1.26$ μM), and a significant increase in the presence of ATPγS ($S_{0.5} = 70.5$ nM; $(K\omega^{-1} = 65.8$ nM). We have now been able to separate out the components of this binding event, namely, the intrinsic affinity of RecA for ssDNA $vs.$ cooperative subunit-subunit interactions. We show that the ATPγS-induced increase in affinity is accounted for almost exclusively by an increase in the cooperativity parameter of the protein (ω increases $\cong$ 11 fold; Table III). This implies that NTP-induced structural changes in the protein may alter the position of residues whose association increases the cooperative nature of subunit-subunit interactions, as opposed to residues that interact directly with DNA. Interestingly, this is consistent with the proposal of Voloshin et $al.,$ (Voloshin et $al.,$ 1996) that induction of a high-affinity DNA binding state of RecA involves an ATP-dependent movement of parts of the protein which result in greater access of the DNA binding domain to the DNA substrate. Additionally, the increase in n_{app} (3.5-fold; Table II), suggests that a larger number of RecA subunits are playing a role in establishing the cooperative nature of the NTP-induced high affinity binding of RecA to ssDNA, while an 11-fold increase in ω reveals that the probability of the next subunit in the assembly process binding to a contiguous $vs.$ an isolated site on DNA is increased by this value.

Unlike RecA, hRad51 binds to ssDNA in the absence of nucleotide cofactor both cooperatively ($n_{app} = 2.7$, $\omega = 27.1$) and with high affinity ($S_{0.5} = 35.3$ nM; $(K\omega)^{-1} = 29.3$ nM). We find that, although ATP and ATPγS increase the

cooperative nature of hRad51 nucleoprotein filament formation, the inherent affinity of the protein is decreased by an order of magnitude by the presence of either cofactor. The net result is that NTP has very little effect on the equilibrium binding affinity of hRad51 for ssDNA, again, a result that is very different from the effect of nucleotide cofactors on RecA-ssDNA interactions. Determination of the kinetic rate constants k_a and k_d also show significant differences regarding the effect of NTP on ssDNA binding by hRad51 *vs.* RecA. For example, while ATPγS results in a significant stabilization of RecA-ssDNA complexes, it has no such effect on hRad51-ssDNA complexes. In fact, k_d for hRad51-ATPγS-ssDNA complexes is equal to that for RecA-ssDNA complexes in the absence of ATPγS.

In summary, these results suggest that ATP plays a fundamentally different role in hRad51 *vs.* RecA-mediated processes. Although high affinity ssDNA binding by hRad51 does not require a nucleotide cofactor, we note that all activities catalyzed by hRad51 measured thus far, e.g. duplex DNA unwinding (Benson *et al.*, 1994) and strand exchange (Baumann *et al.*, 1996; Benson *et al.*, 1998; Gupta *et al.*, 1997) require the presence of a nucleotide cofactor. Given the fact that efficient hRad51-mediated strand exchange requires the presence of other protein factors (Baumann *et al.*, 1996; Benson *et al.*, 1998), it is interesting to speculate that, in contrast to the ATP-induced increase in ssDNA binding affinity for RecA, NTP-induced allosteric effects for hRad51 may be manifest more in its interaction with other recombination proteins, e.g. hRPA, hRad52 or hRad54. Physical interactions between hRad51 and each of these proteins have been demonstrated (Golub *et al*, 1997; Golub *et al.*, 1998; Shen *et al.*, 1996), but the effect

of nucleotide cofactors on these interactions is not known. Additionally, functional interactions between hRad51 and both hRPA and hRad52 have been shown to lead to an increase in strand exchange efficiency (Baumann & West, 1997; Benson *et al.*, 1998). Our data is consistent with the idea that rather than regulating binding of hRad51 to ssDNA, ATP may serve as an allosteric effector of hRad51 interactions with other proteins important for efficient catalysis of genetic recombination. It is also possible that ATP may alter the conformation of the nucleoprotein filament itself, possibly exposing a secondary DNA binding site within hRad51. Ongoing experiments are testing these possibilities.

We not only find differences between hRad51 and RecA, but significant differences are also apparent between the DNA binding properties of the hRad51 and *Sc*Rad51 proteins. Both Namsaraev and Berg (Namsaraev & Berg, 1998) and Zaitseva *et al.* (Zaitseva *et al.*, 1999) have reported that under conditions similar to those in this study, *Sc*Rad51 binds poorly to ssDNA or εDNA in the absence of ATP, concluding that binding to ssDNA is dependent on the presence of ATP. Both studies also showed that ATPγS promotes DNA binding only at elevated *Sc*Rad51 protein concentrations. Namsaraev and Berg (Namsaraev & Berg, 1998) estimated a $K_D = 1.1$ μM for *Sc*Rad51 binding to εDNA in the presence of ATP, a value that indicates a significantly weaker affinity than we find for hRad51.

We find it quite striking that nucleotide cofactors have such different effects on the ability of hRad51, *Sc*Rad51 and RecA to perform one of the most fundamental aspects of recombinase function, binding to ssDNA. Our results suggest that

although the processes catalyzed by each of these proteins is similar, the energy source provided by ATP and its role as an allosteric effector are used by the hRad51 protein in a fundamentally different way than by RecA and *Sc*Rad51. Further characterization of the mechanistic differences between these 3 proteins, as well as the effect of other hRad proteins on the binding of hRad51 to ssDNA and the effect that ATP has on various protein-protein interactions within this system will provide valuable information regarding the role of ATP in homologous recombination and DNA repair. This will undoubtedly provide important insights regarding how different organisms have adapted to catalyze similar recombination events within different cellular contexts.

Chapter VI

Conclusions and Future Directions

Allosteric regulation of enzyme function is a classic example of how cells regulate critical biological pathways. More specifically, the binding of ATP is involved in many of these processes. Even though many enzymes are controlled in this fashion, the structural and mechanistic details have only been elucidated in a handful of instances. In the work presented here, we have provided a molecular description of not only how RecA is activated by the binding of ATP, but also how this information is transmitted through the protein structure, from one monomer to the next. We clearly show that Gln194 serves as the "γ-phosphate sensor" within the ATP binding site of a RecA monomer. Following the binding of ATP, Gln194 effects a change in disordered loop L2, which assumes a conformation conducive to high affinity DNA binding. In addition to promoting this change, conformational changes within L2 are propagated into helix G, which contains several important determinants of the subunit interface, including Phe217. We propose that it is the insertion of the Phe217 side chain into a hydrophobic pocket within the neighboring monomer that mediates the ATP-induced cooperativity of RecA filament formation. Although we have made considerable progress in dissecting the mechanism of ATP mediated allosteric regulation of RecA function, many questions remain. For example, how are the ATP mediated changes within one monomer of RecA "sensed" by the surface of the neighboring monomer? What residues or structural elements in

the opposing monomer mediate this information transfer? What conformational changes are afforded to support the cooperative nature of ATP binding and hydrolysis within the context of the nucleoprotein filament? Future studies will address these very important aspects of RecA structure and function in detail.

Future studies will also define a role for ATP in hRad51 mediated processes. We have shown that unlike RecA, hRad51 binds to ssDNA cooperatively and with high affinity both in the presence and absence of any nucleotide cofactor. Therefore, in a sense, hRad51 is always "primed" for high affinity binding to ssDNA. This also suggests, interestingly enough, that RecA and hRad51 use ATP in a fundamentally different way to catalyze similar reactions. We have also shown that ATP does not regulate the binding of hRad51 to dsDNA. All of the activities catalyzed by hRad51, however, require the presence of a nucleotide cofactor, reinforcing the idea that ATP does indeed play a critical role in the regulation of these processes. It is becoming clearer by the day that eukaryotic recombination and DNA repair are both highly regulated, complex series of events that involve a vast array of factors. It is therefore possible that ATP may function to regulate the association of hRad51 with one or more of these factors. For example, the binding of ATP may result in an increase in the affinity of hRad51 for hRad52, effectively potentiating the recruitment of hRad51 to the site of DNA repair. Ongoing experiments in our laboratory are currently addressing these questions. It is also possible that ATP affects the conformation of the hRad51-ssDNA nucleoprotein filament. In this regard, upon the binding of ATP, conformational changes would occur within the filament structure, exposing a

secondary dsDNA-binding site within hRad51. Such a change would allow the initiation of the strand exchange reaction. Experiments using limited proteolytic digestion of purified hRad51 in the presence and absence of ATP as well as both single and double-stranded DNA cofactors will address this possibility. Once a role for ATP in hRad51 mediated processes is clearly defined, the allosteric regulation of these events can be determined. Alignment of RecA, ScRad51 and hRad51 reveals that Gln194, the "γ-phosphate sensor" within RecA, is conserved in both proteins. It will be interesting to determine whether the molecular determinants of ATP mediated allosteric regulation are conserved from bacteria to yeast to humans.

In addition to the questions outlined above, we have begun to use alanine scanning mutagenesis to identify the functional domains of the hRad51 protein, specifically, residues involved in ssDNA binding and oligomerization. Using the published alignment of the RecA and hRad51 proteins, we have directed mutations to areas within hRad51 which have been shown to be critical in RecA for either ssDNA binding or oligomerization. In addition, we have embarked upon a systematic mutagenesis of the entire hRAD51 gene.

We have divided the hRAD51 sequence into 75 "mutagenic regions" coding for 3-5 consecutive alanine mutations per mutant. Currently, we have obtained approximately 50% of these alanine scanning mutants (See Table V). To determine the effect of mutations on both the ssDNA binding capability as well as the oligomeric distribution of Rad51, we have devised assays to screen wt

Table V. hRad51 Alanine Scanning Mutagenesis and Characterization

Mutant	Induction	ssDNA	Gel Filtration
35-39			
40-43			
44-48	+		
49-53			
54-58			
59-62	+		
63-66	+	-	9mer
67-71	+		
72-76	+		12mer
77-81	+		
82-86			
87-91	+		
92-94	+		
95-98	+		
99-101			
102-106			
107-110			
111-113			
114-118	+		
119-123			
124-128			
129-132			
133-136			
137-140	-		
141-144			
145-149			
150-154			
155-159			

Mutant	Induction	ssDNA	Gel Filtration
160-164			
165-169			
170-174			
175-179			
180-184			
185-189			
237-241	+	-	12mer
242-244	+	-	
245-248	+	-	9mer
249-251	+		
252-256	-		
257-261	-		
262-266			
267-271	-		
272-276			
277-281	+		
282-286	+	+	22mer
287-290	+		mono/dimer
291-295	+		
296-300	+		
301-303	+		
304-306	+		

Table V. hRad51 Alanine Scanning Mutagenesis and Characterization.
Progress in this large-scale mutagenesis project is summarized in this table.
Mutants confirmed by sequencing are listed. Presence or absence of the mutant
protein in crude cell extracts following induction with IPTG is indicated with a
(+) or (-).   ssDNA binding and oligomerization properties are characterized
using ssDNA cellulose and Superose 6 gel filtration chromatography,
respectively.

hRad51 for these properties, using ssDNA-cellulose affinity chromatography and Superose-6 gel filtration chromatography, respectively. wt hRad51 binds well to ssDNA using this technique (Figure 34). Typical Superose 6 profiles of wt hRad51 are shown in Figure 35. At high concentrations hRad51 forms long oligomers in the absence of any DNA cofactor, much like its homolog RecA (Logan *et al.*, 1997). Furthermore, the oligomerization of hRad51 is concentration dependent; as the concentration of hRad51 is decreased, oligomer size also decreases (Figure 35). This result is consistent with that reported for the RecA protein (Logan *et al.*, 1997).

At this time, only a limited number of mutants have been screened for defects in either ssDNA binding or oligomerization. Several of these alanine mutants have shown interesting results. The 63-66 mutant shows a disrupted oligomeric profile (Figure 36). Due to the fact that the RecA and hRad51 sequences are aligned only within the "core domain", the N and C-terminal domains show a certain degree of flexibility in their alignments. This mutant protein contains a lysine residue, which aligns with Lys6 of RecA, which has been shown to be a critical determinant of the subunit interface. The 63-66 mutant protein also shows an apparent defect in ssDNA binding. This is supported by data published by Ahira, *et al.*, 1999 (Aihara *et al.*, 1999), which implicates these residues as critical components of the DNA binding site of hRad51. Additionally, the oligomeric properties of 237-241, 245-248 and 287-290 are disrupted. The 287-290 mutant is of particular interest due to the fact that it

Figure 34.

L   FT   W   B
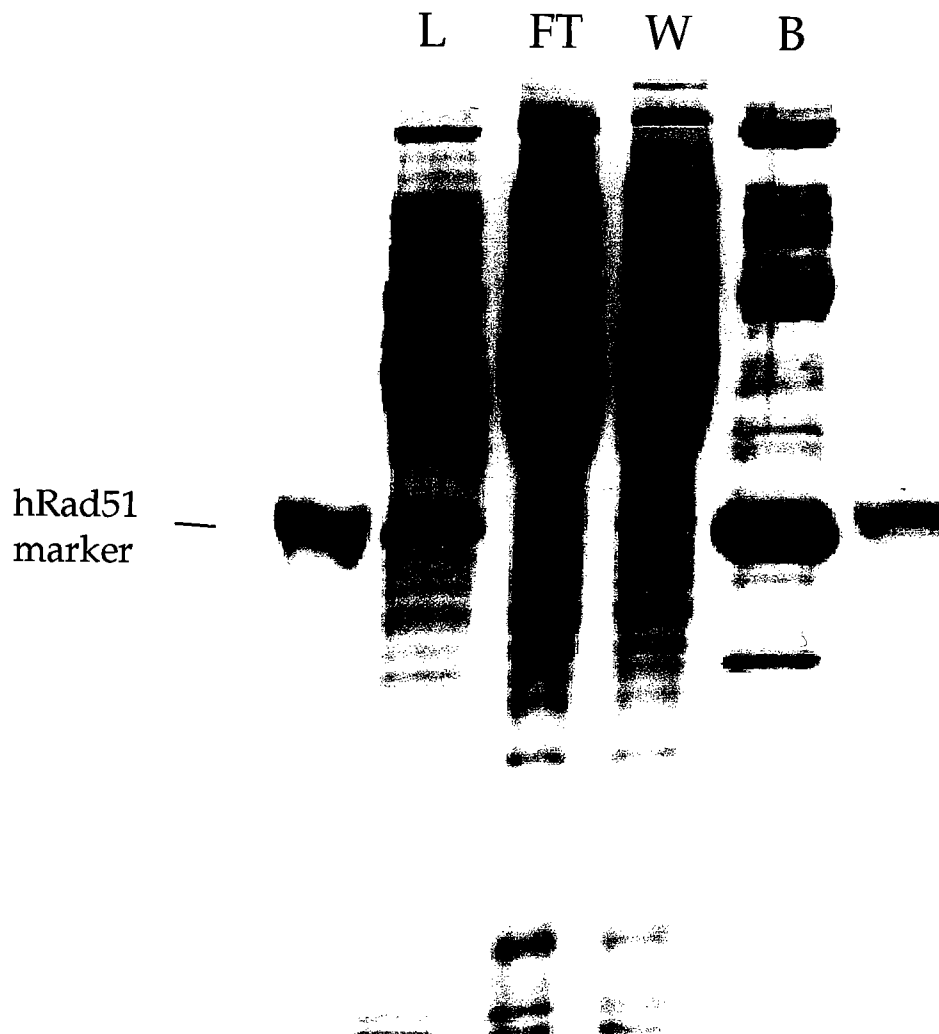
hRad51
marker

Figure 34.. wt hRad51 ssDNA cellulose binding screen. Extracts containing wt hRad51 were prepared as described in Methods and Materials. M is an hRad51 protein marker. L is the load onto the ssDNA cellulose column, F is the flow-through (unbound), W is a wash fraction and B indicates proteins that bind to the column and elute in high salt.

Figure 35.
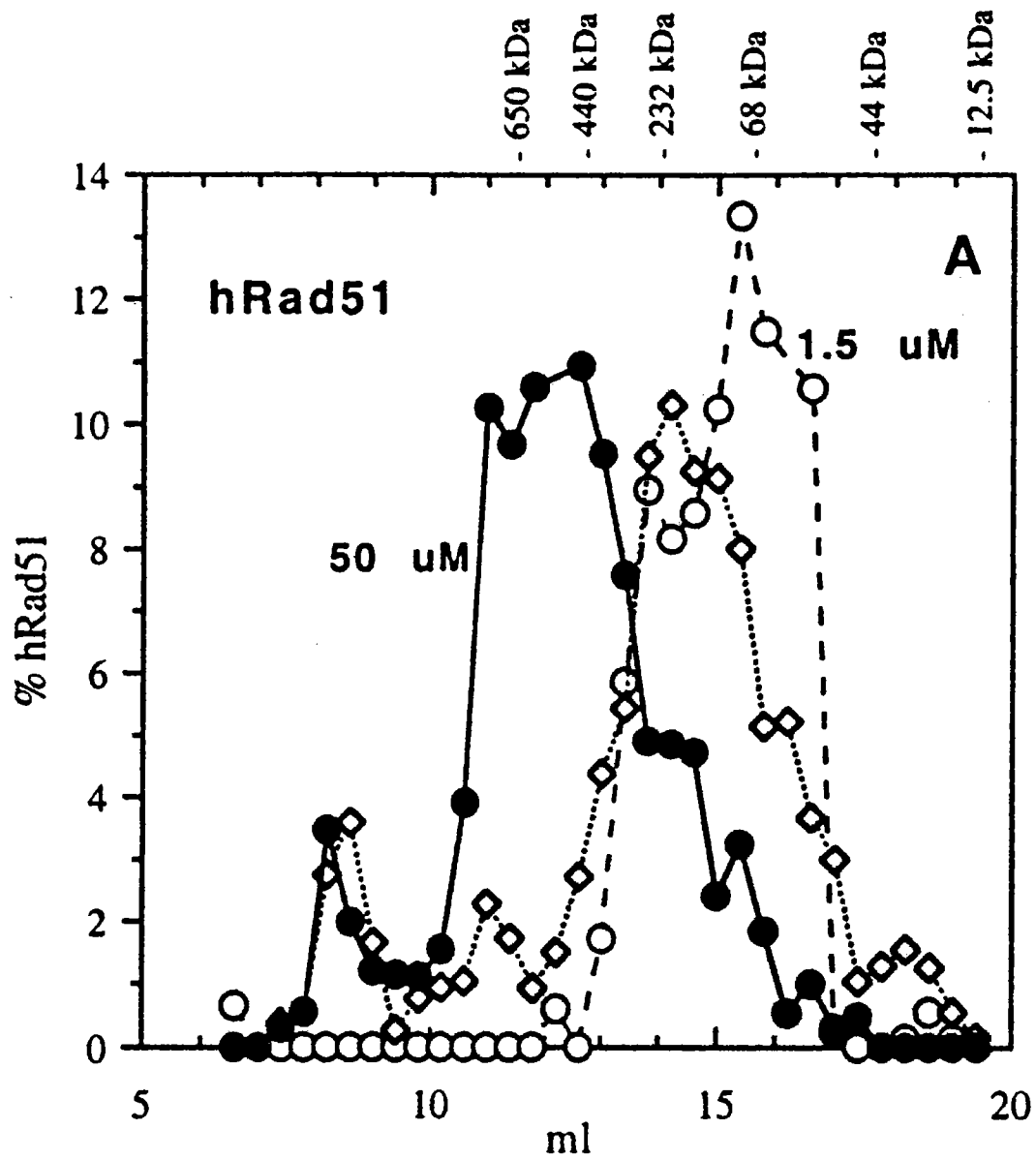
Figure 35. Superose 6 gel filtration profiles of crude cell extracts containing wt hRad51. Superose 6 gel filtration profiles of varying concentrations of wt hRad51 (50, 25 and 1.5uM hRad51) showing that filament formation is concentration dependent. Molecular weight markers are thyroglobulin (650 kDa), apoferritin (450 kDa), β-amylase (206 kDa), bovine serum albumin (68 kDa) and cytochrome C (12.5 kDa).

contains a double glycine (G288-G289), which are conserved in both RecA and ScRad51. This double glycine is proposed to be an important structural element within RecA, possibly being involved in conformational changes within the protein (Story *et al.*, 1993). This mutant shows an estimated molecular weight equivalent to dimeric or monomeric hRad51 (Figure 36), suggesting that residues in this region play an important role in oligomer formation or stability. At this time, the Gly288Ala point mutation has been constructed and screened, and it does not appear to have any disruption in either ssDNA binding or oligomerization. Analysis of the Gly289→Ala mutant will prove to be interesting in identifying specific residues involved and whether this defect is a result of a direct or indirect effect on oligomer stability. ssDNA binding is also disrupted in both the 237-241 and 245-248 mutants. Residues 237-241 align with residues within disordered loop L1 of RecA, which has been implicated in dsDNA binding. Further characterization of these mutant proteins will more specifically define the roles of residues in this region in oligomerization of hRad51.

To date, considerable progress has been made in this large-scale mutagenesis project. To conclusively identify key functional domains of the hRad51 protein, however, further biochemical characterization is necessary. Future studies will include the characterization of novel alanine block mutants as well as continued characterization of mutants in hand. In particular, those mutants that show defects in oligomerization will be further studied to investigate the concentration dependence of filament formation. Additional techniques such as analytical

Figure 36.
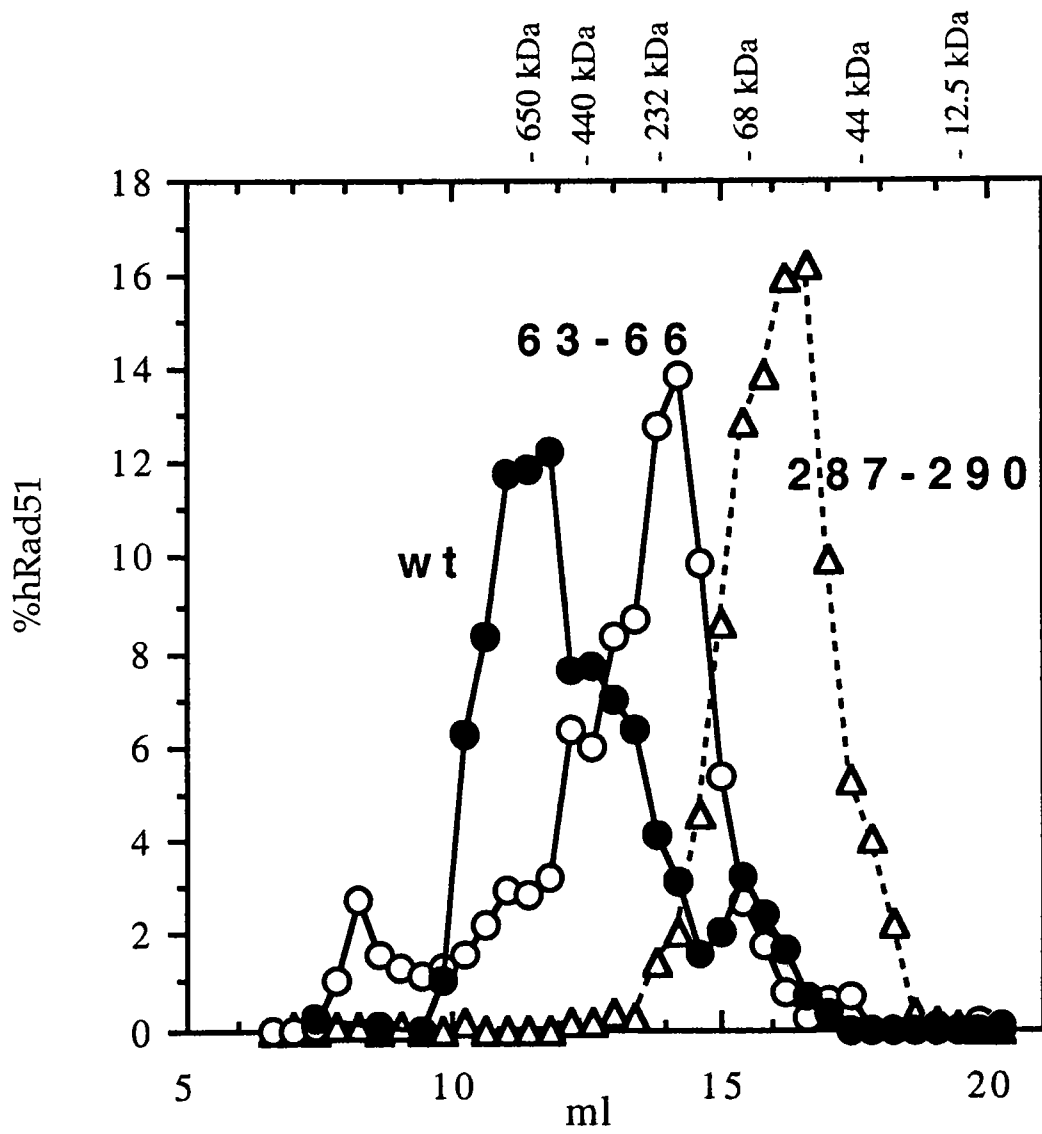
Figure 36. Superose 6 gel filtration profiles of crude cell extracts containing mutant hRad51 proteins. Superose 6 gel filtration profiles of wt hRad51 and alanine scanning mutants 63-66 and 287-290. Molecular weight markers are thyroglobulin (650 kDa), apoferritin (450 kDa), β-amylase (206 kDa), bovine serum albumin (68 kDa) and cytochrome C (12.5 kDa).

ultracentrifugation and electron microscopy will be employed to pinpoint the oligomeric size of these mutant proteins. In addition to the identification of ssDNA binding defects by affinity chromatography, mutants that show interesting characteristics will be purified and studied using a more quantitative approach, such as the IAsys Affinity Biosensor. Using this technology, it will be possible to address important kinetic considerations of hRad51 single and double-stranded-DNA binding properties.

In the future, this "library" of mutant proteins will prove to be an invaluable tool in the identification of the functional domains of the hRad51 protein. To date, hRad51 has been shown to interact with numerous other proteins. Using these alanine mutants, it will be possible to identify the determinants of each of these interacting domains within hRad51. Mechanistic studies of enzyme function will also be addressed. For example, strand exchange capabilities of mutant proteins in the presence of various cofactors such as hRad52 and RPA can be defined and the transfer of allosteric information can be studied. In total, these experiments will provide a detailed, in-depth understanding of the structural and mechanistic components of this complex protein.

Acknowledgements

I would like to thank Erin Wallace, an undergraduate at the College of the Holy Cross (now a graduate student at U.C.S.D.) for her considerable effort in the construction and characterization of the hRad51 mutants.

References

Aihara, H., Ito, Y., Kurumizaka, H., Yokoyama, S. & Shibata, T. (1999). The N-terminal domain of the human Rad51 protein binds DNA: structure and a DNA binding surface as revealed by NMR. *J Mol Biol* **290**(2), 495-504.

Alani, E., Thresher, R., Griffith, J. D. & Kolodner, R. D. (1998). Characterization of DNA-binding and strand-exchange stimulation properties of y-RPA, a yeast single-strand-DNA-binding protein. *Mol Cell Biol* **18**(7), 4400-6.

Auzat, I., Le Bras, G. & Garel, J. R. (1995). Hypercooperativity induced by interface mutations in the phosphofructokinase from Escherichia coli. *J Mol Biol* **246**(2), 248-53.

Barlow, A. L., Benson, F. E., West, S. C. & Hulten, M. A. (1997). Distribution of the Rad51 recombinase in human and mouse spermatocytes. *EMBO J* **16**(17), 5207-15.

Baumann, P., Benson, F. E. & West, S. C. (1996). Human Rad51 protein promotes ATP-dependent homologous pairing and strand transfer reactions *in vitro*. *Cell* **87**(4), 757-66.

Baumann, P. & West, S. C. (1997). The human Rad51 protein: polarity of strand transfer and stimulation by hRP-A. *EMBO J* **16**(17), 5198-206.

Baumann, P. & West, S. C. (1998). Role of the human RAD51 protein in homologous recombination and double- stranded-break repair. *Trends Biochem Sci* **23**(7), 247-51.

Benson, F. E., Baumann, P. & West, S. C. (1998). Synergistic actions of Rad51 and Rad52 in recombination and DNA repair [see comments]. *Nature* **391**(6665), 404-7.

Benson, F. E., Stasiak, A. & West, S. C. (1994). Purification and characterization of the human Rad51 protein, an analogue of E. coli RecA. *EMBO J* **13**(23), 5764-71.

Bezzubova, O., Shinohara, A., Mueller, R. G., Ogawa, H. & Buerstedde, J. M. (1993). A chicken RAD51 homologue is expressed at high levels in lymphoid and reproductive organs. *Nucleic Acids Res* **21**(7), 1577-80.

Bianco, P. R., Tracy, R. B. & Kowalczykowski, S. C. (1998). DNA strand exchange proteins: a biochemical and physical comparison. *Front Biosci* **3**, D570-603.

Bogdarina, I., Fox, D. G., & Kneale, G. G. (1998). Equilibrium and kinetic binding analysis of the N-terminal domain of the Pf1 gene 5 protein and its interaction with single-stranded DNA. *J Mol Biol* **275**, 443-452.

Brenner, S. L., Zlotnick, A. & Griffith, J. D. (1988). RecA protein self-assembly. Multiple discrete aggregation states. *J Mol Biol* **204**(4), 959-72.

Chen, J., Silver, D. P., Walpita, D., Cantor, S. B., Gazdar, A. F., Tomlinson, G., Couch, F. J., Weber, B. L., Ashley, T., Livingston, D. M. & Scully, R. (1998). Stable interaction between the products of the BRCA1 and BRCA2 tumor suppressor genes in mitotic and meiotic cells. *Mol Cell* **2**(3), 317-28.

Clark, A. J. & Marglies, A. D. (1965). Isolation and characterization of recombination deficient mutants of E. coli K-12. *Proc Natl Acad Sci USA* **53**, 451-459.

Clever, B., Interthal, H., Schmuckli-Maurer, J., King, J., Sigrist, M. & Heyer, W. D. (1997). Recombinational repair in yeast: functional interactions between Rad51 and Rad54 proteins. *Eur J Immunol* **27**(5), 1292-5.

Cornille, F., Emery, P., Schule, W., Lenoir, C., Mach, B., Roques, B. P. and Reith, W. (1998) DNA binding properties of a chemically synthesized DNA binding domain of hRFX1. *Nuc Ac ids Res* **26**, 2143-2149.

Cox, M. M. (1994). Why does RecA protein hydrolyse ATP? *Trends Biochem Sci* **19**(5), 217-22.

Cox, M. M. (1999). Recombinational DNA repair in bacteria and the RecA protein. *Prog Nucleic Acid Res Mol Biol* **63**, 311-66.

Craig, N. L. & Roberts, J. W. (1980). E. coli recA protein-directed cleavage of phage lambda repressor requires polynucleotide. *Nature* **283**(5742), 26-30.

De Zutter, J. K. & Knight, K. L. (1999). The hRad51 and RecA proteins show significant differences in cooperative binding to single-stranded DNA. *J Mol Biol* **293**(4), 769-80.

DiCapua, E., Ruigrok, R. W. & Timmins, P. A. (1990). Activation of recA protein: the salt-induced structural transition. *J Struct Biol* **104**(1-3), 91-6.

Egelman, E. H. (1993). What do X-ray crystallographic and electron microscopic structural studies of the RecA protein tell us about recombination? *Curr Opin Struct Biol* **3**, 189-197.

Egelman, E. H. (1998). Bacterial helicases. *J Struct Biol* **124**, 123-128.

Egelman, E. H. & Stasiak, A. (1986). Structure of helical RecA-DNA complexes. Complexes formed in the presence of ATP-gamma-S or ATP. *J Mol Biol* **191**(4), 677-97.

Eggleston, A. K. & West, S. C. (1996). Exchanging partners: recombination in *E. coli. Trends Genet* **12**, 20-26.

Eldin, S., Forget, A. L., Lindenmuth, D., Logan, K. M. & Knight, K. L. (2000). Mutations in the N-terminal region of the RecA protein that disrupt stability of free protein filaments but not nucleoprotein filaments. *J Mol Biol* **299**, 91-101.

Fisher, A. J., Smith, C. A., Thoden, J. B., Smith, R., Sutoh, K., Holden, H. M. & Rayment, I. (1995). X-ray structures of the myosin motor domain of Dictyostelium discoideum complexed with MgADP.BeFx and MgADP.AlF4. *Biochemistry* **34**(28), 8960-72.

Gallivan, J. P. & Dougherty, D. A. (1999). Cation-pi interactions in structural biology. *Proc Natl Acad Sci USA* **96**, 9459-9464.

Gardner, R. V., Voloshin, O. N. & Camerini-Otero, R. D. (1995). The identification of the single-stranded DNA-binding domain of the Escherichia coli RecA protein. *Eur J Biochem* **233**(2), 419-25.

Gasior, S. L., Wong, A. K., Kora, Y., Shinohara, A. & Bishop, D. K. (1998). Rad52 associates with RPA and functions with rad55 and rad57 to assemble meiotic recombination complexes. *Genes Dev.* **12**(14), 2208-21.

Golub, E. I., Kovalenko, O.V., Gupta, R.C., Ward, D.C. & Radding, C.M. (1997). Interaction of human recombination proteins Rad51 and Rad54. *Nucleic Acids Res* **25**, 4106-4110.

Golub, E. I., Gupta, R. C., Haaf, T., Wold, M. S. & Radding, C. M. (1998). Interaction of human Rad51 recombination protein with single-stranded DNA binding protein, RPA. *Nucleic Acids Res* **26**, 5388-5393.

Griffith, J. & Formosa, T. (1985). The uvsX protein of bacteriophage T4 arranges single-stranded and double-stranded DNA into similar helical nucleoprotein filament. *J Biol Chem* **260**, 4484-4891.

Gupta, R. C., Bazemore, L. R., Golub, E. I. & Radding, C. M. (1997). Activities of human recombination protein Rad51. *Proc Natl Acad Sci USA* **94**(2), 463-8.

Haaf, T., Golub, E. I., Reddy, G., Radding, C. M. & Ward, D. C. (1995). Nuclear foci of mammalian Rad51 recombination protein in somatic cells after DNA damage and its localization in synaptonemal complexes. *Proc Natl Acad Sci USA* **92** (6), 2298-302.

Habu, T., Taki T., West A., Nishimune, Y. & Morita, T. (1996). The mouse and human homologs of DMC1, the yeast meiosis-specific homologous recombination gene, have a common unique form of exon-skipped transcript in meiosis. *Nucleic Acids Res* **24,** 470-477.

Hays, S. L., Firmenich, A. A. & Berg, P. (1995a). Complex formation in yeast double-strand break repair: participation of Rad51, Rad52, Rad55, and Rad57 proteins. *Proc Natl Acad Sci USA* **92**(15), 6925-9.

Hays, S. L., Firmenich, A. A., Massey, P., Banerjee, R. & Berg, P. (1995b). Studies of the interaction between Rad52 protein and the yeast single- stranded DNA binding protein RPA.

Heuser, J. & Griffith, J. (1989). Visualization of RecA protein and its complexes with DNA by quick- freeze/deep-etch electron microscopy. *J Mol Biol* **210** (3), 473-84.

Holliday, R. (1964). A mechanism for gene conversion in fungi. *Genet Res* **5**, 282-304.

Hörtnagel, K., Voloshin, O. N., Kinal, H. H., Ma, N., Schaffer-Judge, C. & Camerini-Otero, R. D. (1999). Saturation mutagenesis of the *E. coli* RecA Loop L2 homologous DNA pairing region reveals residues essential for recombination and recombinational DNA repair. *J Mol Biol* **286**, 1097-1106.

Johnson, R. D. & Symington, L. S. (1995). Functional differences and interactions among the putative RecA homologs Rad51, Rad55, and Rad57. *Mol Cell Biol* **15** (9), 4843-50.

Joseph, J. W. & Kolodner, R. (1983). Exonuclease VIII of Escherichia coli. II. Mechanism of action. *J Biol Chem* **258** (17), 10418-24.

Kelley, J. A. & Knight, K. L. (1997). Allosteric regulation of RecA protein function is mediated by Gln194. *J Biol Chem* **272** (41), 25778-82.

Kobayashi, N., Knight, K. & McEntee, K. (1987). Evidence for nucleotide-mediated changes in the domain structure of the recA protein of *Escherichia coli*. *Biochemistry* **26**(21), 6801-10.

Konola, J. T., Logan, K. M. & Knight, K. L. (1994). Functional characterization of residues in the P-loop motif of the RecA protein ATP binding site. *J Mol Biol* **237**(1), 20-34.

Konola, J. T., Nastri, H. G., Logan, K. M. & Knight, K. L. (1995). Mutations at Pro67 in the RecA protein P-loop motif differentially modify coprotease function and separate coprotease from recombination activities. *J Biol Chem* **270**(15), 8411-9.

Kowalczykowski, S. C. (1991). Biochemistry of genetic recombination: energetics and mechanism of DNA strand exchange. *Annu Rev Biophys Biophys Chem* **20**, 539-75.

Kowalczykowski, S. C., Dixon, D. A., Eggleston, A. K., Lauder, S. D. & Rehrauer, W. M. (1994). Biochemistry of homologous recombination in Escherichia coli. *Microbiol Rev* **58**(3), 401-65.

Kowalczykowski, S. C. & Eggleston, A. K. (1994). Homologous pairing and DNA strand-exchange proteins. *Annu Rev Biochem* **63**, 991-1043.

Kowalczykowski, S. C. & Krupp, R. A. (1987). Effects of Escherichia coli SSB protein on the single-stranded DNA- dependent ATPase activity of Escherichia coli RecA protein. Evidence that SSB protein facilitates the binding of RecA protein to regions of secondary structure within single-stranded DNA. *J Mol Biol* **193**(1), 97-113.

Kowalczykowski, S. C. & Krupp, R. A. (1995). DNA-strand exchange promoted by RecA protein in the absence of ATP: implications for the mechanism of energy transduction in protein- promoted nucleic acid transactions. *Proc Natl Acad Sci USA* **92**(8), 3478-82.

Kowalczykowski, S. C., Lonberg, N., Newport, J. W. & von Hippel, P. H. (1981). Interaction of bacteriophage T4-coded gene 32 protein with nucleic acids: I. Characterization of the binding interactions. *J Mol Biol* **145**, 75-104.

Kowalczykowski, S. C., Paul, L. S., Lonberg, N., Newport, J. W., McSwiggen, J. A. & von Hippel, P. H. (1986). Cooperative and noncooperative binding of protein ligands to nucleic acid lattices: experimental approaches to the determination of thermodynamic parameters. *Biochemistry* **25**(6), 1226-40.

Lambright, D. G., Noel, J. P., Hamm, H. E. & Sigler, P. B. (1994). Structural determinants for activation of the alpha-subunit of a heterotrimeric G protein. *Nature* **369**(6482), 621-8.

Leahy, M. C. & Radding, C. M. (1986). Topography of the interaction of recA protein with single-stranded deoxyoligonucleotides. *J Biol Chem* **261**(15), 6954-60.

Leipe, D. D., Aravind, L., Grishin, N. V. & Koonin, E.V. (2000). The bacterial replicative helicase DnaB evolved from a RecA duplication. *Genome Res* **10**, 5-16.

Lim, D. S. & Hasty, P. (1996). A mutation in mouse *rad51* results in an early embryonic lethal that is suppressed by a mutation in *p53*. *Mol Cell Biol* **16**, 7133-7143.

Lindsley, J. E. and Cox, M. M. (1990). Assembly and disassembly of RecA protein filaments occur at opposite filament ends. Relationship to DNA strand exchange. *J Biol Chem* **265**, 9043-54.

Little, J. W., Edmiston, S. H., Pacelli, L. Z. & Mount, D. W. (1980). Cleavage of the *Escherichia coli* lexA protein by the recA protease. *Proc Natl Acad Sci USA* **77**(6), 3225-9.

Logan, K. M. & Knight, K. L. (1993). Mutagenesis of the P-loop motif in the ATP binding site of the RecA protein from Escherichia coli. *J Mol Biol* **232**(4), 1048-59.

Logan, K. M., Skiba, M. C., Eldin, S. & Knight, K. L. (1997). Mutant RecA proteins which form hexamer-sized oligomers. *J Mol Biol* **266**(2), 306-16.

Lovett, S. T. & Kolodner, R. D. (1989). Identification and purification of a single-stranded-DNA-specific exonuclease encoded by the recJ gene of Escherichia coli. *Proc Natl Acad Sci U S A* **86**(8), 2627-31.

Maeshima, K., Morimatsu, K., Shinohara, A. & Horii, T. (1995). RAD51 homologues in Xenopus laevis: two distinct genes are highly expressed in ovary and testis. *Gene* **160**(2), 195-200.

Malkov, V. A. & Camerini-Otero, R. D. (1995). Photocross-links between single-stranded DNA and Escherichia coli RecA protein map to loops L1 (amino acid residues 157-164) and L2 (amino acid residues 195-209). *J Biol Chem* **270**(50), 30230-3.

Maraboeuf, F., Voloshin, O., Camerini-Otero, R. D. & Takahashi, M. (1995). The central aromatic residue in loop L2 of RecA interacts with DNA. Quenching of the fluorescence of a tryptophan reporter inserted in L2 upon binding to DNA. *J Biol Chem* **270**(52), 30927-32.

McEntee, K., Weinstock, G. M. & Lehman, I. R. (1981). Binding of the recA protein of Escherichia coli to single- and double- stranded DNA. *J Biol Chem* **256**(16), 8835-44.

McGhee, J. D. & von Hippel, P. H. (1974). Theoretical aspects of DNA-protein interactions: Co-operative and non-co-operative binding of large ligands to a one-dimensional homogeneous lattice. *J Mol Biol* **86**, 469-489.

Mecozzi, S., West, A.P. & Doherty, D.A., (1996). Cation-pi interactions in aromatics of biological and medicinal interest: electrostatic potential surfaces as a useful qualitative guide. *Proc Natl Acad Sci USA* **93**, 10566-10571.

Menetski, J. P., Bear, D. G. & Kowalczykowski, S. C. (1990). Stable DNA heteroduplex formation catalyzed by the Escherichia coli RecA protein in the absence of ATP hydrolysis. *Proc Natl Acad Sci USA* **87**(1), 21-5.

Menetski, J. P. & Kowalczykowski, S. C. (1985a). Interaction of recA protein with single-stranded DNA. Quantitative aspects of binding affinity modulation by nucleotide cofactors. *J Mol Biol* **181**(2), 281-95.

Menetski, J. P. & Kowalczykowski, S. C. (1985b). Interaction of recA protein with single-stranded DNA: Quantitative aspects of binding affinity modulation by nucleotide cofactors. *J Mol Biol* **181**, 281-295.

Meselson, M. S. & Radding, C. M. (1975). A general model for genetic recombination. *Proc Natl Acad Sci USA* **72**(1), 358-61.

Michalopoulos, I & Hays, R. T. (1999). Role of the conserved lysine 80 in stabalisation of NF-kappaB p50 DNA binding. *Nuc Acids Res* **27**, 503-509.

Mikawa, T., Masui, R. & Kuramitsu, S. (1998). Rec A protien has extremely high cooperativity for substrate in its ATPase activity. *J Biochem* **123**, 450-457.

Milburn, M. V., Tong, L., deVos, A. M., Brunger, A., Yamaizumi, Z., Nishimura, S. & Kim, S. H. (1990). Molecular switch for signal transduction: structural differences between active and inactive forms of protooncogenic ras proteins. *Science* **247**(4945), 939-45.

Morimatsu, K. & Horii, T. (1995). The DNA-binding site of the RecA protein. Photochemical cross-linking of Tyr103 to single-stranded DNA. *Eur J Biochem* **228**(3), 772-8.

Morimatsu, K., Horii, T. & Takahashi, M. (1995). Interaction of Tyr103 and Tyr264 of the RecA protein with DNA and nucleotide cofactors. Fluorescence study of engineered proteins. *Eur J Biochem* **228**(3), 779-85.

Morita, T., Yoshimura, Y., Yamamoto, A., Murata, K., Mori, M., Yamamoto, H. & Matsushiro, A. (1993). A mouse homolog of the Escherichia coli recA and Saccharomyces cerevisiae RAD51 genes. *Genes Dev* **7**(9), 1755-65.

Morrical, S. W. & Cox, M. M. (1985). Light scattering studies of the RecA protein of *Escherichia coli*: relationship between free RecA filaments and RecA-ssDNA complex. *Biochemistry* **24**, 760-767.

Myszka, D. G., Jonsen, M. D. & Graves B. J. (1998). Equilibrium analysis of high affinity interactios using BIACORE. *Anal Biochem* **265**, 326-330.

Namsaraev, E. & Berg, P. (1998). Binding of Rad51p to DNA: Interaction of Rad51p with single- and double- stranded DNA. *J Biol Chem* **273**, 6177-6182.

Nastri, H. G. & Knight, K. L. (1994). Identification of residues in the L1 region of the RecA protein which are important to recombination or coprotease activities. *J Biol Chem* **269**(42), 26311-22.

New, J. H., Sugiyama, T., Zaitseva, E. & Kowalczykowski, S. C. (1998). Rad52 protein stimulates DNA strand exchange by Rad51 and replication protein A. *Nature* **393**(6683), 301.

Ogawa, T., Yu, X., Shinohara, A. & Egelman, E.H. (1993a). Similarity of the yeast Rad51 filament to the bacterial RecA filament. *Science* **259**, 1896-1899.

Ogawa, T., Shinohara, A., Nabetani, A., Ikeya, T., Yu, X., Egelman, E. H. & Ogawa, H. (1993b). RecA-like recombination proteins in eukaryotes: functions and structures of RAD51 genes. *Cold Spring Harbor Symp Quant Biol* **58**, 567-576.

Ogawa, T., Yu, X., Shinohara, A. & Egelman, E. H. (1993c). Similarity of the yeast RAD51 filament to the bacterial RecA filament. *Science* **259**(5103), 1896-9.

Park, M. S., Ludwig, D. L., Stigger, E. & Lee, S. H. (1996). Physical interaction between human RAD52 and RPA is required for homologous recombination in mammalian cells. *J Biol Chem* **271**(31), 18996-9000.

Petes, T. D., Malone, R. E. & Symington, L. S. (1991). Recombination in Yeast. In *The Molecular and Cellular Biology of the Yeast Saccharomyces*, pp. 407-522. Cold Spring Harbor Laboratory Press, New York.

Petukhova, G., Stratton, S. & Sung, P. (1998). Catalysis of homologous DNA pairing by yeast Rad51 and Rad54 proteins. *Nature* **393**, 91-94.

Pugh, B. F. & Cox, M. M. (1988). High salt activation of recA protein ATPase in the absence of DNA. *J Biol Chem* **263**(1), 76-83.

Radding, C. M. (1989). Helical RecA nucleoprotein filaments mediate homologous pairing and strand exchange. *Biochem Biophys Acta* **1008**, 131-145.

Register, J. C. & Griffith, J. (1985). The direction of RecA protein assembly onto single strand DNA is the same as the direction of strand assimilation during strand exchange. *J Biol Chem* **260**, 12308–12312.

Rehrauer, W. M. & Kowalczykowski, S. C. (1993). Alteration of the nucleoside triphosphate (NTP) catalytic domain within *Escherichia coli* RecA protein attenuates NTP hydrolysis but not joint molecule formation. *J Biol Chem* **268**, 1292-1297.

Resnick, M. A. (1976). The repair of double-strand breaks in DNA; a model involving recombination. *J Theor Biol* **59**(1), 97-106.

Roca, A. I. & Cox, M. M. (1990). The RecA protein: structure and function. *Crit. Rev Biochem Mol Biol* **25**(6), 415-56.

Roca, A. I. & Cox, M. M. (1997). RecA protein: structure, function, and role in recombinational DNA repair. *Prog Nucl Acid Res Mol Biol* **56**, 129-222.

Roman, L. J. & Kowalczykowski, S. C. (1986). Relationship of the physical and enzymatic properties of Escherichia coli recA protein to its strand exchange activity. *Biochemistry* **25**(23), 7375-85.

Royer, W. E., Jr., Pardanani, A., Gibson, Q. H., Peterson, E. S. & Friedman, J. M. (1996). Ordered water molecules as key allosteric mediators in a cooperative dimeric hemoglobin. *Proc Natl Acad Sci, USA* **93**, 14526-14531.

Ruigrok, R. W. & DiCapua, E. (1991). On the polymerization state of recA in the absence of DNA. *Biochimie* **73**(2-3), 191-8.

Sablin, E. P., Kull, F. J., Cooke, R., Vale, R. D. & Fletterick, R. J. (1996). Crystal structure of the motor domain of the kinesin-related motor ncd [see comments]. *Nature* **380**(6574), 555-9.

Sambrook, J., Fritsch, E.F. & Maniatis, T. (1989). *Molecular Cloning: A Laboratory Manual, 2nd ed.*, Cold Spring Harbor Laboratory, Cold Spring Harbor, NY.

Sawaya, M. R., Guo, S., Tabor, S., Richardson, C. C. & Ellenberger, T. (1999). Crystal structure of the helicase domain from the replicative helicase-primase of bacteriophage T7. *Cell* **99**, 167-177.

Schild, D., Lio, Y., Collins, D. W., Tsomondo, T. & Chen, D. J. (2000). Evidence for simultaneous protein interactions between human Rad51 paralogs. *J Biol Chem* **275**, 16443-16449.

Schindelin, H., Kisker, C., Schlessman, J. L., Howard, J. B. & Rees, D. C. (1997). Structure of ADP x AIF4(-)-stabilized nitrogenase complex and its implications for signal transduction. *Nature* **387**(6631), 370-6.

Scully, R., Chen, J., Plug, A., Xiao, Y., Weaver, D., Feunteun, J., Ashley, T. & Livingston, D. M. (1997). Association of BRCA1 with Rad51 in mitotic and meiotic cells. *Cell* **88**(2), 265-75.

Segel, I. H. (1975). *Enzyme Kinetics*, John Wiley & Sons, Inc.

Shan, Q., Bork, J. M., Webb, B. L., Inman, R. B. & Cox, M. M. (1997). RecA protein filaments: end-dependent dissociation from ssDNA and stabilization by RecO and RecR proteins. *J Mol Biol* **265**(5), 519-40.

Sharan, S. K., Morimatsu, M., Albrecht, U., Lim, D.-S., Regal, E., Dinh, C., Sands, A., Eichele, E. & Bradley, A. (1997). Embryonic lethality and radiation hypersensitivity mediated by Rad51 in mice lacking *Brac2*. *Nature* **386**, 804-810.

Shen, Z., Cloud, K. G., Chen, D. J. & Park, M. S. (1996). Specific interactions between the human RAD51 and RAD52 proteins. *J Biol Chem* **271**(1), 148-52.

Shinohara, A., Ogawa, H., Matsuda, Y., Ushio, N., Ikeo, K. & Ogawa, T. (1993). Cloning of human, mouse and fission yeast recombination genes homologous to RAD51 and recA. *Proc Natl Acad Sci, USA* **90**(14), 6577-80.

Shinohara, A., Ogawa, H. & Ogawa, T. (1992). Rad51 protein involved in repair and recombination in *S. cerevisiae* is a RecA-like protein. *Cell* **69**(3), 457-70.

Shinohara, A. & Ogawa, T. (1997). Stimulation by Rad52 of yeast Rad51-mediated recombination. *Mutat Res* **384**(2), 65-72.

Shinohara, A. & Ogawa, T. (1998). Stimulation by Rad52 of Rad51-mediated recombination. *Nature* **391**, 404-407.

Silver, M. S. & Fersht, A. R. (1982). Direct observation of complexes formed between recA protein and a fluorescent single-stranded deoxyribonucleic acid derivative. *Biochemistry* **21**, 6066-6072.

Silver, M. S. & Fersht, A. R. (1983). Investigation of binding between recA protein and single-stranded polynucleotides with the aid of a fluorescent deoxynucleic acid derivative. *Biochemistry* **22**, 2860-2866.

Singleton, M. R., Sawaya, M. R., Ellenberger, T. & Wigley, D. B. (2000). Crystal structure of T7 gene 4 ring helicase indicates a mechanism for sequential hydrolysis of nucleotides. *Cell* **in press**.

Skiba, M. C. & Knight, K. L. (1994). Functionally important residues at a subunit interface site in the RecA protein from Escherichia coli. *J Biol Chem* **269**(5), 3823-8.

Skiba, M. C., Logan, K. M. & Knight, K. L. (1999). Intersubunit proximity of residues in the RecA protein as shown by engineered disulfide cross-links. *Biochemistry* **38**(37), 11933-41.

Soultanas, P. & Wigley, D. B. (2000). DNA helicases: 'inching forward'. *Curr Opin Struct Biol* **10**, 124-128.

Stasiak, A., Di Capua, E. & Koller, T. (1981). Elongation of duplex DNA by recA protein. *J Mol Biol* **151**(3), 557-64.

Stasiak, A. & Egelman, E. H. (1994). Structure and function of RecA-DNA complexes. *Experientia* **50**(3), 192-203.

Stole, E. & Bryant, F. R. (1994). Introduction of a tryptophan reporter group into loop 1 of the recA protein. Examination of the conformational states of the recA-ssDNA complex by fluorescence spectroscopy. *J Biol Chem* **269**(11), 7919-25.

Story, R. M., Bishop, D. K., Kleckner, N. & Steitz, T. A. (1993). Structural relationship of bacterial RecA proteins to recombination proteins from bacteriophage T4 and yeast. *Science* **259**(5103), 1892-6.

Story, R. M. & Steitz, T. A. (1992). Structure of the recA protein-ADP complex [see comments]. *Nature* **355**(6358), 374-6.

Story, R. M., Weber, I. T. & Steitz, T. A. (1992). The structure of the E. coli recA protein monomer and polymer. *Nature* **355**(6358), 318-25.

Sturzbecher, H. W., Donzelmann, B., Henning, W., Knippschild, U. & Buchhop, S. (1996). p53 is linked directly to homologous recombination processes via RAD51/RecA protein interaction. *EMBO J.* **15**(8), 1992-2002.

Subramanya, H. S., Bird, L. E., Brannigan, J. A. & Wigley, D. B. (1996). Crystal structure of a DExx box DNA helicase. *Nature* **384**, 379-383.

Sugiyama, T., Zaitsev, E. M. & Kowalczykowski, S. C. (1997). A single-stranded DNA-binding protein is needed for efficient presynaptic complex formation by the *Saccharomyces cerevisiae* Rad51 protein. *J Biol Chem* **272**, 7940-7945.

Sung, P. (1994). Catalysis of ATP-dependent homologous DNA pairing and strand exchange by yeast RAD51 protein. *Science* **265**(5176), 1241-3.

Sung, P. (1997). Function of yeast Rad52 protein as a mediator between replication protein A and the Rad51 recombinase. *J Biol Chem* **272**, 28194-28197.

Sung, P. & Robberson, D. L. (1995). DNA strand exchange mediated by a RAD51-ssDNA nucleoprotein filament with polarity opposite to that of RecA. *Cell* **82**(3), 453-61.

Sung, P. & Stratton, S. A. (1996). Yeast Rad51 recombinase mediates polar DNA strand exchange in the absence of ATP hydrolysis. *J Biol Chem* **271**(45), 27983-6.

Szostak, J. W., Orr-Weaver, T. L., Rothstein, R. J. & Stahl, F. W. (1983). The double-strand-break repair model for recombination. *Cell* **33**(1), 25-35.

Takata, M., Sasaki, M., Sonoda, E., Fukushima, T., Morrison, C., Albala, J., Kannar, R., Thompson, L. & Takeda, S. (2000). *Mol Cell Biol*, in press.

Tsuzuki, T., Fujii, Y., Sakumi, K., Tominaga, Y., Nakao, K., Sekiguchi, M., Matsushiro, A., Yoshimura, Y. & Morita T. (1996). Targeted disruption of the RAD51 gene leads to lethality in embryonic mice. *Proc Natl Acad Sci USA* **93**(13), 6236-40.

Ullsperger, C. J. & Cox, M. M. (1995). Quantitative RecA protein binding to the hybrid duplex product of DNA strand exchange. *Biochemistry* **34**(34), 10859-66.

Umezu, K., Nakayama, K. & Nakayama, H. (1990). Escherichia coli RecQ protein is a DNA helicase [published erratum appears in Proc Natl Acad Sci U S A 1990 Nov;87(22):9072]. *Proc Natl Acad Sci USA* **87**(14), 5363-7.

Voloshin, O. N., Wang, L. & Camerini-Otero, R. D. (1996). Homologous DNA pairing promoted by a 20-aminio acid peptide derived from RecA. *Science* **272**, 868-872.

Wang, L., Voloshin, O. N., Stasiak, A. & Camerini-Otero, R. D. (1998). Homologous DNA pairing domain peptides of RecA protein: intrinsic propensity to form beta-structures and filaments. *J Mol Biol* **277**, 1-11.

Weinstock, G. M., McEntee, K. & Lehman, I. R. (1981). Hydrolysis of nucleoside triphosphates catalyzed by the recA protein of Escherichia coli. Steady state kinetic analysis of ATP hydrolysis. *J Biol Chem* **256**(16), 8845-9.

West, S. C. (1992). Enzymes and molecular mechanisms of genetic recombination. *Annu Rev Biochem* **61**, 603-40.

Wilson, D. H. & Benight, A. S. (1990). Kinetic analysis of the pre-equilibrium steps in the self-assembly of RecA protein from *Escherichia coli*. *J Biol Chem* **265**, 7351-7359.

Wong, I. & Lohman, T. M. (1993). A double-filter method for nitrocellulose-filter binding: Application to protein-nucleic acid interactions. *Proc Natl Acad. Sci USA* **90**, 5438-5432.

Yoshimura, Y., Morita, T., Yamamoto, A. & Matsushiro, A. (1993). Cloning and sequence of the human RecA-like gene cDNA. *Nucleic Acids Res* **21**, 1665.

Yoshioka, K., Saito, K., Tanabe, T., Yammamoto, A. Ando, Y., Nakamura, Y., Shirakawa, H. & Yoshida, M. (1999). Differences in DNA recognition and conformational change activity between boxes A and B inHMG2 protein. *Biochemistry* **38**, 589-595.

Yu, X. & Egelman, E. H. (1992). Structural data suggest that the active and inactive forms of the RecA filament are not simply interconvertible. *J Mol Biol* **227**, 334-346.

Yuan, Z. M., Huang, Y., Ishiko, T., Nakada, S., Utsugisawa, T., Kharbanda, S., Wang, R., Sung, P., Shinohara, A., Weichselbaum, R. & Kufe, D. (1998). Regulation of Rad51 function by c-Abl in response to DNA damage. *J Biol Chem* **273**(7), 3799-802.

Zagursky, R. J. & Berman, M. L. (1984). Cloning vectors that yield high levels of single-stranded DNA for rapid DNA sequencing. *Gene* **27**, 183-191.

Zaitseva, E. M., Zaitsev, E. N. & Kowalczykowski, S. C. (1999). The DNA binding properties of Saccharomyces cerevisiae Rad51 protein. *J Biol Chem* **274**(5), 2907-15.

Zlotnick, A., Mitchell, R. S., Steed, R. K. & Brenner, S. L. (1993). Analysis of two distinct single-stranded DNA binding sites on the recA nucleoprotein filament. *J Biol Chem* **268**(30), 22525-30.